1-1-2013

Study the Carrier Frequency Offset (CFO) for Wireless OFDM

Saeed Mohseni
University of Denver

STUDY THE CARRIER FREQUENCY OFFSET (CFO) FOR WIRELESS OFDM

_____

A Dissertation

Presented to

the Faculty of Engineering and Computer Science

University of Denver

_____

In Partial Fulfillment

of the Requirements for the Degree

Doctor of Philosophy

_____

by

Saeed Mohseni

June 2013

Advisor: Dr. Mohammad A. Matin

Author: Saeed Mohseni
Title: STUDY THE CARRIER FREQUENCY OFFSET (CFO) FOR WIRELESS OFDM
Advisor: Dr. Mohammad A. Matin
Degree Date: June 2013

Abstract

Due to high proficiency with high bandwidth efficiency, orthogonal frequency division multiplexing (OFDM) has been selected for broadband wireless communication systems. Since OFDM can provide large data rates with sufficient robustness to radio channel impairments, and due to its robustness against the multipath delay spread, OFDM has always been a designated technique for broadband wireless communication mobile systems. Nevertheless, OFDM suffers from Carrier Frequency Offset (CFO). CFO has been recognized as a major disadvantage of OFDM. CFO can lead to the frequency mismatch in transmitter and receiver oscillator. Lack of the synchronization of the local oscillator signal, for down conversion in the receiver with the carrier signal contained in the received signal, can cause the performance of OFDM to degrade. In other words, the orthogonality of the OFDM relies on the condition that the transmitter and receiver operate with exactly the same frequency reference. If this is not the case, the perfect orthogonality of the subcarrier will be lost, which can result in CFO. In this research, the source of creating CFO and the major CFO estimation algorithms have been reviewed and discussed in literature. We then proposed some algorithms and techniques for estimating and compensating for the effect of CFO. We showed that our proposed methods have a better performance with low complexity.

Although this research focuses on CFO, high Peak-to-Average Power Ratio (PAPR) has been named as the other main drawback of the OFDM modulation format.

The chapter 4 is dedicated to PAPR. In this chapter after investigating PAPR, we proposed a technique that leads to the reduction of PAPR. On the other hand, in wireless communication path loss is the main power loss that occurs between the transmitter and the receiver antenna. Therefore, chapter 5 is dedicated to investigate indoor and outdoor path loss. We then proposed an extended model that can be used to cover the outdoor and indoor environment for predicting the path loss. Chapter 6 contains the results and conclusion.

Acknowledgements

I am most grateful to my advisor, Dr. Mohammad A. Matin, for his consistence support, encouragement, expertise, and exquisite guidance throughout my PhD study. I also appreciate the members of my committee, Dr. Jun Jason Zhang, Dr. George Edwards and Dr. Davor Balzar for their guidance and support.

I would like to express my deepest gratitude to my mother and my brother, Mansour for their willing encouragement and support during my study over the years. Special thanks go to my beloved wife, Sima, for her consistence love and support, and to my lovely children, Sarina and Daniel, for bringing me all the joy and happiness in the world.

I send my blessings to my late father for all he had done for his children, especially for the love of learning that he planted in his children's hearts. Even though he is not alive, I am sure his soul gets happy when he sees that his children are successful. I also wish to express my appreciation to all those who have cared for me.

Table of contents

List of figures

List of tables

List of abbreviations

3GPP	3rd Generation Partnership Project
ADSL	Asynchronous Digital Subscriber Line
A/D	Analog-to-Digital
AOI	Angle of Incident
ASK	Amplitude Shift Keying
AWGN	Additive White Gaussian Noise
BER	Bit Error Rate
BP	Break Point
BW	Bandwidth
CAF	Clipping and Filtering
CAZAC	Constant Amplitude Zero Autocorrelation
CBC	Complement Block Coding
CC	Classical-Clipping
CCDF	Complementary Cumulative Distribution Function
CDMA	Code Division Multiple Access
CE	Cyclic Extension
CFO	Carrier Frequency Offset
CP	Cyclic Prefix
DAB	Digital Audio Broadcasting
dB	Decibel
DC	Deep-Clipping

DCR	Direct Conversion Receivers
DE	Doppler Effect
DFT	Discrete Fourier Transform
DMB	Digital Mobile Broadcasting
DPSD	Doppler Power Spectrum Density
DSBW	Directional Scattering Bandwidth
DVB	Digital Video Broadcasting
ESPRIT	Estimation of Signal Parameter via Rotational Invariance Techniques
EVD	Eigenvalue Decomposition
FAF	Floor Attenuation Factor
FFT	Fast Fourier Transform
FSP	Free Space Propagation
GB	Guard Band
HC	Heavy side-Clipping
HPA	High Power Amplifier
HST	High Speed Transportation
ICI	Inter-Carrier Interference
ISI	Inter Symbol Interference
IEEE	Institute of Electrical and Electronics Engineers
IFFT	Inverse Fast Fourier Transform
IDFT	Inverse Discrete Fourier Transform
I/Q	In-phase and Quadrature

ISI	Inter Symbol Interference
LOS	Line Of Sight
LOSC	Local Oscillator Signal
LSF	Large Scale Fading
SSF	Small Scale Fading
MASK/M-ary ASK	M-ary Amplitude Shift Keying
MC-CDMA	Multi Carrier Code Division Multiple Access
MLE	Maximum Likelihood Estimate
MPSK/M-ary PSK	M-ary Phase Shift Keying
MQAM/M-ary QAM	M-ary Quadrature Amplitude Modulation
MSE	Mean Square Error
MUSIC	MUltiple SIgnal Classifier
NLOS	No Line Of Sight
OFDM	Orthogonal Frequency Division Multiplexing
OSC	Oscillator
PA	Power Amplifier
PAPR	Peak to Average Power Ratio
PCS	Personal Communication System
PL	Path Loss
PSD	Power Spectrum Density
PSK	Phase Shift Keying
PTS	Partial Transmission Sequence
QAM	Quadrature Amplitude Modulation

QPSK	Quadrature Phase-Shift Keying
RF	Radio Frequency
SBCC	Sub-Block Complement Coding
SC	Smooth-Clipping
SCD	Sampling Clock Drift
SCs	Sub-Carriers
ScFO	Sampling clock Frequency Offset
SINR	Signal-to-Interference-plus-Noise-Ratio
SISO	Single-Input Single-Output
SLM	Selective Mapping
SMOPT	Selective Mapping of Partial Tones
SNR	Signal-to-Noise Ratio
SSF	Small Scale Fading
STO	Symbol Time Offset
SVD	Spectral Value Decomposition
TDE	Time Domain Equalizer
TDR	Transmission Data Rate
TI	Tone Injection
TR	Tone Reservation
VTD	Vehicle Travel Direction
WAF	Wall Attenuation Factor
UTD	Uniform Theory of Diffraction

Chapter 1

Introduction

1.1 Background

The Orthogonal Frequency Division Multiplexing (OFDM) system was suggested for the first time during the Second World War and gradually was studied for use as a high speed modem and for digital mobile communication. Approximately 55 years ago, Doelz et al. [1] published the idea of dividing the transmitting data into the number of interleaved bit streams and modulate numerous carriers. Then Chang [2], in the middle of the 1960's, presented the basic idea of multicarrier modulation. But it was Weinstein and Ebert [3] that brought it to fruition. They showed how to apply the Discrete Fourier Transform (DFT) to perform the baseband modulation and demodulation. They showed how, by using the DFT, we can increase and improve the efficiency of the modulation and demodulation.

However, due to the high proficiency with high bandwidth and its ability to provide large data rates and its robustness against the multipath delay spread, OFDM has been selected for the broadband wireless systems. But in order to efficiently modulate and demodulate the OFDM signals, and preventing the degradation of the OFDM wireless systems, a few pre and post tasks must be done. The most important in an

OFDM transceiver are estimating and compensating the Carrier Frequency Offset (CFO), frequency synchronization, and Peak-to-Average Power Reduction (PAPR).

1.2 Problem statement

Although OFDM has many advantages, OFDM systems are very sensitive to the CFO. CFO is one of the most important drawbacks of the OFDM wireless communication system. CFO destroys the orthogonality relationship between the subcarrier and creates Inter-Carrier Interference (ICI). ICI can create frequency mismatch between the transmitter and receiver. This frequency mismatch can lead to the severe performance degradation issue for OFDM wireless systems. Therefore, for a reliable receiver, the effect of the CFO must be estimated and compensated. In short, no matter which method to be used, the carrier frequency offset should be estimated and compensated to keep the orthogonality in OFDM systems.

1.3 Objective

The main focus of this research is on CFO. In this research we have investigated the reasons of creating CFO and we have analyzed its effects on the performance of the OFDM systems. We have reviewed and discussed the major CFO estimation algorithms and techniques in literature and have evaluated their performance and efficiency. Then we have proposed some algorithms and techniques for estimating and compensating for the effect of CFO. Our goal is to propose the algorithm and method that can compensate for the effect of CFO and gain better performance with lower complexity.

1.4 Scope of research work

In this research the main focus is on exploring and using advanced mathematical tools to overview the available algorithms and techniques and then to propose an algorithm for reducing the complexity and computational process for CFO estimation in wireless OFDM systems. As we mentioned since PAPR and path loss are the other issues that degrade the OFDM performance, in Chapter 4, after briefly investigating them, we have proposed a method with lower complexity for PAPR and then we have presented an analytical model for optimizing indoor and outdoor radio propagation prediction for path loss in wireless OFDM communication systems.

1.5 Methodology

To achieve our objectives we use different mathematical approaches and Matlab software version R2011-a.

- Mathematical tools are used for investigating the available algorithms, techniques and methods and obtaining an analytical algorithm or method for improving the existence methods.
- MATLAB is used for simulation and comparing the proposed algorithm with the algorithms and techniques that were suggested by the others.

1.6 Contribution and publications

This research is on the study of the effects of carrier frequency offset (CFO) for wireless orthogonal frequency-division multiplexing (OFDM) systems. Most of the research and contributions have already published in various peer review journals

(publications list is in page 168). Following paragraph will concise in respect to each of the publications.

One of the major drawbacks for OFDM system is Carrier frequency offset (CFO). A training based technique for estimating and compensation for the bigger range of CFO has been presented. A method for CFO estimation which is based on cost function and uses the structure of the subcarrier has been suggested. Then the research continued by investigating the effect of carrier frequency offset and frequency synchronization on different parameters on OFDM systems. The research showed the dependency of the SNR to the frequency offset and a better approach by using the repetitive pattern to increase the range of estimation has been showed.

In addition to CFO research my initial research was in Peak-to-Average Power Ratio (PAPR) and path loss which were published in peer review journal as stated below.

A method has been presented which in compare with the conventional OFDM, the separation of subcarriers (SCs) is forth. Thus, in each OFDM symbol, only the first $1 + N/4$ samples will be sent while the rest will be ignored, which leads to decrease the maximum of PAPR. In this case, the rest of the samples by using the partial symmetry of Fourier transform can be constructed.

An approach for the path loss propagation model for indoor/outdoor path loss has proposed which is on the base of calculating a new initial value plus the field measurements.

1.7 Chapter organization

The dissertation is divided into five chapters. The layouts for these chapters are as follows:

Chapter 1 includes background, the problem statement, the objective, the scope of the research work, methodology, and the chapter organization.

Chapter 2 provides a brief history and background of OFDM system in wireless communication, and its applications; and a study of the principles of OFDM system in detail, including the concept of OFDM systems, OFDM theory, OFDM modulation and demodulation techniques, key components of OFDM transmission (OFDM related issues), advantages and disadvantages of using OFDM for communication systems, and OFDM transceiver architecture.

Chapter 3 includes: the study of Carrier Frequency Offset (CFO), sources of frequency offset, effects of frequency synchronization errors in OFDM systems, challenges in CFO estimation, the effect of CFO on degradation of OFDM systems and phase shift, the relation between frequency offset and SNR, a blind and semi-blind CFO estimation for OFDM systems, a training based algorithm, CAZAC sequences for joint CFO. A review of the pilot based and non-pilot based estimation are studied in detail, and our proposed our algorithms for estimating CFO are then presented.

Chapter 4 covers the High Peak to Average Power Ratio (PAPR). In this chapter we briefly study the High Peak to Average Power Ratio (PAPR) and the techniques that have been used for reduction PAPR such as Selecting Mapping (SLM), Partial Transmission Sequence (PTS), Clipping and Filtering (CAF) and then we have proposed an algorithm for reducing the PAPR with lower complexity.

Chapter 5 has dedicated to the study of the outdoor and indoor path loss for mobile wireless channel and then we proposed a method that can be used for estimating indoor and outdoor path loss for wireless OFDM systems.

Chapter 6 includes: summary, conclusions and Future works. This chapter is followed by the list of our publications, bibliography, and published journal and conference papers.

Chapter 2

Concept of OFDM

2.1 Introduction

One generation ago, we would have been astonished if we could see today's wireless technology growth. The growth of wireless communication has depended upon many factors such as communication technology, consumers' and business professionals' needs, multimedia communication desires, computer technology and finally price/expenses for providing the wireless communication services. Today, the people want to be able to have access to the applications and services that they had with a fixed wire-line connection through the wireless communication at any moment, any place and any condition (mobile or stationary).

2.2 The history of OFDM

We have recently witnessed a dramatic flow of interest in orthogonal frequency division multiplexing (OFDM). The evidence is in the numerous publications and the number of stunning experimental demos that have been accomplished in OFDM area [4]. Although the concept of OFDM is not new and dates back to the decade of 1950's, then its usage was not common or popular due to the limitations in practical implementation.

In 1971, Weinstein and Ebert [5] suggested using Discrete Fourier Transform (DFT) to implement OFDM. This good idea decreased the complexity of implementation. The passing of time and the introduction of the Fast Fourier Transform (FFT) and then using it for implementation of OFDM began a new era where OFDM became popular and common.

OFDM can be used in different schema; it can be used both as a modulation scheme and as a multiple access scheme. Multi Carrier Code Division Multiple Access (MC-CDMA) is the combination of the OFDM with Code Division Multiple Access (CDMA). In the first step of this technique, the signal spreads with a spreading code in frequency domain and is then sent over the subcarriers. In short, the concept of Orthogonal Frequency Division Multiplexing (OFDM) has been considered for many decades and it took a long time for OFDM to evolve to where it is today, and to be utilized by various standards, such as 802.11 a/g and 802.16 [6][7]. However it is good to mention that using and expanding the OFDM system is determined by three requirements:

1. Available bandwidth;
2. Tolerable delay spread;
3. Doppler account.

2.3 OFDM

OFDM is a multiplexing technique that divides the bandwidth into multiple frequency sub-carriers. The multiple sub-carriers are closely spaced to each other without

causing interference. Due to the high flexibility that Orthogonal Frequency Division offers and the efficiency of OFDM in using the bandwidth (BW) and its high tolerance for induced distortion, the OFDM has been considered as the modulation process for diverse applications in wireless communication systems.

Some of these applications are: Multiple Input Multiple Output (MIMO); Asynchronous Digital Subscriber Line (ADSL); Digital Audio Broadcasting (DAB); Digital Video Broadcasting (DVB); Local Area Network (LAN); Mobile Broad Band Wireless Access (MBWA); and 3rd Generation Partnership Project (3GPP) Long Term Evolution (LTE) [8].

2.4 Concept of overlapping modulation

The figures 2.1-a, and 2.1-b illustrate the concept of using overlapping multicarrier modulation techniques compared with non-overlapping multicarrier techniques. As seen in figure 2.1 [9], applying this technique can save fifty percent of the bandwidth (BW). But for reducing the cross talk between subcarriers (SCs) and preventing adjacent carrier interference, the carrier must be mathematically orthogonal.

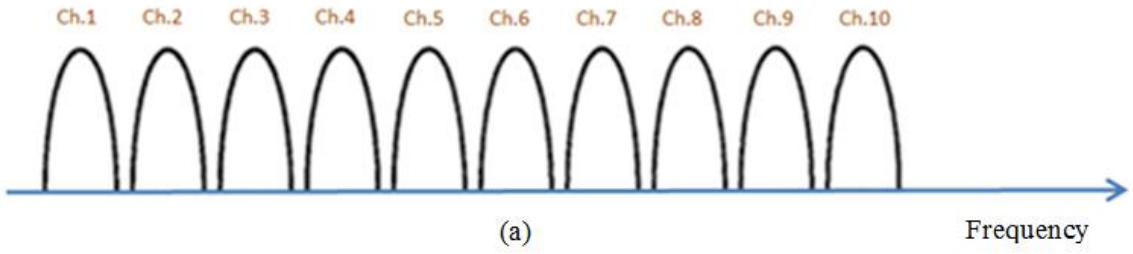

Figure 2.1-a Concept of OFDM signal in conventional multicarrier technique

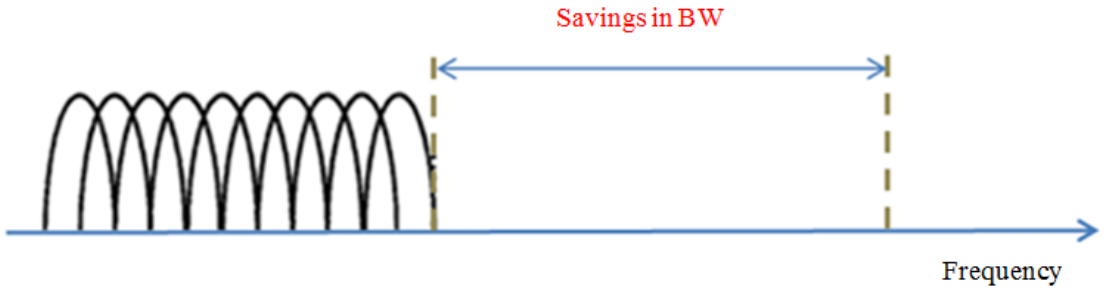

Figure 2.1-b Concept of OFDM signal in orthogonal multicarrier modulation technique

Figure 2.2 is an example of the OFDM spectrum. Figure 2.2 (a) shows the spectrum of the individual data of the sub-channel. The OFDM signal, multiplexed in the individual spectra with frequency spacing equal to the transmission speed of each SC, is shown in Figure 2.2 (b).

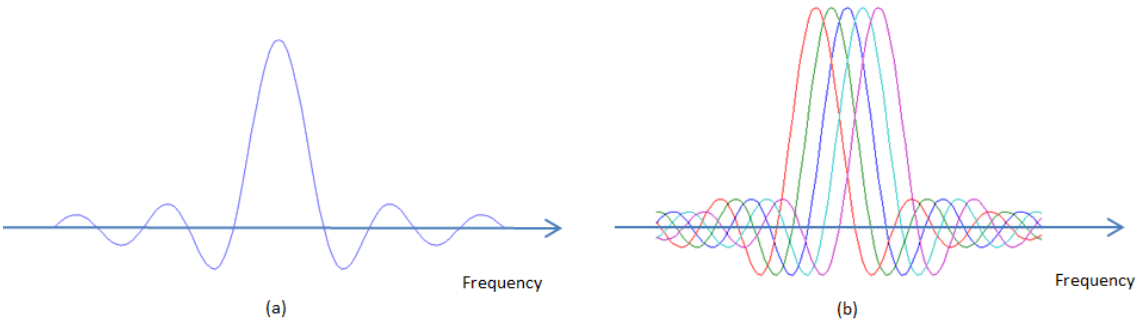

Figure 2.2 Spectra of (a) an OFDM sub-channel (b) an OFDM signal

Orthogonality between two signals allows the multiple information signals to be transmitted and detected without problem and interference. As illustrated in figure 2.3 [10], carrier centers are in orthogonal frequencies and there is an orthogonality relationship between signals. In figure 2.3 the peak of every single signal coincides with

the lowest part of the other signals (trough), and there is $1/T_s$ space between the subcarriers (SCs).

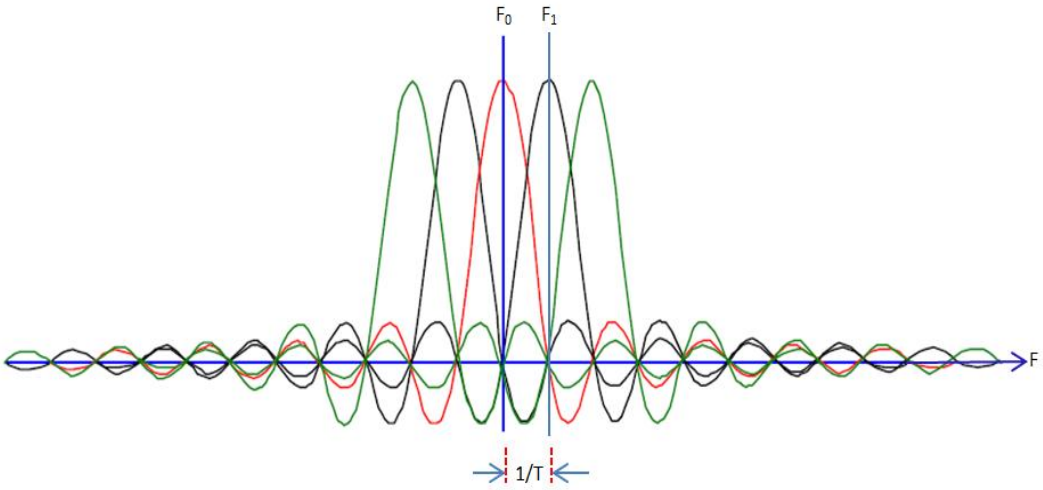

Figure 2.3 Illustration of the orthogonality relationship between signals

2.5 The methods of organizing the subcarriers in OFDM

The OFDM organizes the subcarriers (SCs) in the frequency domain by assigning the information signal onto the different subcarriers. Assigning the subcarriers (SCs) can be done by two methods. Consider a set of subcarriers that are assigned to an OFDM frame. The methods are as follows:

Method 1: In this method, first, OFDM reads the bits/symbol and then allocates one subcarrier to it. In the second step, it reads another group of bits per symbols and then allocates the subcarrier which is orthogonal to the subcarrier in step one. This procedure is then repeated.

Method 2: In this method, first OFDM reads the bits/word of the entire OFDM frame and then constructs a matrix that each element of this matrix represents one word.

Figure 2.4 (a) illustrates five subcarriers modulated by assigned symbols to it, and Figure 2.4 (b) illustrates the entirely bandwidth (BW).

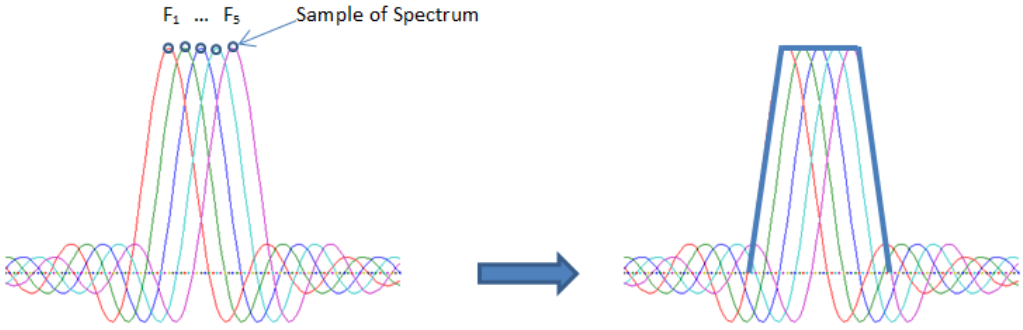

Figure 2.4 (a) Spectral setting (b) OFDM Transmission BW

Briefly, in the OFDM modulation, the existing channel divides into numerous independent subcarriers then all of these subcarriers transmit at a time. However, in order to avoid inter-carrier interference (ICI), the orthogonality of all the subcarriers should be kept to each other.

It is necessary to mention that the selection of the orthogonal frequency differences is based on the data rate or symbol time, and therefore it should be selected carefully, not randomly or arbitrarily.

2.6 The role of cyclic prefix

A signal going through a time dispersive channel leads to Inter Symbol Interference (ISI) and Inter Carrier Interference (ICI). These two phenomena destroy the orthogonality between the subcarriers. Peld and Ruiz [11], by introducing the Cyclic Extension (CE) which today is called Cyclic Prefix (CP), solved these problems. CP is

actually a copy of the last samples from IFFT, which is placed in front of the symbol. Figure 2.5 shows the use of CP. In Figure 2.5 T_{CP} is the length of the cyclic prefix and T_S is the length of the OFDM symbol and $T = T_{CP} + T_S$.

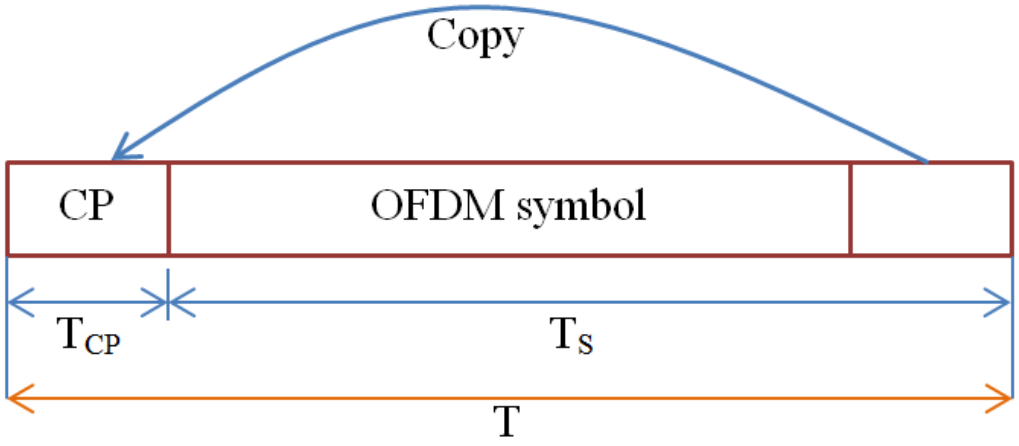

Figure 2.5 Cyclic Prefix (CP)

To escape Inter-Symbol Interference (ISI) and Inter Carrier Interference (ICI), the length of the CP must be as long as the noteworthy part of the impulse response. If the Cyclic Prefix is shorter than the impulse response, the convolution is not going to be circular. This leads to the creation of ISI. On the other hand, since CP does not carry any useful data, the transmission rate will be reduced by increasing the number of samples in CP.

It is important to note that the transmitted energy will be amplified with the length of the CP. However, the insertion of the Cyclic Prefix causes the loss of Signal to Noise Ratio (SNR) which is stated as follows:

$$SNR_{loss} = -10 \log_{10}\left(1 - \frac{T_{CP}}{T}\right) \quad (2.1)$$

On the other hand, inserting the CP leads to the decrease of the number of symbols which are transmitted per second. Therefore, the length of the CP should not be longer than necessary.

2.7 The effect of subcarriers and Guard Band on system performance

The result of increasing the number of Subcarriers (SCs) and Guard Band (GB) can be pointed out as follows:

- Increasing the number of SCs can lead to the increase of the power efficiency but it can make the system be more sensitive to the Doppler spread.

- Increasing the number of SCs and increasing the bandwidth can lead to the reduction of the Inter Symbol Interference (ISI) but at the cost of reducing the bandwidth (BW) efficiency and power efficiency.

2.8 Modulation

Modulation can be accomplished by changing the amplitude, frequency and phase of the sinusoidal carrier. In general there are two different modulation methods: coherent and non-coherent modulation. The coherent modulation techniques use the reference phase between the transmitter and receiver which results in a precise demodulation on the receiver side. The non-coherent modulation is used in low data rate systems like Digital Audio Broadcasting (DAB). Generally in case of the lack of knowledge of the carrier phase, the non-coherent is more useful. Since it does not need carrier or phase tracking and channel estimation, the structure of the receiver will be simpler.

2.8.1 Coherent Modulation for OFDM systems

The suitable coherent modulation methods for OFDM systems are: Amplitude Shift Keying (ASK), Phase Shift Keying (PSK), and Quadrature Amplitude Modulation (QAM). Since each of these methods can be represented as an M-ary modulation schemas, we have M-ary ASK, M-ary PSK and M-ary QAM.

2.8.2 M-ary Amplitude Shift Keying (MASK/M-ary ASK)

In this modulation the information will be carried in amplitude. So if we assume a set of $\{A_1, A_2, \dots, A_M\}$, the signal s_i can be stated as:

$$s_i(t) = A_i cos\omega t \tag{2.2}$$

The 2-ASK which is called BPSK is one of the common modulation schemas that has been generally used. The constellation points are located in $\sqrt{2E/T}$ and $-\sqrt{2E/T}$ (E is signal energy per symbol.)

2.8.3 M-ary Phase Shift Keying (MPSK/M-ary PSK)

In this modulation the phase is shifted for different constellation. In this case there is M possible signals which have $\theta_i = 2(i-1)/M$ where each signal is given as:

$$s_i(t) = \sqrt{\frac{2E}{T}} \cos\left(2\pi f_c t + \frac{2\pi}{M}(i-1)\right) \quad where\ i = 1,2, \dots, M \tag{2.3}$$

It is necessary to mention that 2-PSK is the same BPSK.

2.8.4 M-ary Quadrature Amplitude Modulation (MQAM/M-ary QAM)

This modulation is a combination of amplitude and phase modulation. The M signals can be given as follows:

$$s_i(t) = \sqrt{\frac{2E_0}{T}} a_i \cos(2\pi f_c t) + \sqrt{\frac{2E_0}{T}} b_i \cos(2\pi f_c t) \quad where \quad 0 \le t \le T \quad (2.4)$$

Where $\{a_i, b_i\}$ is the element of an $L \times L$ matrix, this matrix can be stated as [12]:

$$\begin{bmatrix} (-L+1, L-1) & (-L+3, L-1) & \dots & (L-1, L-1) \\ (-L+1, L-3) & (-L+3, L-3) & \dots & (L-1, L-3) \\ \vdots & \vdots & \vdots & \vdots \\ (-L+1, -L+1) & (-L+3, -L-1) & \dots & (L-1, L+1) \end{bmatrix} \quad (2.5)$$

For $M = 4$, it is as 4-PSK, which is called Quadrature PSK (QPSK).

2.9 The advantages and disadvantages of OFDM

OFDM has become one of the most exciting developments in the area of modern broadband wireless networks. During recent years, the applications of OFDM, principally in digital communication systems such as Digital Audio Broadcasting (DAB), Digital Video Broadcasting (DVB) and Digital Mobile Broadcasting (DMB) have highlighted some of the important and key advantages of OFDM.

These advantages can be summarized as follows:

- Since narrowband interference hits only a small portion of the Subcarriers (SCs), it is considered to be robust against narrowband;
- For dealing with multipath, OFDM is the best and more efficient method;
- OFDM makes the single frequency network possible;
- Using OFDM leads to the deletion of the need of the high complexity receiver, making it possible to use the low complexity receiver;
- OFDM has a high resistance against selective fading and interference.

Some of the disadvantages of OFDM are:

- Sensitivity to frequency offset and phase noise;
- Having high Peak to Average Power Ratio (PAPR).

2.10 Challenges in the OFDM wireless systems

The OFDM systems are very sensitive to the frequency offset because it can cause the Inter Carrier Interference (ICI). This can lead to the frequency mismatched in transmitter and receiver oscillator. Timing and frequency offsets are the origin of the interference of sub-channels with each other. Since OFDM wireless systems are very sensitive to the CFO, it can severely degrade the performance of the OFDM wireless systems. Therefore it has been recognized as one of the most major drawbacks in OFDM wireless systems. On the other hand, OFDM consists of multiple sinusoids summed together which it can create a huge Peak-to-Average Power Ratio (PAPR). High PAPR has been named as the other drawback of the OFDM modulation format. In RF systems, the major problem resides in the power amplifiers (PA) at the transmitter end, where the

amplifier gain will saturate at high input power. High PAPR is not a trivial issue for OFDM systems because it decreases the efficiency of the power amplifier (PA). Low efficiency of the power amplifier is a problem, especially in small mobile devices on the uplink [13].

In short, two important issues for OFDM challenges are:

1. Carrier Frequency Offset (CFO);
2. Peak-to-Average Power Ratio (PAPR).

2.11 Path losses and fading in OFDM systems

The first obvious difference between the wired and wireless channel is the amount of transmitted power that actually reaches the receiver. Path loss can be caused by many different effects, such as free space loss, refraction, diffraction, environment, weather condition, and the distance between transmitter and receiver.

In wireless communication, due to the mobility of the user, the transmission medium can vary with time. At times, the variation of the transmission medium can be huge. On the other hand, the signal that the receiver gets from the transmitter can come via a number of different propagation paths. This phenomenon can cause fading.

The model for predicting the signal strength that a receiver receives is usually based on the Free Space Propagation (FSP) model. In this model, there is no attenuation between the signal that the transmitter sends and the signal that the receiver receives, and there in no obstacle between them. This means the sending and receiving is based on the Line Of Sight (LOS).

In a real environment, the Radio Frequency waves (RF) are basically affected by three different phenomena: reflection, scattering and diffraction. Fading is another phenomenon that causes the change of the amplitude of the signal over time and frequency. There are two kinds of Fading: shadow fading and multipath induced fading. Shadow fading is produced by an obstacle that affects the propagation of the RF wave and the multipath induced fading. As is obvious from its name, it is created by the multipath propagation. Fading phenomena, unlike the additive noise, is considered as a non-additive degradation. The following figures 2.6 (a), 2.6 (b) and 2.6 (c) illustrate the transmission and receiving of the OFDM signal without considering the effect of noise, path loss and fading.

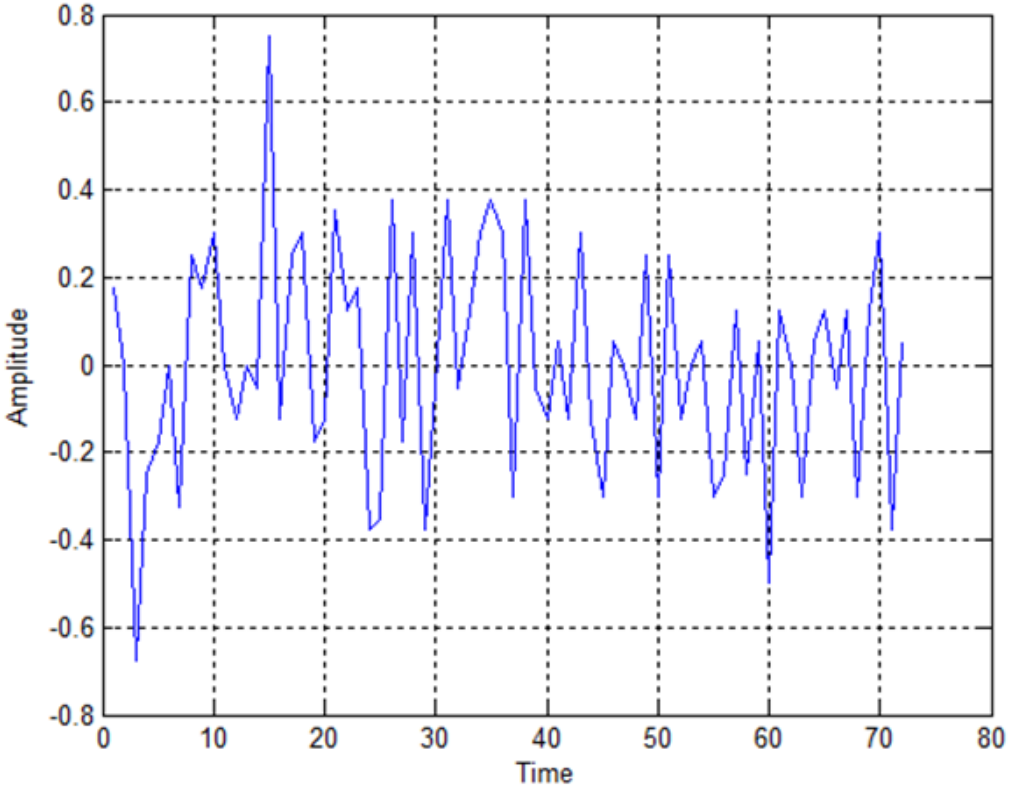

Figure 2.6 (a) OFDM Signal

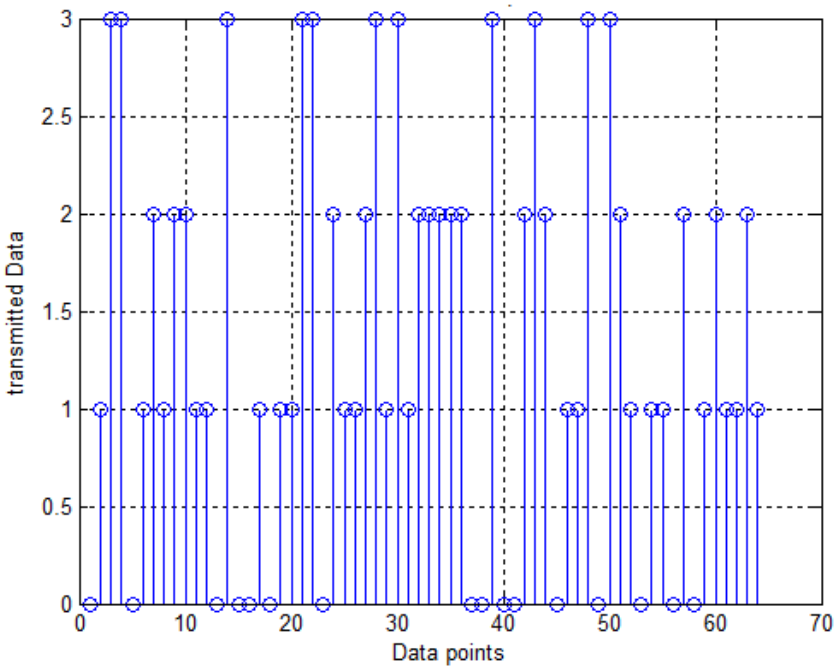

Figure 2.6 (b) Transmitted Data

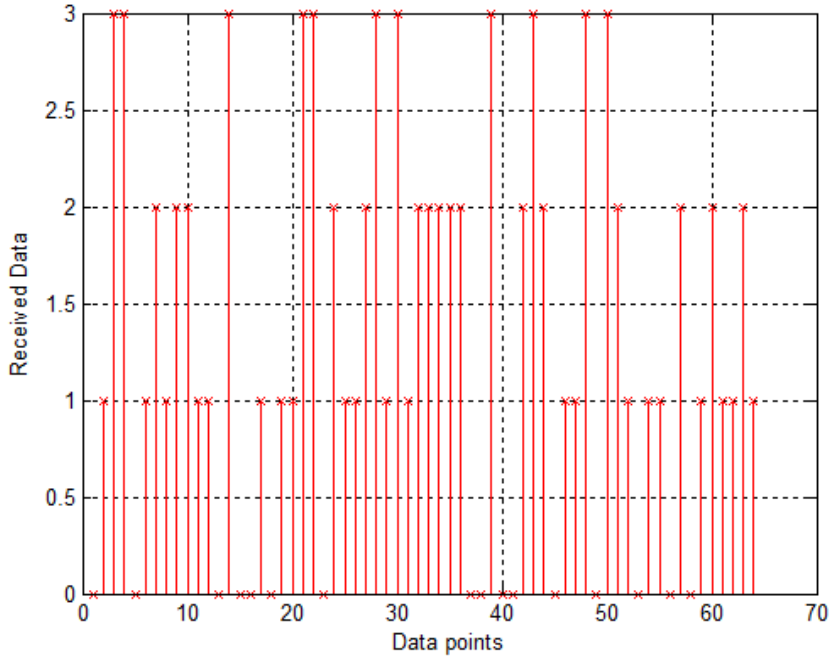

Figure 2.6 (c) Received Data

The table 2.1 shows the path loss exponent.

Environment	Path loss exponent
Free space 2	2
Urban area cellular radio	2.7–3.5
Shadowed urban cellular radio	3–5
In building line-of-sight	1.6–1.8
Obstructed in building	4–6
Obstructed in factories	2–3

Table 2.1 Path Loss Exponent [14]

So many factors can have effect on the total received power. These factors can assign the allowable transmit power. In this part we will study these factors in details, and we will show how these factors should be modeled simply based on the path loss and the distance between the transmitter and receiver.

2.12 Choice of OFDM parameters

The most important parameters that should be considered in any OFDM design are guard time, symbol duration, the number of the subcarriers, subcarrier spacing, and type of the modulation. However, what dictates and assigns the selection of the parameters are the system requirements. Some of the common system requirements are desired bit rate, available bandwidth (BW), Doppler values and acceptable delay spread. It is necessary to mention that some of these requirements can conflict with each other. For example, if we want to have a good delay spread tolerance, we should select a huge

number of the subcarrier with the slight subcarrier spacing. But for a good tolerance against the phase noise, the opposite is true. Therefore, there are different parameters for OFDM systems, and selecting always leads to a tradeoff between them. Basically the three main ones that should be considered are bit rate, bandwidth (BW), and delay spread. Since the guard time must be two to four times the Root Mean Squared of the Delay Spread (RMSDS) among the mentioned parameters, the delay spread is the one that assigns the guard time. This value is related to the type of coding and modulation. It is noteworthy that the higher order of the QAM (i.e. 64-QAM) compared with QPSK has a higher degree of sensitivity to the ICI and ISI. The other prerequisite which has a direct impact on the selection of the parameters is the desired integer number of samples within the FFT/IFFT interval and the symbol interval. The accepted OFDM time related and rate related parameters in IEEE 802.11 are respectively listed in tables 2.2 and 2.3.

Parameters	Values
Number of data sub-carriers	48
Number of pilot sub-carriers	4
Total number of sub-carriers	52
Sub-carrier frequency spacing	0.3125 MHz
IFFT/FFT period	3.2μs $(1/\Delta_F)$
Preamble duration	16μs
Signal duration BPSK-OFDM symbol	4μs $(T_{GI}+T_{FFT})$
Guard Interval (GI) duration	0.8μs $(T_{FFT}/4)$
Training symbol GI duration	1.6μs $(T_{FFT}/2)$
Symbol interval	4μs $(T_{GI}+T_{FFT})$
Short training sequence duration	8μs $(10T_{FFT}/4)$
Long training sequence duration	8μs $(T_{GI}+T_{FFT})$

Table 2.2: The timing related parameters for the OFDM systems [15]

Modulation	Coding rate (R)	Coded bits per subcarrier (N_{BPSC})	Coded bits per OFDM symbol (N_{CBPS})	Data bits per OFDM symbol (N_{DBPS})	Data rate (Mb/s) (20 MHz channel spacing)	Data rate (Mb/s) (10 MHz channel spacing)	Data rate (Mb/s) (5 MHz channel spacing
BPSK	1/2	1	48	24	6	3	1.5
BPSK	3/4	1	48	36	9	4.5	2.25
QPSK	1/2	2	96	48	12	6	3
QPSK	3/4	2	96	72	18	9	4.5
16-QAM	1/2	4	192	96	24	12	6
16-QAM	3/4	4	192	144	36	18	9
64-QAM	1/2	6	288	192	48	24	12
64-QAM	3/4	6	288	216	54	27	13.5

Table 2.3: The rate dependent parameters for the OFDM systems [15]

As you see in table 2.3 the data rate has different values. These values vary according to the type of the modulation. For OFDM-AWGN (OFDM-Additive White Gaussian Noise), the performance of the data rate comparison for the different schemes in IEEE 802.11 is illustrated in figure 2.7. The theoretical values can be calculated as follows:

$$\frac{E_b}{N_0} = \frac{W}{R}\frac{N_g}{N_s}10^{\frac{SNR}{10}} \tag{2.6}$$

$$BER = \frac{1}{2}er\ f_c(\sqrt{E_b/N_0} \tag{2.7}$$

Here w is signal bandwidth. (BW), N_s is symbol length, R is data rate and N_g is guard interval length. The data rate varies according to the type of the modulation and has a different value for BPSK, QPSK, 16QAM, and 64QAM.

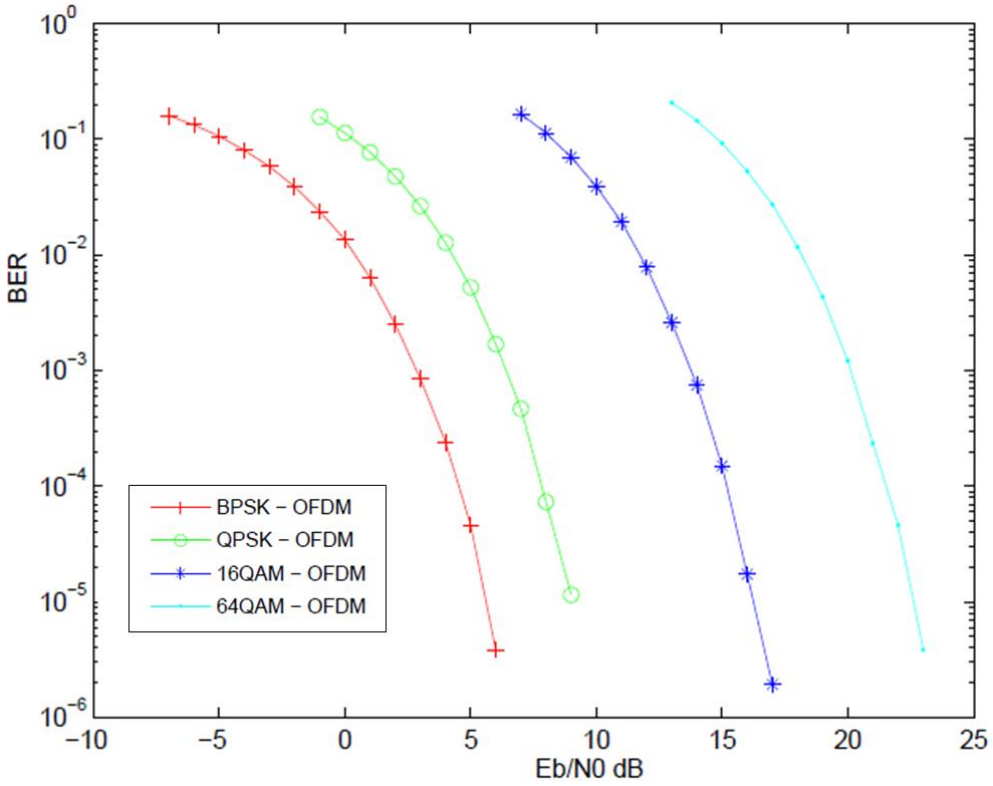

Figure 2.7 Data rates comparison

2.18 A typical schematic of an OFDM transceiver

Figure 2.8 shows a typical schematic diagram of an OFDM transceiver system. The IFFT unit modulates a block of input values to a number of subcarriers. On the receiver side, these subcarriers will be demodulated by the FFT unit which actually is the reverse operation of what is done in IFFT unit. Since these two operations are practically identical, the IFFT can be created by conjugating the input and output of an FFT and then dividing the output by the FFT size.

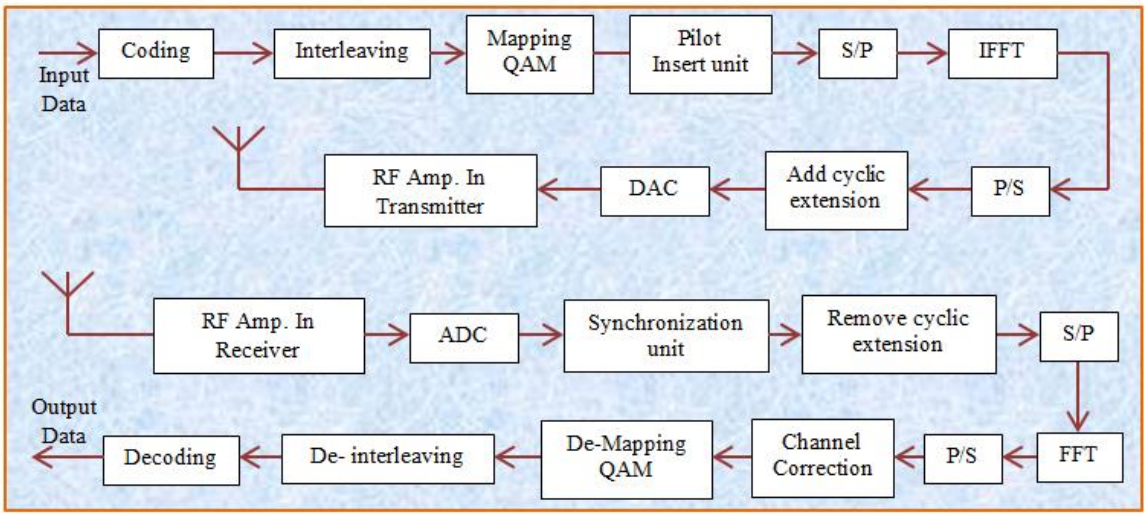

Figure 2.8 A typical schematic diagram of an OFDM transceiver system

2.19 Proprietary OFDM Flavors

At the end of this brief discussion about OFDM, it is worth mentioning that there are four variants of OFDM. These four variants are:

1. Vector OFDM (VOFDM)
2. Wideband OFDM (WOFDM)
3. Adaptive OFDM (AOFDM)
4. Flash OFDM

It is necessary to be mentioned that with regard to the simulation requirements and the comparison of the different algorithms or methods and suggested algorithm and method, the components of each block might be changed or modified related to the discussed model in the related section.

Chapter 3

Carrier Frequency Offset (CFO)

3.1 Introduction

The orthogonality of the OFDM relies on the condition that the transmitter and receiver operate with exactly the same frequency reference. If this is not the case, the perfect orthogonality of the subcarrier will be lost, which can result to subcarrier leakage. This phenomenon is also known as the Inter Carrier Interference (ICI) [16]. In other words, the OFDM systems are sensitive to the frequency synchronization errors in the form of CFO. CFO can lead to the Inter Carrier Interference (ICI). Therefore, CFO plays a key role in frequency synchronization. Basically to get a good performance of OFDM, the CFO should be estimated and compensated.

Lack of the synchronization of the local oscillator signal (L.OSC), for down conversion in the receiver with the carrier signal contained in the received signal, causes Carrier Frequency Offset (CFO) which can create the following factors:

(i) Frequency mismatched in the transmitter and the receiver oscillator;

(ii) Inter Carrier Interference (ICI);

(iii) Doppler Effect (DE).

3.2 Effects of frequency offset on OFDM signals

When CFO happens, it causes the receiver signal to be shifted in frequency (δf). This is illustrated in the figure 3.1. If the frequency error is an integer multiple *I* of subcarrier spacing δf, then the received frequency domain subcarriers are shifted by $\delta f \times I$ [17].

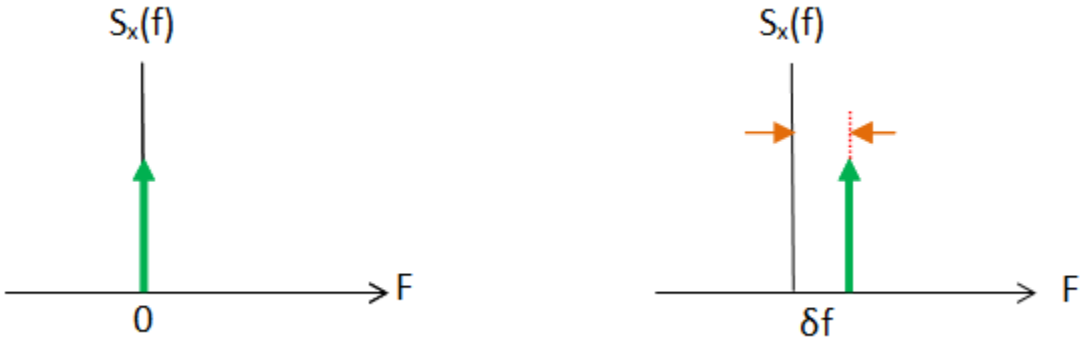

Figure 3.1 Illustration of frequency offset (δf)

On the other hand, as we know the subcarriers (SCs) will sample at their peak, and this can only occur when there is no frequency offset. However, if there is any frequency offset, the sampling will be done at the offset point which is not the peak point. This causes a reduction of the amplitude of the anticipated subcarriers, which can result in the rise of the Inter Carrier Interference (ICI) from the adjacent subcarriers (SCs). Figure 3.2 [18] shows the impact of carrier frequency offset (CFO). It is necessary to mention that although it is true that the frequency errors typically arise from a mismatch between the reference frequencies of the transmitter and the receiver local oscillators, this difference is avoidable due to the tolerance that electronics elements have.

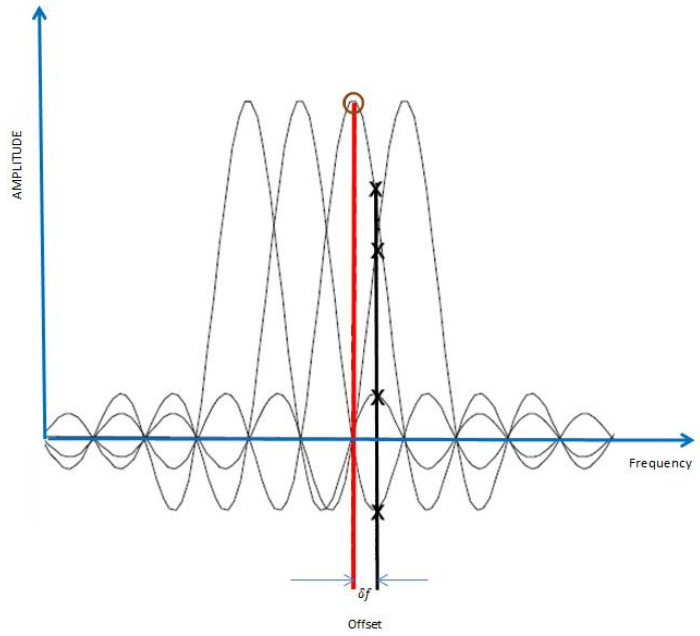

Figure 3.2 Frequency offset (δf)

Therefore, there is always a difference between the carrier frequencies that is generated in the receiver with the one that is generated in transmitter; this difference is called frequency offset (f_{offset}) and is:

$$f_{offset} = f_c - f_c' \tag{3.1}$$

where f_c is the carrier frequency in the transmitter and f_c' is the carrier frequency in receiver.

3.3 Carrier Frequency Offset (CFO)

The OFDM systems are very sensitive to the carrier frequency offset (CFO) and timing. Therefore, before demodulating the OFDM signals at the receiver side, the receiver must be synchronized to the time frame and to the carrier frequency which has been transmitted. In order to help the synchronization, the signals that are transmitted

have the references parameters that are used in the receiver for synchronization. However, in order for the receiver to be synchronized with the transmitter, it needs to know two important factors:

(i) prior to the FFT process, where it should start sampling the incoming OFDM symbol from;

(ii) how to estimate and correct any carrier frequency offset (CFO).

After estimating the symbol boundaries in the receiver and detecting if the symbol is present, the next step is to estimate the frequency offset.

The block diagram of the OFDM transceiver system, including the modulation, digital-to-analog (D/A) converter, channel and noise, the analog-to-digital (A/D) converter, and the demodulation, is illustrated in figure 3.3 [19].

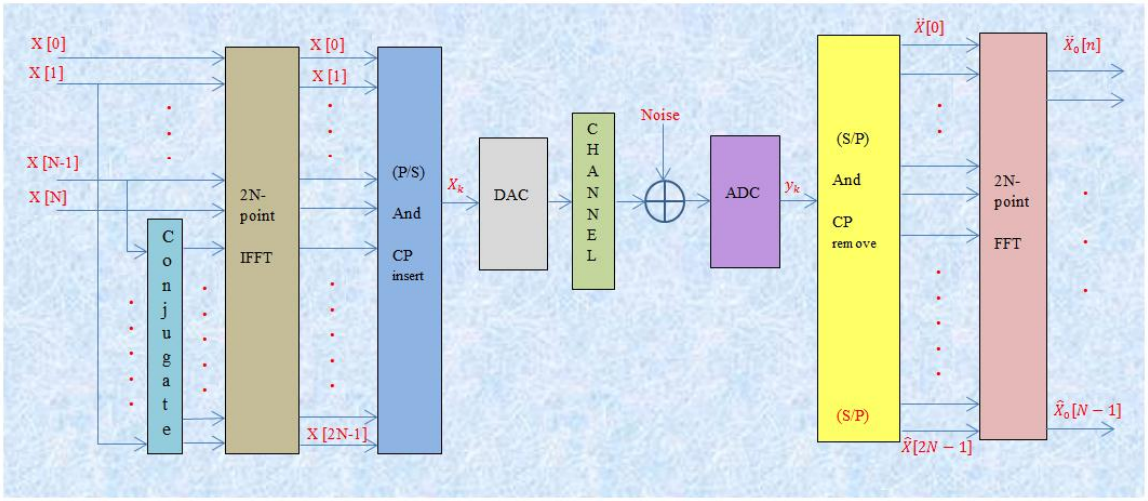

Figure 3.3 Block diagram of the OFDM transceiver system

A received signal without carrier frequency offset can be considered as follows:

$$r[n] = H[n]X(n) + \omega[n] \quad where \quad 0 \le n \le N-1 \tag{3.2}$$

Eq. 3.2 can be considered if and only if the effect of CFO is ignored. In the presence of the CFO the received signal can be stated as [20]:

$$r[n] = H[n]X(n)\frac{\sin(\pi\varepsilon)}{Nsin(\frac{\pi\varepsilon}{N})}e^{\frac{j\pi\varepsilon(N-1)}{N}} + \tag{3.3}$$

$$\sum_{m=0,m\neq n}^{N-1} H[m]X(m)\frac{\sin[\pi(m-n+\varepsilon)]}{Nsin[\frac{\pi(m-n+\varepsilon)]}{N}]}e^{\frac{j\pi(m-n+\varepsilon)(N-1)}{N}} + \omega[n]$$

In Eq. 3.3, ε is the normalized frequency offset. Part two in Eq. 3.3 is the result of the effect of ICI due to the presence of the frequency offset. As can be observed from Eq. 3.3, the CFO causes the amplitude of the signal to be degraded by the following factor:

$$\frac{\sin(\pi\epsilon)}{Nsin(\frac{\pi\epsilon}{N})} \tag{3.4}$$

According to Eq. 3.3, the shift that the received signal experiences is equal to:

$$\theta = e^{j\pi\varepsilon(N-1)/N} \tag{3.5}$$

As we know, the normalized (ε) CFO has two parts: integer part (ε_i), and fractional par (ε_f). Therefore, it can be stated as:

$$\varepsilon = \varepsilon_i + \varepsilon_f \tag{3.6}$$

The integer part leads to the cyclic shift in the received signal, but the fractional part has the effect of phase distortion and amplitude of the received signal. Figure 3.4

[19] illustrates a typical block diagram of the OFDM system with the fractional frequency offset estimation, and integer frequency offset estimation for estimating and compensating for the effect of CFO in the receiver.

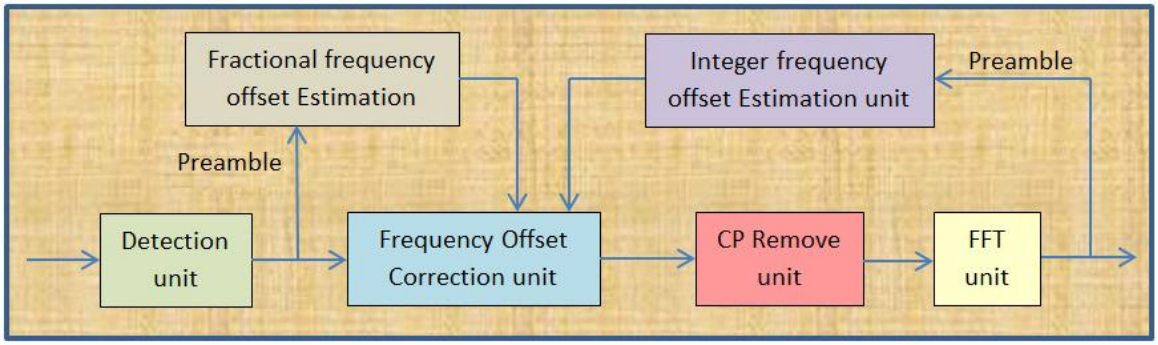

Figure 3.4 Structure of an OFDM system with the required units for estimating and compensating CFO

Figure 3.5 [18], shows the block diagram of the OFDM wireless transceiver system, and the output of the FFT at the receiver. In figure 3.5, y[k] is as follows [21]:

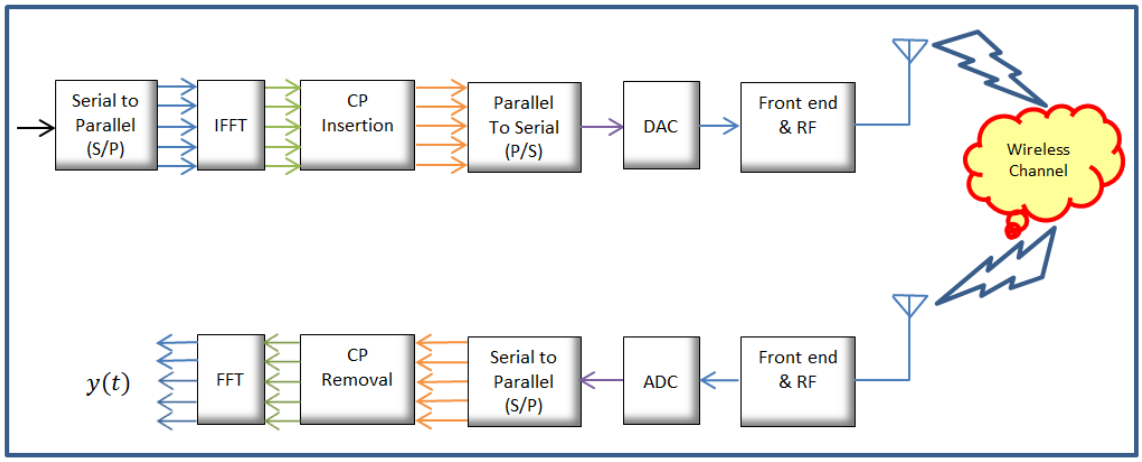

Figure 3.5 Block diagram of the OFDM wireless transceiver system

$$[k] = \frac{1}{N}\sum_{m=0}^{N-1} s[m]H[m]\frac{sin(\pi(m-k+\Delta f))}{sin\left(\frac{\pi(m-k+\Delta f)}{N}\right)} * exp\left(j\left(\frac{N-1}{N}\right)(m-k+\Delta f)\right) \quad (3.7)$$

(3.8)

$$y[k] = \frac{1}{N}s[k]H[k]\left(\frac{\sin(\pi\Delta f)}{\sin\left(\pi\Delta f/_N\right)}\right)exp\left(\frac{j(N-1)\Delta f}{N}\right) + \frac{1}{N}\sum_{\substack{m=0 \\ m\neq k}}^{N-1} s[m]H[m]\left[\frac{\sin(\pi(m-k+\Delta f))}{sin\left(\frac{\pi(m-k+\Delta f)}{N}\right)}\ exp\left(j\left(\frac{N-1}{N}\right)(m-k+\Delta f)\right)\right]$$

For simplicity, set α equal to:

$$\alpha_{m-k} = \left[\frac{\sin(\pi(m-k+\Delta f))}{sin\left(\frac{\pi(m-k+\Delta f)}{N}\right)}\ exp\left(j\left(\frac{N-1}{N}\right)(m-k+\Delta f)\right)\right]$$

$if\ m = k \quad then$

$$\alpha_{m-k} = \alpha_0 = \left[\frac{\sin(\pi\Delta f)}{sin\left(\frac{\pi\Delta f)}{N}\right)}\ exp\left(j\left(\frac{N-1}{N}\right)(\Delta f)\right)\right] \quad (3.9)$$

Therefore

$$y[k] = \frac{1}{N}s[k]H[k]\left(\frac{\sin((\pi\Delta f)}{\sin\left(\pi\Delta f/_N\right)}\right)exp\left(\frac{j(N-1)\Delta f}{N}\right) + \frac{1}{N}\sum_{\substack{m=0 \\ m\neq k}}^{N-1} s[m]H[m]\alpha_0 \quad (3.10)$$

The result in Eq. 3.10 indicates, in the case of the existence of any frequency offset, the estimation of the output symbol depends on the input values.

On the other hand, if there is no frequency offset, i.e. $\Delta f = 0$, then the received signal is:

$$if \quad \Delta f = 0 \qquad \rightarrow \qquad y[k] = \frac{1}{N} s[k] H[k] \tag{3.11}$$

Due to the frequency mismatch, the performance of an OFDM system can be reduced. This loss of performance can be compensated by estimating the frequency offset on the receiver side. Figure 3.6 [18] shows an OFDM Receiver with frequency synchronization.

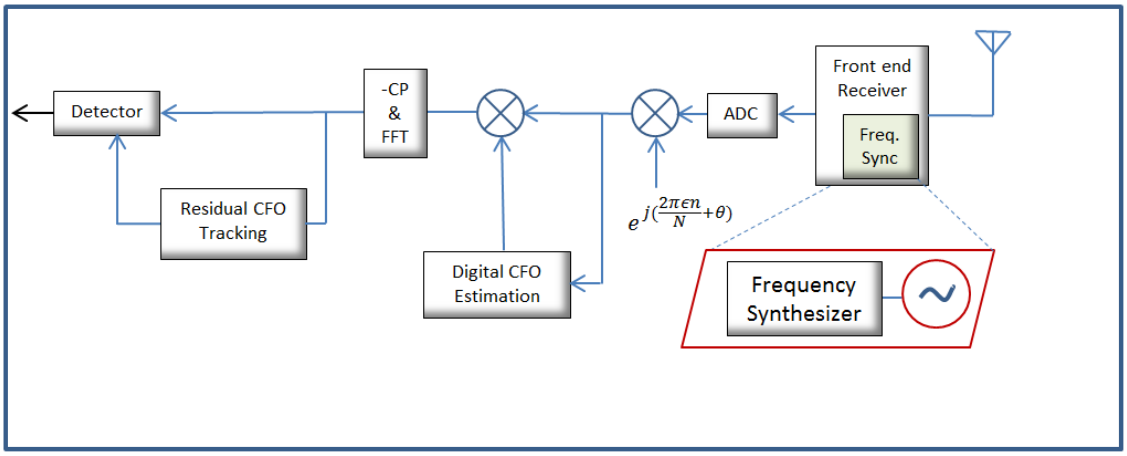

Figure 3.6 OFDM receiver with frequency synchronization

Table 3.1 [18] is a cliff notes for the effect of CFO on a transmitted signal in time domain and frequency domain.

	Received signal	Effect of CFO on received signal
Time domain	$y[n]$	$e^{j2\pi\varepsilon/n}x[n]$
Frequency domain	$Y[k]$	$X[k-\varepsilon]$

Table 3.1 Effect of the CFO on transmitted signal

3.4 Sources of frequency offset

A few sources can cause frequency offset, such as frequency drifts in transmitter and receiver oscillators, Doppler shift, radio propagation, and the tolerance that electronics elements have in local oscillators in the transmitter and the receiver. When there is a relative motion between transmitter and receiver, the Doppler can happen [22]. It is worth mentioning that the radio propagation talks about the behavior of radio waves when they are broadcasted from transmitter to receiver. In terms of propagation, the radio waves are generally affected by three phenomena which are diffraction, scattering and reflection.

3.5 Doppler Effect

The Doppler Effect (DE) is defined as follows:

$$f_d = \frac{v.f_c}{c} \tag{3.12}$$

Here f_d is Doppler Frequency, c is the speed of light, and v is the velocity of the moving receiver. The normalized CFO can be stated as:

$$\varepsilon = \frac{\mathrm{f_{offset}}}{\Delta \mathrm{f}} \tag{3.13}$$

Where Δf is the subcarrier spacing, ε has two parts, one integer (ε_i) and one fractional (ε_f). So we have:

$$\varepsilon = \varepsilon_i + \varepsilon_f \tag{3.14}$$

where $\varepsilon_i = \lfloor \varepsilon \rfloor$

3.6 The effect of integer and fractional part of CFO

As previously mentioned, the normalized CFO has made of two parts: integer part (ε_i), and fractional part (ε_f). The integer part causes the received signal to the receiver to experience a cyclic shift. The effect of the fractional part is as follows. The received signal in time domain can be considered [23]:

$$Y_l[k] = \sum_{n=0}^{N-1} y_l[n] e^{-j2\pi kn/N} = H_l[k]X_l[k] + Z_l[k] \tag{3.15}$$

Here, $Y_l[k]$, $H_l[k]$, $X_l[k]$and $Z_l[k]$ represent the received symbol, channel frequency response, transmitted symbol, and the noise in the frequency domain for the k^{th} subcarrier.

$$IDFT\{Y_l[k]\} = y_l[n] = \frac{1}{N}\sum_{k=0}^{N-1} H[k]X_l[k]e^{2j\pi(k+\varepsilon)(n+\delta)/N} + Z_l[n] \tag{3.16}$$

Here, $Z_l[n] = IDFT\ \{Z_l[k]\}$.

To see the effect of the CFO, we discard the phase noise and merely consider the CFO [24]. Therefore, Eq. 3.16 can be written as:

$$y_l[n] = \frac{1}{N}\sum_{k=0}^{N-1} H[k]X_l[k]e^{2j\pi(k+\varepsilon)/N} + Z_l[n] \tag{3.17}$$

The FFT of Eq. 3.17 yields [23]:

$$y_l[k] = FFT\{y_l(n)\} \tag{3.18}$$

$$y_l[k] = \frac{sin\pi\varepsilon_f}{Nsin(\pi\varepsilon_f/N)}\, e^{j\pi\varepsilon_f(N-1))/N} H_l[k]X_l[k] + I_l[k] + Z_l[k] \tag{3.19}$$

The first part of Eq. 3.19 shows the effect of the fractional part of the CFO. Figures 3.7 and 3.8 [25] show its effect. However, as expected, by growing the fractional part of the CFO, the effect increases on phase distortion and amplitude. This can be seen in figures 3.7 and 3.8. In these figures the effect of noise and Symbol Time Offset (STO) are not reflected at all.

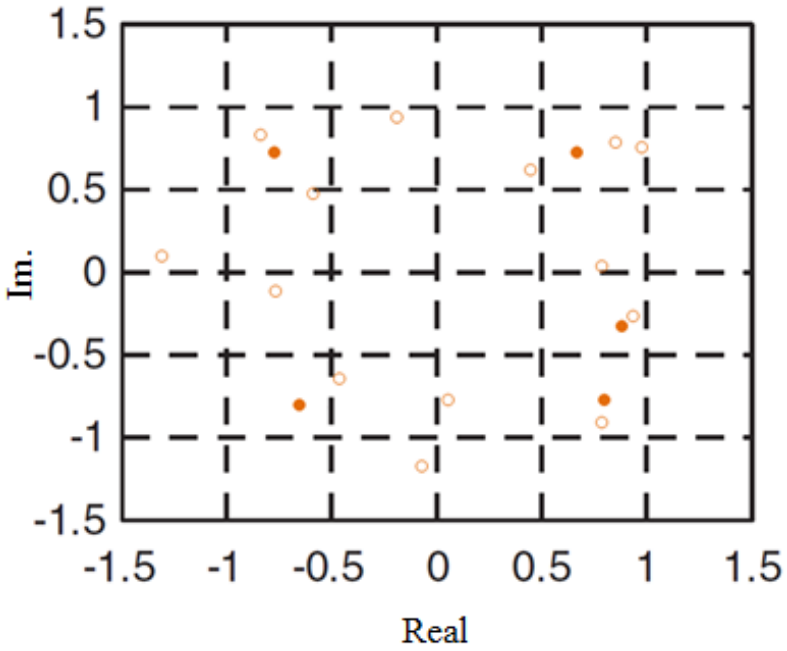

Figure 3.7 Effect of CFO when $\varepsilon = 0.4$

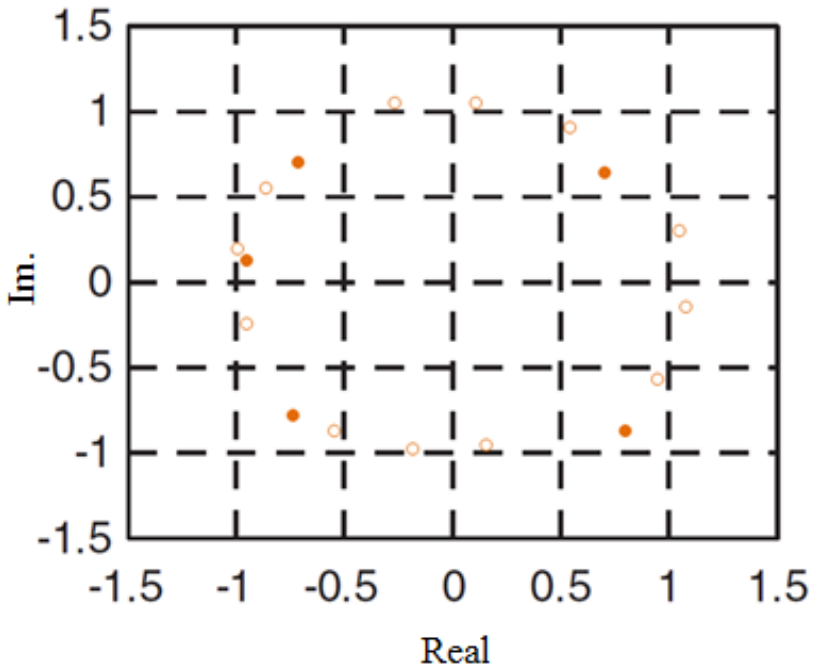

Figure 3.8 Effect of CFO when $\varepsilon = 0.06$

3.7 Effect of CFO on phase shift

To see the effect of CFO on phase shift, we consider there is no phase noise. Therefore, the time domain received signal considering Eq. 3.17 can be considered as follows:

$$y_l[n] = \frac{1}{N}\sum_{k=0}^{N-1} H[k]X_l[k]e^{2j\pi(k+\varepsilon)n/N} + Z_l[n] \tag{3.20}$$

Figure 3.9 [25] illustrates the effect of CFO on the phase in the time domain and Figure 3.10 [25] presents the phase change between them. Here we consider that the system is not exposed to any noise. The solid line in Figure 3.9 shows when there is no CFO (i.e. perfect case), and dash lines show when the amount of the CFO in the system is equal to 1.4.

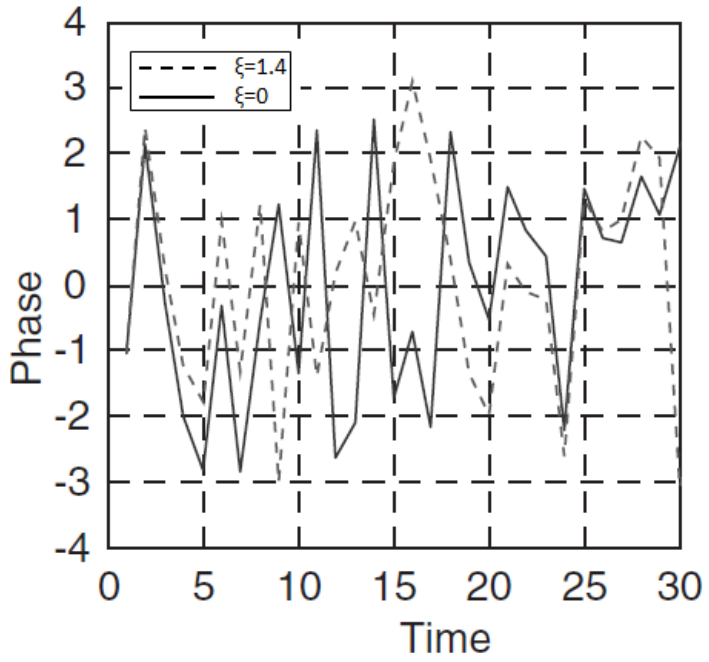

Figure 3.9 Effect of CFO (ξ) on phase in the time domain

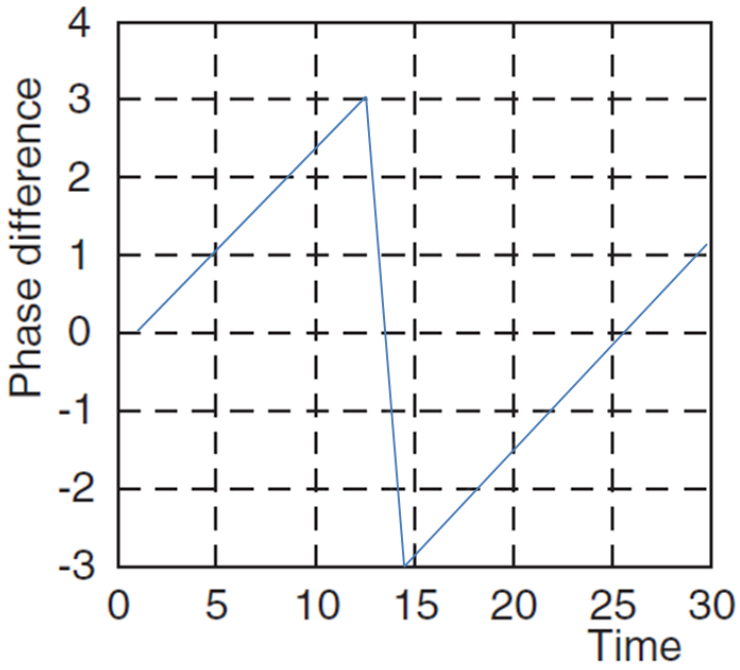

Figure 3.10 Effect of CFO (ξ) on phase difference

3.8 Effect of CFO on degradation of OFDM systems

The complex transmitted OFDM signal in a period T at the frequency m/T can be stated as [26]:

$$s(t) = \left(\sum_{m=0}^{N-1} a_m e^{\frac{j2\pi mt}{T}}\right) e^{j\theta(t)} \tag{3.21}$$

in which a_m is data symbol and the term $\theta(t)$ represents the time varying phase due to the carrier frequency offset between the transmitter and receiver.

With a reasonable approximation, the degradation in terms of dB is defined as [26]:

$$D \cong \frac{10}{Ln\ 10}\left(\left(1 - {E_0}^2\right) + V_0 \frac{E_s}{N_0}\right) \tag{3.22}$$

in which the signal to noise ratio (SNR) is: E_s/N_0, V_0 is the variance for others noises, and ${E_0}^2$ is the power of the component.

In case of the presence of frequency offset (Δf) between the transmitter and receiver, the $\theta(t)$ in Eq. 3.21 is defined as:

$$\theta(t) = 2\pi\Delta f t + \theta_0 \tag{3.23}$$

Therefore, the degradation (D) for OFDM is defined as [26]:

$$D \cong \frac{10}{3Ln\ 10}\left(\pi N \frac{\Delta f}{R}\right)^2 \frac{E_s}{N_0} \tag{3.24}$$

From Eq. (7) it can be observed that the degradation for an OFDM is proportional with the square root of the frequency offset and it is also proportional with E_s/N_0. In

other words, OFDM is very sensitive to frequency offset and frequency offset can cause severe degradation in OFDM systems.

Figure 3.11 [19] illustrates the SNR degradation as a function of the frequency offset to the subcarrier spacing. For this illustration, the values for E_s/N_0 will be 18 and 16 db. However, the maximum acceptable frequency offset can only happen when the frequency offset is less than one percent of the subcarrier space. As a result, for overcoming the mentioned problem, the frequency synchronization must be used before the FFT.

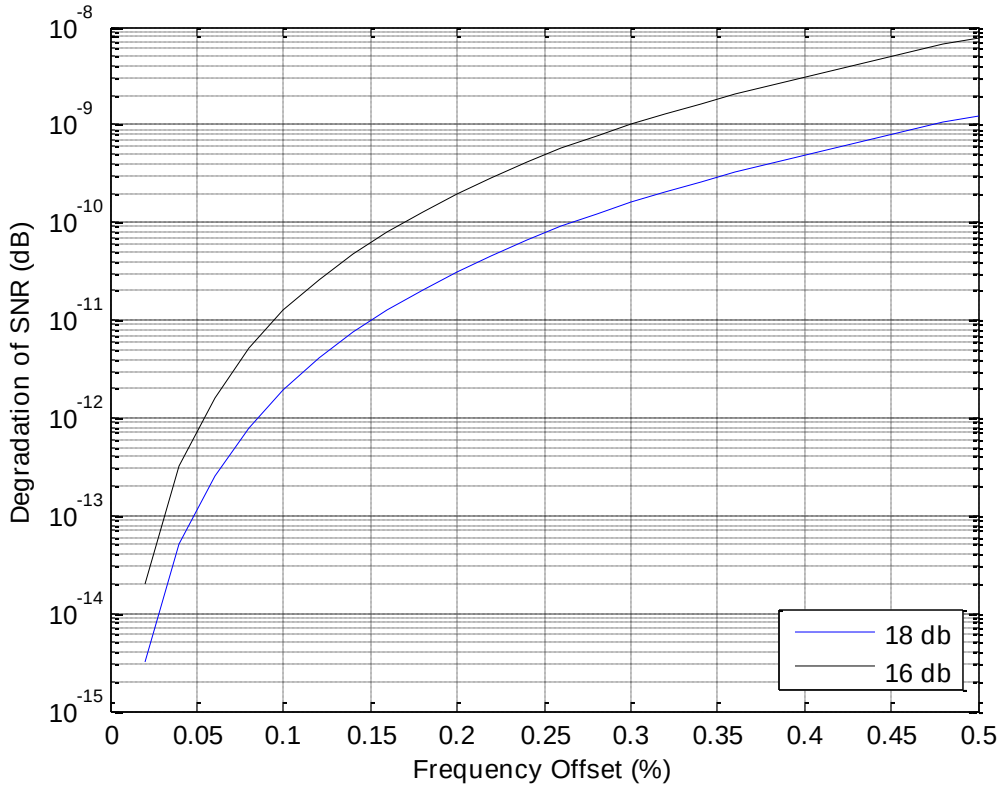

Figure 3.11 SNR degradation as a function of the frequency offset

3.9 The effect of CFO, phase noise, and Rayleigh fading

As previously mentioned, two key parameters that should be considered in designing any OFDM communication system are CFO and phase noise. In this part we show the effect of CFO, phase noise, and Rayleigh fading on the performance of the OFDM wireless systems.

The effect of CFO with the phase noise, Rayleigh fading and time jitter on the performance of the OFDM wireless systems can be stated as follows [27,28]:

$$SINR(\varepsilon, \sigma_u^2, \xi, \alpha) \geq \tag{3.25}$$

$$\frac{\gamma_{in}\alpha^2(1-\xi)\{sinc^2(\pi)\}}{1+\gamma_{in}\alpha^2(1-\xi)[0.5947sinc^2(\pi)+\{\frac{\sigma_u^2}{2N}sinc^2(\pi)\sum_{r=1}^{N-1}\frac{1}{sin^2\left(\frac{\pi\varepsilon r}{N}\right)}\}]+\gamma_{in}\alpha^2\xi}$$

$$|\varepsilon| \leq 0.5\,, \quad |\xi| \leq 1$$

where:

ε Normalized CFO

γ_{in} Input SNR (Signal-to-Noise-Ratio)

ξ Time jitter

σ_u^2 Variance of the noise phase

α Rayleigh fading

N Number of subcarriers

In the case of the absence of time jitter and assuming a nonfading environment (i.e. α=1), Eq. 3.25 will be as follows:

$$SINR(\varepsilon,\sigma_u^2) \geq \frac{\gamma \sin\{sinc^2(\pi)\}}{1+\gamma_{in}[0.594(sin\pi)^2+\{\frac{\sigma_u^2}{2N}sinc^2(\pi)\sum_{r=1}^{N-1}\frac{1}{sin^2(\frac{\pi\varepsilon r}{N})}\}]}$$

$$|\varepsilon| \leq 0.5 \tag{3.26}$$

Figures 3.25 and 3.13 illustrate the effect of SINR VS the CFO, considering the different values of the SNR.

In figures 3.12 and 3.13 the variance of phase noise is respectively equal to 0.018 and 1.25. As can be seen in figures 3.12 and 3.13, by increasing the value of the variance of phase noise, the amount of SINR reduces. Figures 3.12 and 3.13 also display that the value of SINR will also be decreased by growing the SNR.

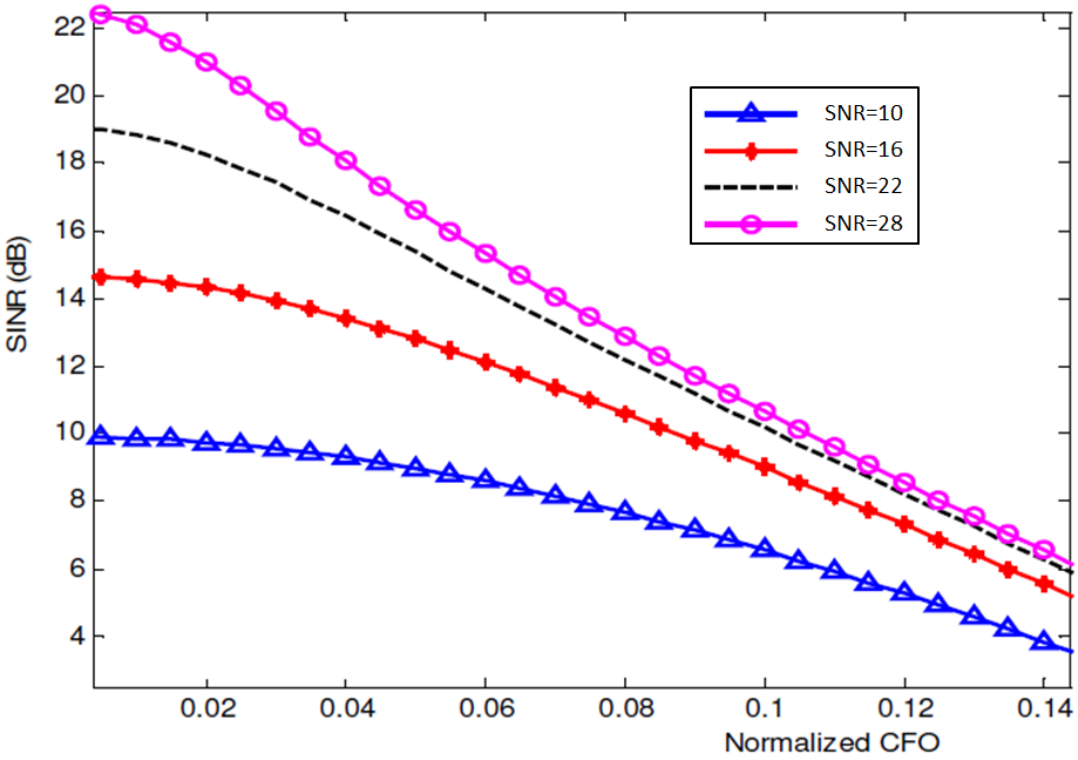

Figure 3.12 Signal-to-Interference-plus-Noise-Ratio (SINR)

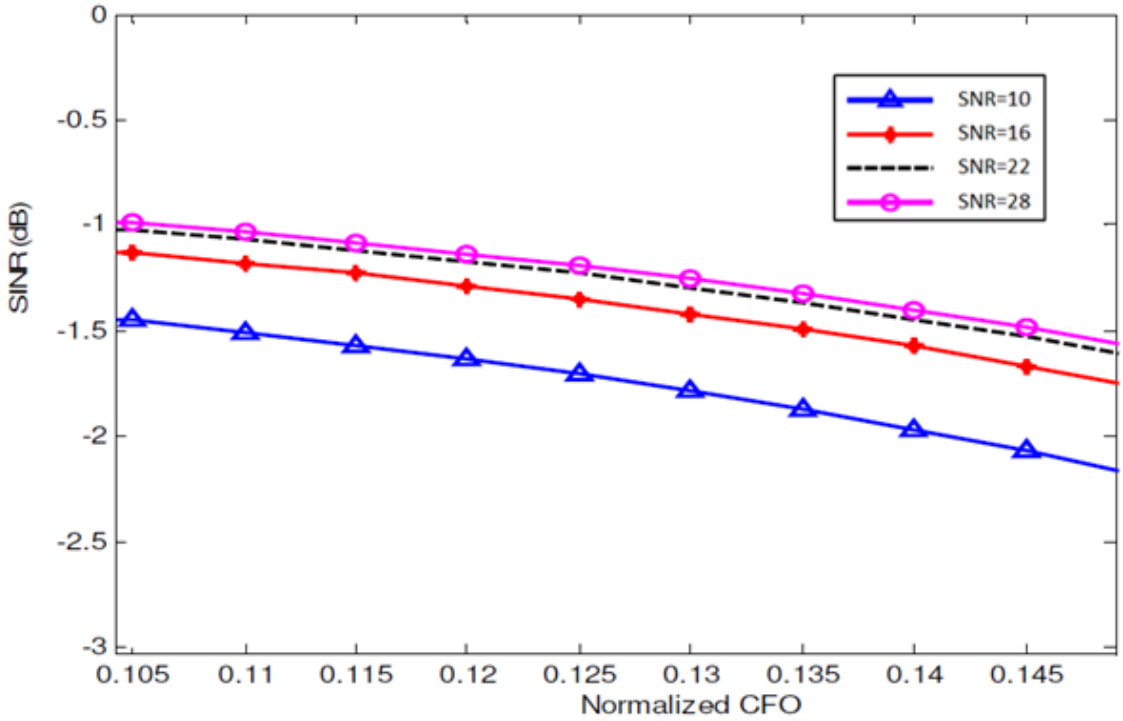

Figure 3.13 Signal-to-Interference-plus-Noise-Ratio (SINR)

3.10 The relation between frequency offset and SNR

The effect of CFO on Signal-to-Noise Ratio (SNR) in OFDM systems was studied by Pollet et al. [29]. The impact of the CFO on the degradation in terms of dB is given by [30]:

$$D_{freq} \cong \frac{10}{3ln10}(\pi \Delta f T)^2 \frac{E_b}{N_0} \tag{3.27}$$

$D_{freq}, T, E_b \; and \; N_0$ are frequency offset, symbol duration, energy per bit (for OFDM signal), and one sided noise power spectrum density (PSD).

The effect of frequency offset is similar to the effect of noise and it may cause degradation of the Signal-to-Noise Ratio (SNR) where SNR is:

$$SNR = \frac{E_b}{N_0} \tag{3.28}$$

Figure 3.14 [19] illustrates the impact of the sampling offset on the degradation of SNR. As Figure 3.14 shows, by increasing the number of subcarriers, the degradation of OFDM increases.

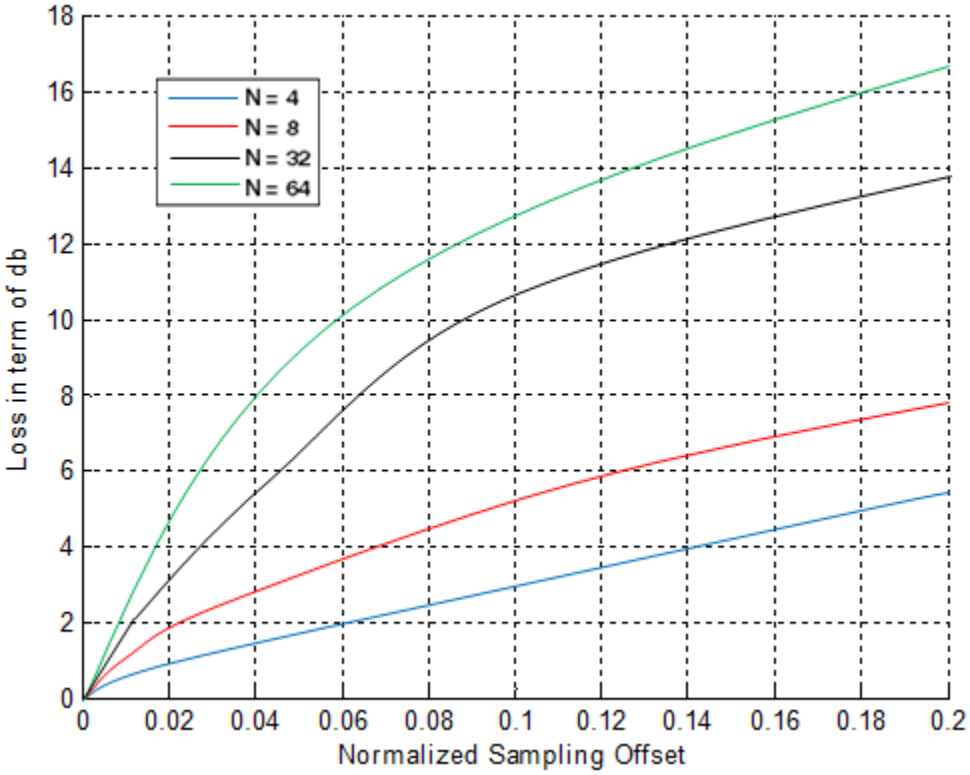

Figure 3.14 SNR degradation versus sampling offset

3.11 Frequency synchronization

The frequency synchronization for OFDM systems can be classified by two methods: data aided and non-data aided. While the data aided uses the pilot symbols for estimation, the non-data aided uses a Cyclic Prefix (CP) correction.

In wireless OFDM systems, synchronization is the most important issue. In order for the receiver to regenerate the signal that the transmitter sends, it must be synchronized in frequency, time, and phase with the transmitter. Since the mobile OFDM systems work

in a dynamic environment, this is not an easy case. However, in the OFDM wireless systems, two reasons that lead to frequency offset between the receiver and the transmitter are:

(i) sampling clock mismatch

(ii) misalignment

3.12 Sampling clock mismatch

The Analog-to-Digital (A/D) on the receiver side is responsible for determining the sampling time. A/D does not have always the exact sampling clock. This can cause a relative drift between the receiver's sampling in respect to the transmitter. This drift, called Sampling Clock Drift (SCD) (or sampling clock error), reduces the OFDM system performance. The SCE produces the rotation of subcarriers which leads to ICI and finally destroys the orthogonality between the subcarriers. Many researchers have discussed and evaluated the effect of SCD on OFDM wireless systems [31]. The normalized sampling error can be stated as follows:

$$t_\delta = \frac{T_{RX} - T_{TR}}{T} \tag{3.29}$$

where, T_{RX} is the received sampling period and T_{TR} is the transmit sampling period. The total effect can be shown as [32]:

$$R_{l,k} = exp\left[j2\pi k t_\delta l \frac{T_s}{T_u}\right] X_{l,k} \sin c(\pi k t_\delta) H_{l,k} + W_{l,k} + N_{t_\delta}(l,k) \tag{3.30}$$

Here $R_{l,k}$ is the received subcarrier, $l\ and\ k$ are OFDM symbol index and subcarrier index, $W_{l,k}$ is Additive White Gaussian Noise (AWGN), T_s is total symbol duration, T_u is useful sample duration, and $N_{t\delta}$ is additional interference because of the

sampling frequency offset. The degradation of OFDM systems, due to this effect, can be given by [33]:

$$D_n \approx 10\log_{10}\left[1+\frac{\pi^2}{3}\frac{E_s}{N_0}(kt_\delta)^2\right] \tag{3.31}$$

As it can be seen from Eq. 3.31, the degradation performance of OFDM wireless systems increase by the square power of the frequency offset.

3.13 The effect of STO on OFDM Synchronization

The effect of the STO depends to the estimated starting point of the OFDM symbol. Three main possibilities can be considered as follows: the estimated starting point of the OFDM symbols can occur at the exact timing point, before the exact timing point, and after the exact timing point. In the first situation, the OFDM symbols will be recovered and there will be no type of the interference. In the second situation, the orthogonality among the subcarrier will be well-preserved but a phase offset will be introduced which will be proportional to the STO. In the third situation, the signal will contain a portion of the current and a portion of the next OFDM symbol. Therefore, the received signal contains the ISI which is caused by the next symbol, and the orthogonality between the subcarriers will be destroyed. By taking the FFT of the signal which is the combination of the current and the next OFDM symbol we have:

$$Y_l(k) = \sum_{n=0}^{N-1-\delta} x_l(n+\delta)e^{-j2\pi k/N} + \sum_{n=N-\delta}^{N-1} x_l + (n+2\delta-N_g)e^{-j2\pi nk/N} \tag{3.32}$$

where δ and ε are the normalized STO and CFO.

After extending and simplifying Eq. 3.32, the following terms appears in it, which relates to the presence of the ICI and indicate the lack of orthogonality:

$$\sum_{p=0,p\neq k}^{N-1} x_l(p)\, e^{j2p\delta/N} \sum_{n=0}^{N-1-\delta} e^{\frac{j2\pi(p-k)n}{N}} \tag{3.33}$$

When the extreme delay of the multipath channel is longer than the length of the Cyclic Prefix (CP), the end portion of the OFDM symbol will affect the head portion of the following symbol. This effect appears as the Inter-Symbol Interference (ISI). The other factor that has effect on creating the ISI and ICI is the timing of the FFT window start point, even though the length of the CP will be enough long. Note that when the FFT window start point is later than the start of the symbol, both ISI and ICI will be occur.

3.14 The effect of ISI on OFDM systems

The signals that arrive to the receiver come from the different paths. Therefore, there is a time delay between the signals which can cause inter-symbol interference (ISI). ISI causes the degradation of performance in the reception of the receiver. Consider the output of the modulator unit in the transmitter as:

$$x(t) = \sum_{n=-\infty}^{\infty}\left[\sum_{k=0}^{N-1} d_{n,k}\emptyset_k(t - nT_d)\right] \tag{3.34}$$

Respectively $T_d, d_{n,k}, N$ are: symbol duration, data symbol and block size, and f_k is kth subcarrier frequency where $f_k = f_0 + \frac{k}{T_d} \quad and \quad k = 0,1,\dots,N-1$ and

$$\emptyset_k(t) = \begin{cases} e^{j2\pi f_k t} & t \in [0, T_d] \\ 0 & otherwise \end{cases} \tag{3.35}$$

Eq. 3.34 can be stated as follows:

$$x_n(t) = \sum_{k=0}^{N-1} d_{n,k} \emptyset_k (t - nT_d) \tag{3.36}$$

The transmitted signal can be stated as:

$$s(t) = \sum[\sum_{k=0}^{L-1} x_n(k) \delta(t - (nL + k)T_d)] \tag{3.37}$$

L is the data symbol length.

The received OFDM signal considering the AWGN and multipath condition can be presented as follows [34]:

$$r_n(k) = \sum_{i=0}^{L-1} x_n(i) h(k - i) + \sum_{i=0}^{L-1} x_{n-1}(i) h(k + L - i) + v_n(k) \tag{3.38}$$

If we consider Q=L-N and the length of the multipath channel (L_h) to be as long as the guard interval, Eq. 3.38 can be separated and stated in two time intervals as follows:

$$r_n(k) = \tag{3.39}$$

$$r_n(k) = \begin{cases} \sum_{i=0}^{L-1} x_n(i) h(k - i) + \sum_{i=0}^{L-1} x_{n-1}(i) h(k + L - i) + v_n(k) & 0 \le k0 \le Q - 1 \\ \sum_{i=0}^{L-1} x_n(i) h(k - i) + v_n(k) & Q \le k \le L - 1 \end{cases}$$

As it can be seen, the first interval has the ISI from the previous symbol and desired symbol, but the next interval merely has the wanted data symbol. However, the advantage of the OFDM wireless systems is their robustness against the multipath delay spread. Decreasing the effect of ISI can be accomplished by using the long symbol period.

3.15 Effect of CFO on creating ICI

As previously noted, the lack of orthogonality in the received signal to the OFDM receiver creates carrier frequency offset. CFO introduces the ICI in the system. However, Figure 3.15 [19] illustrates the ICI due to the frequency offset. Figure 3.15 was created for different values of frequency offset. As it can be seen from figure 3.15, increasing the frequency offsets the ICI increases.

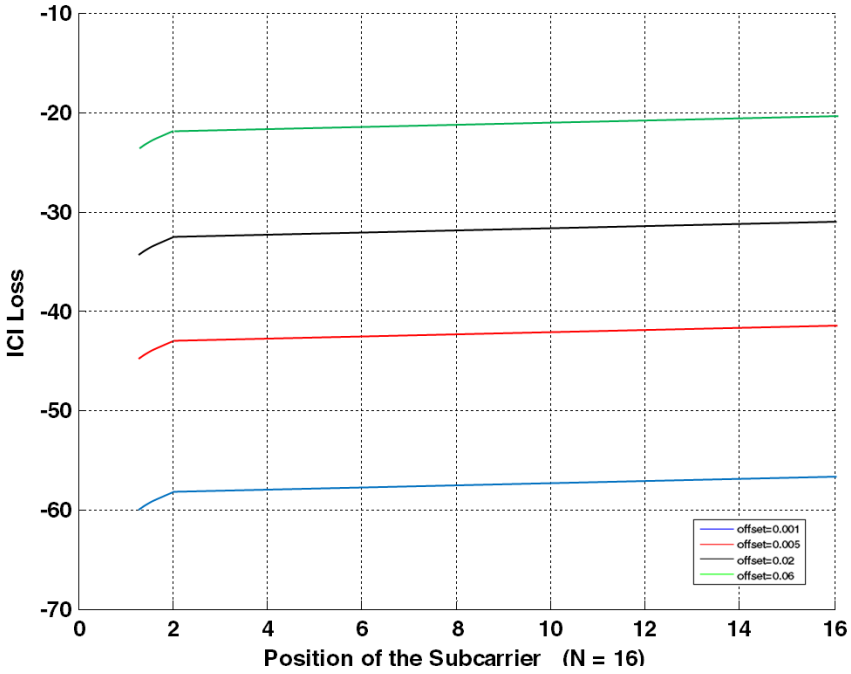

Figure 3.15 The overall ICI created by frequency offset

3.16 The effect of Symbol and Sample Timing Offset

When the data blocks in the input of the FFT in receiver are exactly matched with the ones from the transmitted IFFT block in transmitter, we can claim that we have achieved a perfect synchronization. There is two kind of synchronization: late synchronization, and early synchronization. If the synchronization tick comes after the

perfect synchronization point, it is called the late synchronization. This can destroy the orthogonality of the subcarrier and cause ICI. By getting the Cyclic Prefix (CP) enough long, we can eliminate the major effects of the early synchronization. It is worth mentioning that we must avoid the late synchronization in all the cases. However, the late synchronization can also cause a chunk of the channel response to fall out of the channel estimation window, which can create an additional noise. Therefore, consider an Additive White Gaussian Noise (AWGN) channel which the vector received signal can presented as:

$$y_m = \left[y_{p,m}, \dots, y_{N_c-1,m}, y_{0,m+1}, \dots, y_{p-1,m+1}\right] \tag{3.40}$$

After the demodulation via FFT unit, it is [35]:

(3.41)

$$\hat{X}_{k,m} = \frac{N_c - P}{N_c} X_{k,m} e^{j2\pi\left(\frac{K}{N_c}\right)P} + \frac{1}{N_c} \sum_{n=0}^{N_c-1-P} e^{-j2\pi(n/N_c)k} \sum_{i=N_d/2; i\neq k}^{N_d/2-1} e^{j2\pi(i/N_c)(n+p)}$$

$$+ \frac{1}{N_c} \sum_{n=N_c-p}^{N_c-1} e^{-j2\pi(n/N_c)k} \sum_{i=N_d/2}^{N_d/2-1} X_{i,m+1} e^{j2\pi(i/N_c)(n+p)} + n_{k,m}$$

As it is obvious from Eq. 3.41, the symbol timing offset can create three effects: ISI, ICI and phase rotation.

Carrier Frequency Offset Δf_c (CFO) and Sampling clock Frequency Offset (ScFO) cause the phase rotation in the received signals which can be stated as:

$$\theta(t) = 2\pi\left(1 + \left(\frac{T_s - T}{T}\right)\right).\Delta f_c t \tag{3.42}$$

T_s is actual sampling interval and T is perfect sampling interval. The effect of the phase rotation is:

(3.43)

$$y_{k,m} = \frac{1}{T}\left\{ X_{k,m} \int_0^T e^{j\theta(t)} dt + \sum_{i=0, i\neq k}^{N_c-1} X_{i,m} \int_0^T e^{-j2\pi(k-i/T)t} e^{j\theta(t)} dt \right\} + n_{k,m}$$

Considering Eq. 21, it is obvious that not only do the CFO and ScFO destroy the orthogonality between the subcarriers but they also create the OFDM subcarrier symbol rotation and OFDM symbol window drift.

Considering [36], the degradation of OFDM systems due to the ICI can be stated as follows:

$$D(db) \approx \frac{10}{3ln10}\left[\pi \frac{N_c \Delta f_c}{B}\right]^2 \frac{E_s}{N_0} \tag{3.44}$$

3.17 The effect of using DCR on CFO

Using Direct Conversion Receivers (DCR) is another case that causes CFO. Numerous investigators and researchers have studied the effects of the In-phase and Quadrature (I/Q) mismatch of the local oscillators (LOSC) in OFDM wireless systems [37, 38, 39]. They have revealed that an I/Q mismatch destroys the orthogonality of the subcarriers, which leads the OFDM systems to suffer from Inter Carrier Interference (ICI) and CFO. However, since Direct Conversion Receivers (DCR) are very cost effective with lower power consumption, they are getting more and more popular.

Although DCRs have some advantages, they bring a challenging issue which is called In-phase/Quadrature phase (I/Q) imbalance. This issue causes ICI at the received

signals to lead to CFO. It is well known that OFDM systems are sensitive to CFO, and many CFO and I/Q imbalance estimation and compensation methods and techniques have been proposed. Some of these techniques assume a perfect timing synchronization, which makes it very difficult to accomplish in practice. To show the impact of I/Q imbalance on the received signal, consider Figure 3.16 [19] which shows the block diagram of the DCR with I/Q and CFO compensation configuration.

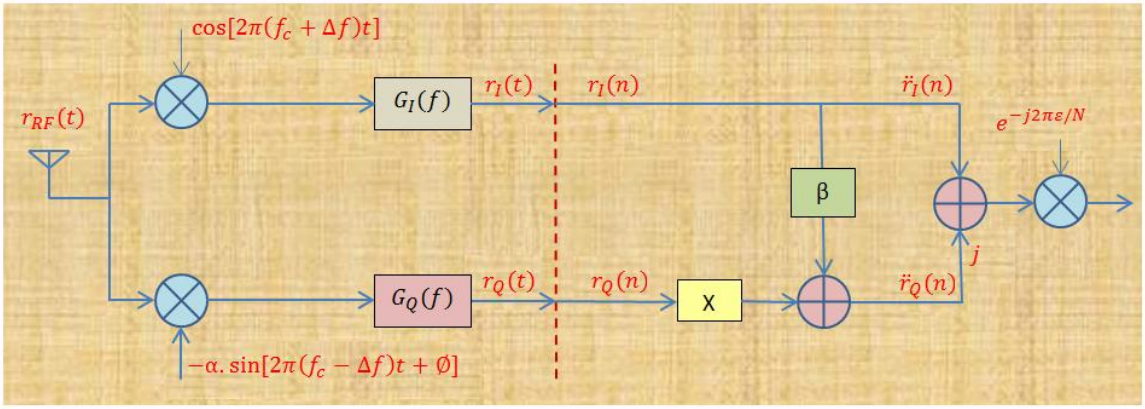

Figure 3.16 Block diagram of the DCR with I/Q and CFO compensation configuration

The received RF signals to the DCR receiver antenna can be stated as [40]:

$$rRF(t) = \mathcal{R}\{[s(t) \otimes h(t)].e^{j2\pi f_c t}\} \tag{3.45}$$

where $h(t)$, $s(t)$ and f_c in order are: baseband equivalent channel, baseband transmitted signal, and carrier frequency. According to the [40], [41] and [42], the down converted signal at the receiver side can be presented as:

$$r(t) = \left\{e^{j2\pi\Delta ft}.[s(t) \otimes h(t)] \otimes c_1(t) + \left\{e^{-j2\pi\Delta ft}.[s^*(t) \otimes h^*(t)]\right\} \otimes c_2(t) + w(t)\right\} \quad (3.46)$$

In Eq. 3.46, you can see the presence of the frequency offset (Δf) in the down converted signal at the receiver side, which needs to be estimated and compensated.

3.18 The effect of increasing the range of CFO estimation

The algorithms that use CP for estimating CFO can only estimate the CFO in a limited range. This limited range is:

$$-\frac{1}{2} \leq \varepsilon \leq \frac{1}{2} \quad (3.47)$$

To increase this limit, the distance between two blocks of samples for correction need to be decreased by using a training symbol. To increase the CFO estimation within a bigger range we can use Eq. 3.47 [43, 44].

$$\hat{\varepsilon} = \frac{D}{2\pi} arg\left\{\sum_{n=0}^{N/D-1} y_l^*[n] y_l[n + N/D]\right\} \quad (3.48)$$

where N/D is an integer. Here the range is:

$$-\frac{D}{2} \leq \varepsilon \leq \frac{D}{2} \quad (3.49)$$

The CFO estimation range by using Eq. 3.48 will be increased to $|\varepsilon| \leq D$. However this increase costs in the degradation of the MSE performance. Figure 3.17 [25] shows the effect of increasing the estimation range of CFO versus the MSE performance for D=1 (red graph) and D=4 (black graph).

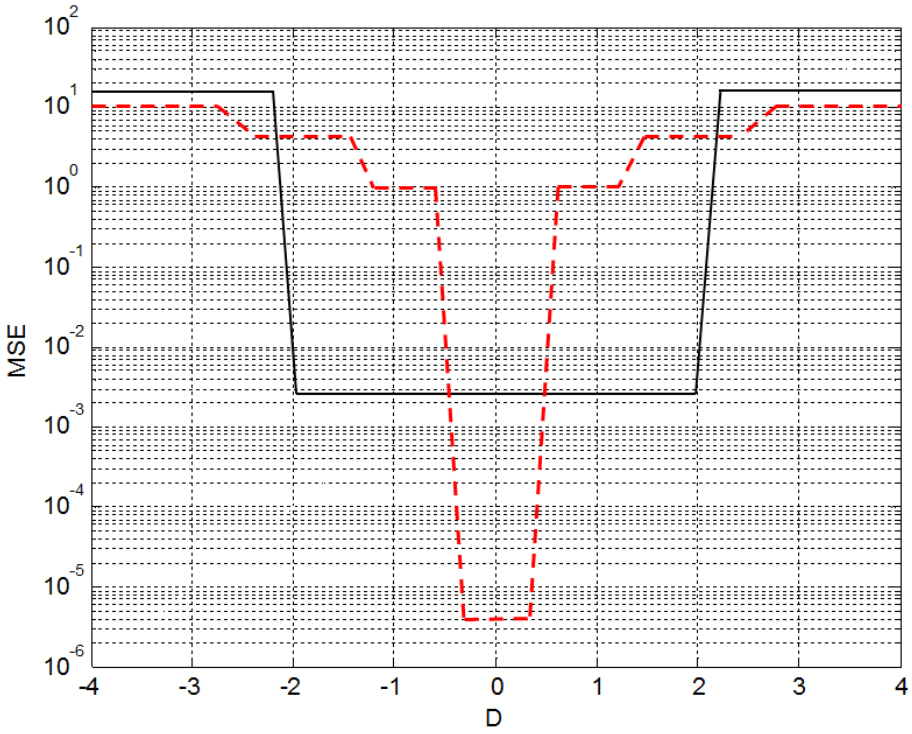

Figure 3.17 MSE versus D

3.19 Using Time domain equalizer (TDE) to combat the effect of ICI and ISI

As we know in the receiver side, the demodulation can be done by an FFT trailed by an equalizer, when the Cyclic Prefix (CP) is longer than the channel impulse response. On the other hand, a long cyclic prefix (CP) (or guard time) leads to a large amount of overhead in respect to the Transmission Data Rate (TDR). A typical remedy for decreasing the guard time(T_G), and combating with the effect of ICI and ISI, that creates the reduced channel response, is to use a Time Domain Equalizer (TDE) prior to the FFT demodulation. Figure 3.18 shows the block diagram of a TDE for a typical OFDM system.

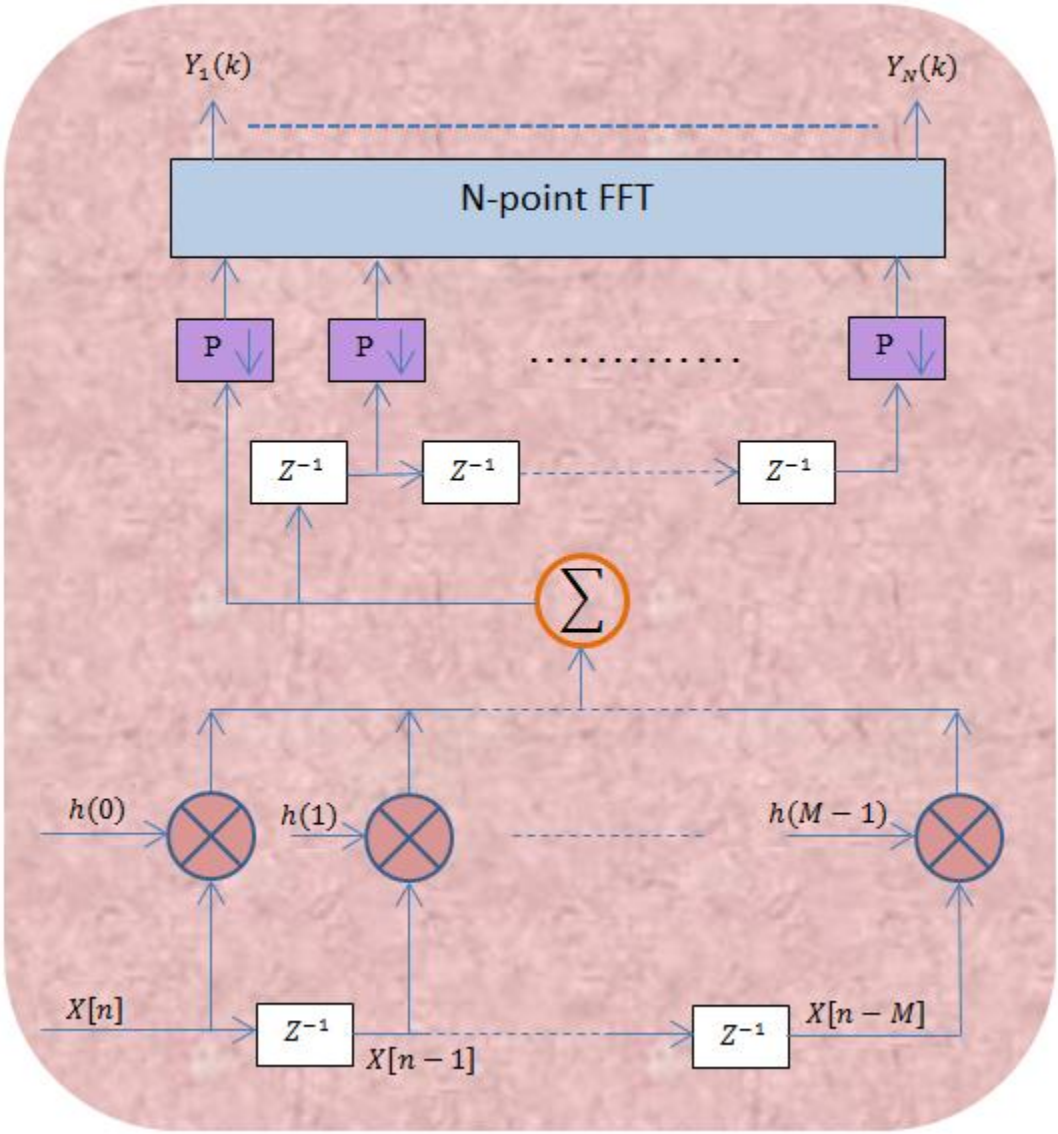

Figure 3.18 Block diagram of a TDE for a typical OFDM system

The matrix form for the figure 3.18 can be given as:

$$Y = WXh \tag{3.50}$$

where W (which is a FFT Matrix$2N \times 2N$), X and h are as follows:

$$W = \begin{bmatrix} 1 & 1 & 1 & \cdots & 1 \\ 1 & e^{\frac{-j2\pi}{2N}} & \left(e^{\frac{-j2\pi}{2N}}\right)^2 & \cdots & \left(e^{\frac{-j2\pi}{2N}}\right)^{2N-1} \\ 1 & \left(e^{\frac{-j2\pi}{2N}}\right)^2 & \left(e^{\frac{-j2\pi}{2N}}\right)^4 & & \left(e^{\frac{-j2\pi}{2N}}\right)^{2(2N-1)} \\ & \vdots & & \ddots & \vdots \\ 1 & \left(e^{\frac{-j2\pi}{2N}}\right)^{2N-1} & \left(e^{\frac{-j2\pi}{2N}}\right)^{2(2N-1)} & \cdots & \left(e^{\frac{-j2\pi}{2N}}\right)^{(2N-1)^2} \end{bmatrix}_{2N\times 2N} \tag{3.51}$$

$$X = \begin{bmatrix} x[kS+v+1] & x[kS+v] & \cdots & x[kS+v-M+2] \\ x[kS+v+2] & x[kS+v+1] & & x[kS+v-M+3] \\ & \vdots & \ddots & \vdots \\ x[S(k+1)] & x[S(k+1)-1] & \cdots & x[S(k+1)-M+1] \end{bmatrix} \tag{3.52}$$

$$h = \{h[0] \quad h[1] \quad \ldots \quad h[M-1] \quad h[M]\}^T \tag{3.53}$$

v is the length of the cyclic prefix and S is the length of a symbol plus the cyclic prefix and is:

$$S = 2N + v \tag{3.54}$$

The output of FFT is:

$$Y = \{Y_1[k] \quad Y_2[k] \quad \ldots \quad Y_{N-1}[K] \quad Y_N[k]\}^T \tag{3.55}$$

3.20 Synchronization using the cyclic extension

One of the properties of the Cyclic Prefix/Cyclic Extension (CP/CE) is that the first portion of every OFDM symbol is identical to the last part. This property can help us to use the cyclic extension for synchronization issue not only for time synchronization but also for frequency synchronization [45, 46]. Figure 3.19 illustrates the usage of the cyclic prefix (CP) for synchronization.

$$x(t) = \int_0^{T_G} r(t-\tau)r(t-\tau-T)dt \tag{3.56}$$

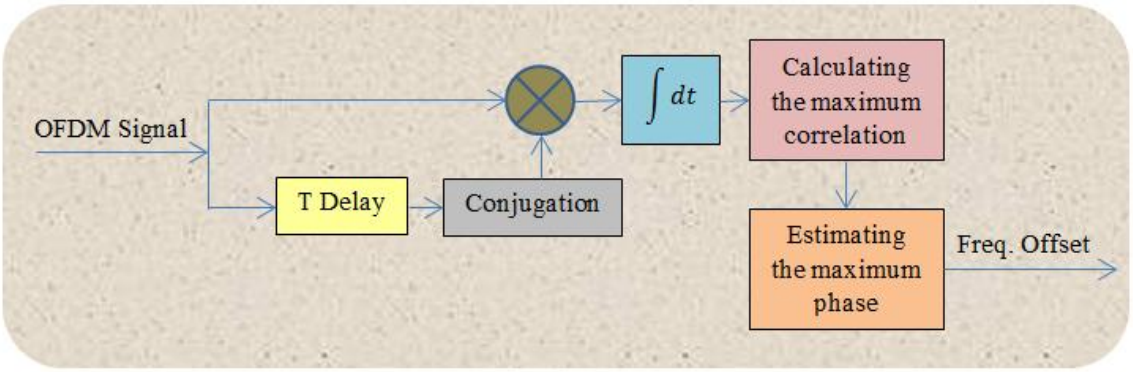

Figure 3.19 Cyclic prefix for synchronization

3.21 CFO estimation algorithm and Techniques

CFO can produce Inter Carrier Interference (ICI) which can be much worse than the effect of noise on OFDM systems. That is why various CFO estimation and compensation algorithms have been proposed.

Its importance is evidenced by the researchers who have proposed numerous and various CFO estimation and compensation techniques and algorithms. These methods can generally be categorized into two major branches:

1. Training based algorithm;

2. Blind algorithm and Semi-blind algorithm.

3.22 Training based algorithm

The training sequence can be designed in a way that can limit the number of computations at the receiver side. Generally, these algorithms have a low computational complexity. However, the negative point of the training based algorithm is that the training sequences must be transmitted from the transmitter during its transmission. This can cause a reduction of the effectiveness of the data throughput.

3.23 Blind and Semi-blind algorithms

Another algorithm that has been used is called the Blind CFO estimation algorithm. In this algorithm, by using the statistical properties of the received signal, the CFO will be estimated. Since the receiver does not have any knowledge of the signal that the transmitter has been sending, the blind algorithm is considered to have a high computational complexity. The high computational complexity is the disadvantage of these algorithms. Compared with training based algorithm, blind algorithms have no need to transmit the training sequences and, therefore, there is no training overhead for these algorithms.

3.24 Study of the training based and blind algorithms

In this part, a few proposed training and Blind algorithms are discussed. For the CFO estimation, Paul H. Moose [47] in his paper "The technique for OFMD frequency offset correction" suggested a training based CFO estimation algorithm. His paper is divided into two major sections. In the first section, he showed the effect of offset errors on the signal to noise (SN). In the second part, he presented an algorithm to estimate the offset, and use it to remove it prior to the demodulation. He presented the algorithm for maximum likelihood estimate (MLE) of frequency offset using the values of a repeated data symbol. In this algorithm, two repetitive OFDM symbols are sent. This algorithm works on the base of knowing the start point of the OFDM symbol. In this paper, the maximum likelihood estimate (MLE) of CFO is defined as follows [47]:

$$\hat{\varepsilon} = \frac{1}{2\pi}\, tan^{-1}\{(\sum_{k=1}^{M} Im[Y_{2k}Y_{1k}^{*}])\ (\sum_{k=1}^{M} Re[\,Y_{2k}Y_{1k}^{*}]\} \tag{3.57}$$

where: $\hat{\varepsilon}$ is the maximum likelihood estimate (MLE) for CFO, Im is the imaginary part, Re is the real part and * means the complex conjugate. In this estimation the mean square error is:

$$Mean\ square\ of\ [\hat{\varepsilon}] = \frac{1}{(2\pi)^2 N\mu} \tag{3.58}$$

where μ is the ratio of the signal to noise for the received signals, and N is the number of subcarriers (SCs).

According to the paper, the limit of accurate estimation (for acquisition range) for this algorithm is $|\varepsilon| \leq 0.5 \Rightarrow (-0.5 \leq \text{Acquisition Range} \leq 0.5)$. Therefore, the acquisition range for subcarrier spacing is between -0.5 and 0.5, which is smaller than the value that is in the IEEE 802.11a. When the acquisition range goes towards the 0.5, $\hat{\varepsilon}$ may jump to -0.5 due to the noise and the discontinuity of the arctangent. When this occurs, the estimate is no longer unbiased and, in practice, it becomes useless. This estimation for the small values of CFO is conditionally unbiased. However, the big weakness of the suggested algorithm in Moose's paper is its dependency to the starting point. Therefore, the algorithm needs to know the start point of the OFDM symbol.

For the CFO estimation, and in order to overcome the weakness in Moose's algorithm, Timothy M. Schmidl and Donald C. Cox, in their paper "Robust Frequency and Timing Synchronization for OFDM [48]" suggest the time domain OFDM system based on the two identical halves in order to solve the problem of determining the starting point of the OFDM symbol,. In this method, finding the symbol timing for OFDM means finding an estimate of where the symbol starts. Figure 3.20, shows an example of the timing metric as a window slides past coincidence for the Additive White Gaussian Noise (AWGN) channel for an OFDM signal with 1000 subcarriers, a carrier frequency offset of 12.4 subcarrier spacing, and an signal-to-noise ratio (SNR) of 10 dB Here the SNR is the total signal (of all the subcarriers) to noise power ratio.

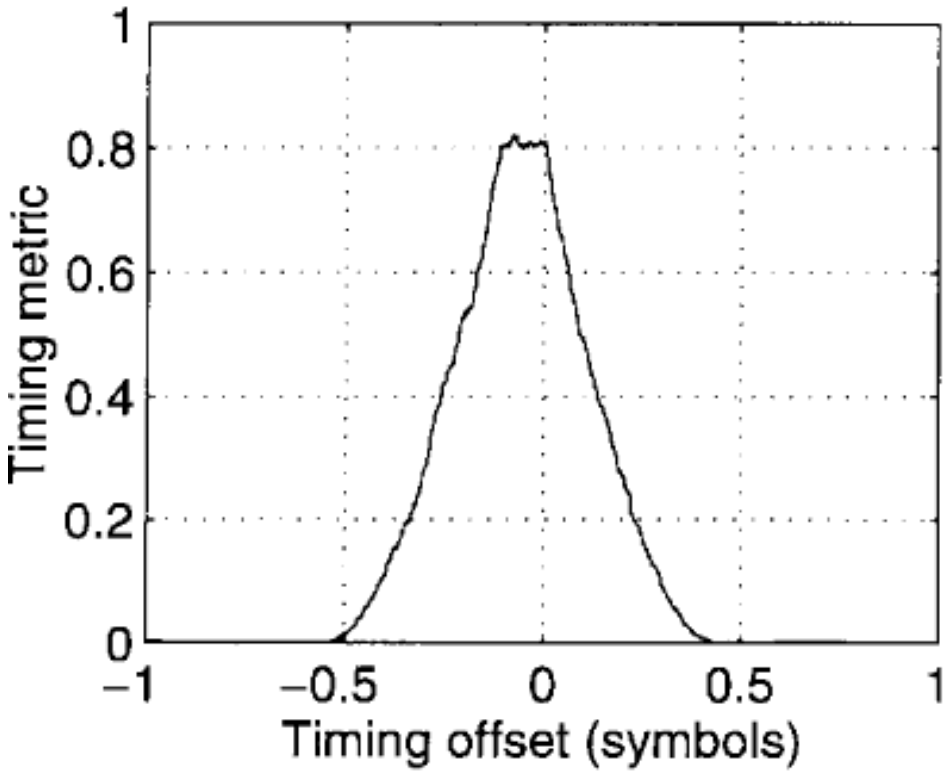

Figure 3.20 Example of the timing metric for the AWGN channel (SNR = 10dB) [48]

As it is shown, the timing metric reaches a plateau. Since there is no Inter Symbol Interference (ISI) within this plateau to distort the signal, the starting point of OFDM can be chosen at any spot on this plateau. The timing metric is defined as follows [48]:

$$M(d) = \frac{|P(d)|^2}{((R(d))^2} \tag{3.59}$$

where

$$P(d) = \sum_{m=0}^{L-1}(r_d^* + mr_d + m + L) \tag{3.60}$$

and

$$R(d) = \sum_{m=0}^{L-1}|r_d + m + L|^2 \tag{3.61}$$

As you see, the $P(d)$ is an auto correlation function and $R(d)$ is a normalized constant. In this estimation, the mean square error is:

$$Mean\ square\ of\ [\widehat{\varepsilon}] = \frac{2}{\pi^2 N\mu} \tag{3.62}$$

The Mean Square Errors (MSE) in both methods (Moose and Timothy) are near and similar to each other.

By comparing the Moose's method and Timothy's method, we can tell that the advantage of Timothy's method is its simplicity. Plus it is not dependent upon the starting point. In Moose' method, the frequency synchronization is done in frequency domain. But in the Timothy's method, the frequency synchronization is achieved in time domain in which the complexity of Fast Fourier Transform (FFT) in time domain is much less than in frequency domain. It should be noted that both of these methods use the periodic training sequence; one in frequency domain and the other in time domain. It is necessary to mention that the time domain periodic training sequences are the ones that have been accepted in various wireless standards. However, there are some limitations for CFO estimation in these methods for SISO-OFDM.

A semi-blind method was proposed for simultaneously estimating the carrier frequency offsets (CFOs) and channels of an uplink for MIMO-OFDM system by Yonghong Zeng, A. Rahim Leyman, and Tung-Sang Ng [49]. In this method, a pilot OFDM block for each user is exploited for resolving the CFOs and the ambiguity matrix. Two dedicated pilot designs, periodical and consecutive, had been discussed. Based on

each pilot design and the estimated shaped channels, two methods were proposed to estimate the CFOs. The algorithm that is used in this method can be summarized as follows [49]:

1. Computing $R_x = E(x_i x_i^{\dagger})$

2. Finding orthogonal eigenvectors of matrix R_x

3. Finding the eigenvalue decomposition (EVD)

After finding the CFOs, the ambiguity matrix obtains. In this method, when the CFOs have been estimated at the base station, recovery of the signal is still a problem [49]. However the complex steps that follow them in semi-blind algorithms make its implementation difficult. Basically, the computational complexity of this algorithm is too high for practical implementation.

Other groups of algorithms, which are called Semi-blind algorithms, are proposed to estimate multiple CFO values. These algorithms have pros and cons. However, most of the proposed algorithms have computational a complexity which make their implementation difficult and their complexity grows nonlinearly. On the other hand, by using the MIMO instead of SISO, the other requirements, both in transmitter side and receiver side, such as multiple clock signals (distributed or centralized clock signal) come into the boarding table.

3.25 Reviewing the Pilot based and Non-pilot base estimation

Generally speaking, CFO estimation and compensation approaches can be divided into two main approaches: Pilot Based Estimation (PBE) and Non-Pilot Based Estimation

(NPBE); NPBE is also called blind estimation. Although many good blind estimation algorithms have been proposed, but it is worth mentioning that the main advantage of the PBE method over NPBE is its accuracy and reliability.

3.26 Model for CFO

Figure 3.21 illustrates the block diagram of the OFDM wireless transceiver system. Consider this figure with N subcarriers with the sampling rate $1/T_s$. Therefore, we have:

$$X(n) = W_P S(n) \tag{3.63}$$

$$y(n) = [y_0(n) y_1(n) y_2(n) \dots y_{N-1}(n)]^T \tag{3.64}$$

$$y(n) = W_P H s(n) \tag{3.65}$$

where

$$H = \begin{bmatrix} H(1) & \cdots & 0 \\ \vdots & \ddots & \vdots \\ 0 & \cdots & H(P) \end{bmatrix} \tag{3.66}$$

After DFT unit, we have:

$$W_P^H y(n) = H\big[s_1(n) \dots s_p(n)\big]^T \tag{3.67}$$

$$y(n) = E W_P H s(n) e^{j\emptyset((N+L)(n-1))} \tag{3.68}$$

$$E = diag\big(1, e^{j\emptyset}, \dots, e^{j(n-1)\emptyset}\big) \tag{3.69}$$

where E is carrier offset matrix, W_p is a $N \times P$ matrix, $s(n)$ is data, H is channel response, and L is length of cyclic prefix.

$$W_P^H y(n) = W_P^H E W_P H s(n) e^{j\emptyset(N+L)(n-1)} \tag{3.70}$$

Here the CFO and ∅ need to be estimated and applied.

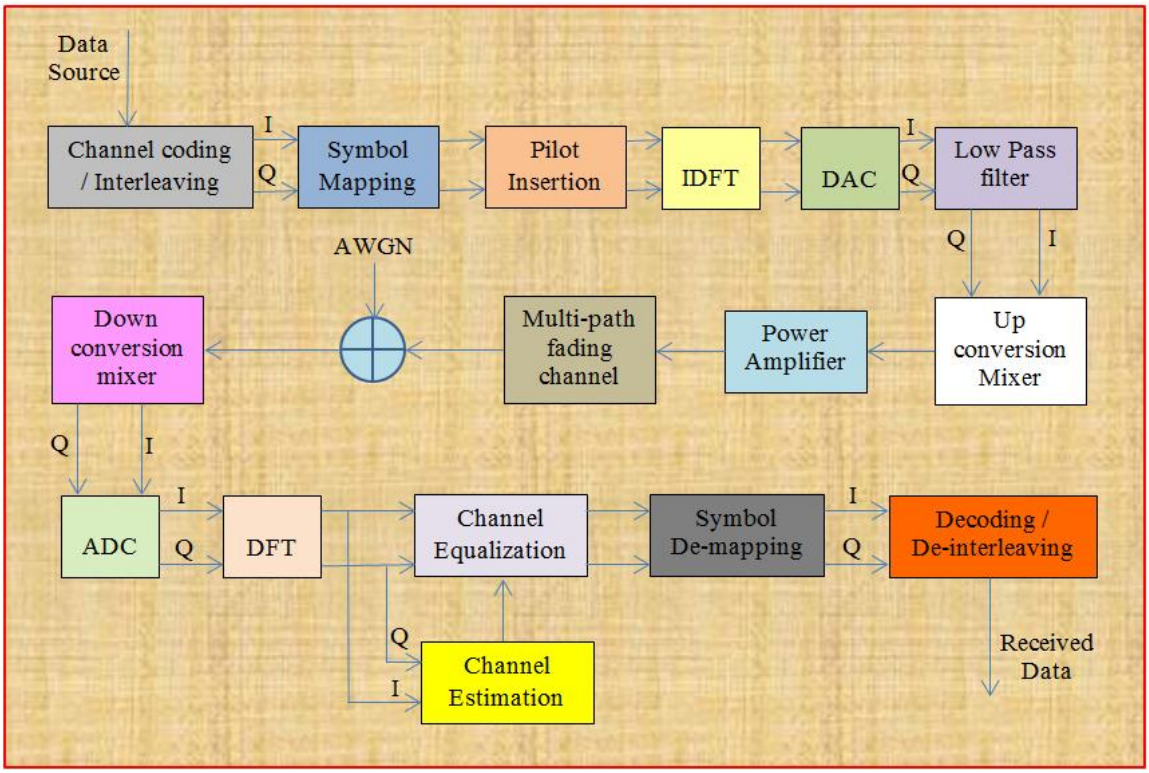

Figure 3.21 A typical block diagram for wireless OFDM system

3.27 Pilot based and Non-pilot base estimation

In pilot based estimation which involves at least one pilot symbol, the receiver signal can be stated as:

$$y(n) = E(\emptyset) W_P H s + n = U(\emptyset) h + n \tag{3.71}$$

The Maximum Likelihood Estimate (MLE) for h and ∅ is as follows:

$$(\widehat{\emptyset}, \hat{h}) = agr_{\emptyset,h} min \|y - U(\emptyset) h\|^2 \tag{3.72}$$

Considering the fact that most of the time during the tracking ICI the residual carrier offset is small. So we can assume that the ICI can be considered as an additional Gaussian noise. Therefore, Eq. 3.68 can approximately be stated as:

$$y(n) = W_P H s(n) e^{j\emptyset((N+L)(n-1))} + \hat{n}(n) \tag{3.73}$$

where $\hat{n}(n)$, consider not only the ICI but also noise. Add p, which corresponds to pilot locations, so we can state:

$$\frac{W_j^H y(n)/s_j(n)}{W_j^H y(n+1)/s_j(n+1)} = e^{-j\emptyset(N+L)} \tag{3.74}$$

where $j \in p \; and \; n = 1, \ldots$

The non-pilot methodology does not use reference symbols to estimating CFO. In this method, on the base of the structure and statistical data of the received signals, the Frequency Offset (FO) will be estimated.

3.28 Blind CFO estimation technique using SPRIT-Like Algorithm

This algorithm uses the shift invariant structure available in the signal subspace of the cissoids to estimate the desired parameters for generalizing the eigenvalues calculation [50]. The k^{th} block of a sample received signal block minus the prefix is stated as:

$$y(k) \stackrel{\text{def}}{=} [y_0(k) \ldots y_{N-1}(k)]^T \tag{3.75}$$

Considering Eq. 3.75, the consecutive samples in forward and backward directions can be expressed as:

$$y_F^i(k) \stackrel{\text{def}}{=} [y_{i-1}(k) \;\; y_i(k) \;\; \ldots \;\; y_{i+M-1}(k)]^T \tag{3.76}$$

$$y_B^i(k) \stackrel{\text{def}}{=} [y_{N-i}(k) \;\; y_{Ni}(k) \;\; \ldots \;\; y_{N-i-M}(k)]^H \tag{3.77}$$

where $i = 1,2,\ldots,N-M$

The operate H in $[.]^H$ means the conjugate is transposed. Considering that, the N-point received signal can be stated as:

$$y(k) = EW_P H_P S(k) e^{j(k-1)\varphi(N+N_g)} \tag{3.78}$$

As the definition, $\check{S}(k) H_P S(k) e^{j(k-1)\varphi(N+N_g)}$, therefore $y(k) = EW_P \check{S}(k)$ and

$$E = diag\left(1, e^{j\varphi}, \ldots, e^{j(N-1)\varphi}\right) \tag{3.79}$$

it can be shown that:

$$y_F^i(k) = E_{M+1} W_{M+1} \Delta^i \check{S}(k) \tag{3.80}$$

where

$$E_{M+1} = diag\left(1, e^{j\varphi}, \ldots, e^{jM\varphi}\right) \tag{3.81}$$

the diagonal matrix is:

$$\Delta = diag(1 + e^{j(\omega+\varphi)}, \ldots, e^{j(P-1)\omega+\varphi}) \tag{3.82}$$

$$where \qquad \omega = 2\pi/N$$

In the same way, backward vector can be stated as follows:

$$y_B^i(k) = E_{M+1}W_{M+1}\Delta^i \times e^{-j\varphi(N-1)}\begin{bmatrix}1 & \cdots & 0\\ 0 & \ddots & \vdots\\ 0 & 0 & e^{j(P-1)(N-1)\omega}\end{bmatrix} \tag{3.83}$$

$where\ as\ the\ definition \qquad r(k) \overset{\text{def}}{=} e^{-j\varphi(N-1)}\begin{bmatrix}1 & \cdots & 0\\ 0 & \ddots & \vdots\\ 0 & 0 & e^{j(P-1)(N-1)\omega}\end{bmatrix}\ therefore:$

$$y_B^i(k) = E_{M+1}W_{M+1}\Delta^i r(k) \tag{3.84}$$

The operate H in $[.]^*$ means the complex conjugate. By assuming $A_{M+1} \overset{\text{def}}{=} E_{M+1}W_{M+1}$, the covariance matrix can be given as follows:

$$R_{M+1} \overset{\text{def}}{=} \frac{1}{K(N-M)} = \sum_{k=1}^{K}\sum_{i=1}^{N-M}\left[y_F^i(k)(y_F^i(k))^H + y_B^i(k)(y_B^i(k))^H\right] \tag{3.85}$$

$$= A_{M+1}\varepsilon[(\tilde{S}(k) + r(k))(\check{S}(k) + r(k))^H]A_{M+1}^H$$

Now by using the Spectral Value Decomposition (SVD), the P eigenvectors of A_{M+1} can be found and the eigenvalues of the diagonal matrix can be presented as follows:

$$\Delta = \left(A_{M+1}(1\colon M, 1\colon P)\right)^{\dagger}(A_{M+1}(2\colon M+1, 1\colon P) \tag{3.86}$$

However the Carrier Frequency Offset in this algorithm can be found from:

$$\exp(j\varphi) = \frac{tr(\Delta)}{\sum_{k=0}^{P-1}\exp(jk\omega)} \qquad where\ \ \omega = 2\pi/N \tag{3.87}$$

where the CFO can be computed as follows:

$$\varphi = Angle\left(\frac{Trace(\Delta)}{\sum_{k=0}^{P-1}e^{jk\omega}}\right) \tag{3.88}$$

Although this algorithm is considered as having a good performance, the selection of K has a key role for having the P eigenvectors of R_{M+1} . However, comparing MUSIC-like searching method, this method is better.

3.29 Blind CFO estimation technique using MUSIC Algorithm

This algorithm uses the known structure of the subspace of the OFDM signals. In brief, the MUSIC algorithm, by using the receiver outputs, constructs polynomial costs function as follows [51]:

$$P(z) = \sum_{i=1}^{L} \sum_{k=1}^{K} \left\| W_{P+i}^{H} Z^{-1} y(k) \right\|^2 = \sum_{i=1}^{L} \sum_{k=1}^{K} W_{P+i}^{H} Z^{-1} y(k) y^{H}(k) Z W_{P+i} \quad (3.89)$$

Here $L \leq N - P$. But, if there are several virtual carriers, we can select $L \ll N - P$ in order to decrease the computational complexity. On the other hand, if $= e^{j\varphi}$, then $P(Z)$ will be equal to zero. This gives us the opportunity to find Carrier Offset by calculating the $P(Z)$ along the unit circle.

It also estimates the CFO as the null of $P(z)$. It should be noted that since this algorithm uses the intrinsic orthogonality among the OFDM sub-channels, , it still has an algebraic structure that is the function of carrier offset when that which receives to the receiver is getting severely modified.

This property is that which the MUSIC algorithm uses to formulate the cost function and it is why the MUSIC search algorithm is highly accurate.

3.30 Study of the CFO estimation using periodic preambles

In this section, the overview of the CFO estimation techniques and comparison with each other is in aspect of computational complexity. As mentioned, CFO has two parts, fractional and integer. Some researchers proposed the algorithms that estimate the integer part and some proposed the methods that estimate the fractional part. Huang and Letaief [52] suggested a method that took care of both parts in CFO. P. Moose [53] suggested the maximum likelihood CFO estimator which worked on the base of a preamble with two identical pilot symbols. This method will not be optimal when the number of periods is more than two. To advance the performance, Morelli et al. [54] proposed a good algorithm using preambles when the periodic is bigger than two. Minn et al. [55] showed that by using the Linear Unbiased Estimation (LUE), the Morelli proposed algorithm can be improved. Yu and et al. [56] suggested the ML CFO Estimator for mentioned proposed algorithm. It is apparent that the problem with these entire algorithms is that they have high computational complexity. To improve and lower the complexity, Yu and et al. [57] proposed a method for CFO estimation. Their algorithm contains few steps which are: constructing the correlation matrix, calculating required coefficient for correlation matrix, finding non-zero roots, and finally finding the CFO. In the following part, we go through the algorithm that Yu and et al. proposed. The received preamble to the receiver can be expressed as:

$$y(k) = e^{\frac{j2\pi\varepsilon k}{N}} x(K) + w(k) \tag{3.90}$$

$w(k)$ is considered as Additive White Gaussian Noise (AWGN), and ε is CFO.

$$x(K) = s(k) * h(k) \tag{3.91}$$

$s(k)$ is preamble signal with period N and length QN, where $k = 0,1,2, \dots, QN-1$, $h(k)$ is channel response, and $x(k)$ is the output signal from transmitter. However, $y(n)$, $X(n)$ and $W(k)$ can be defined as follows:

$$y(n) = [y_1(n) \quad y_2(n) \quad \dots \quad y_k(n)]^T \tag{3.92}$$

$$X(n) = [x_1(n) \quad x_2(n) \quad \dots \quad x_k(n)]^T \tag{3.93}$$

$$W(n) = [w_1(n) \quad w_2(n) \quad \dots \quad w_k(n)]^T \tag{3.94}$$

and

$$Y = [y(0) \quad y(1) \quad \dots \quad y(N-1)] \tag{3.95}$$

$$X = \left[X(0) \quad X(1)e^{\frac{j2\pi\varepsilon}{N}} \quad \dots X(N-1)e^{\frac{j2\pi\varepsilon(N-1)}{N}}\right] \tag{3.96}$$

$$W = [W(0) \quad W(1) \quad \dots W(N-1)] \tag{3.97}$$

$$A = \begin{bmatrix} e^{j2\pi\varepsilon} & 0 & \cdots & 0 \\ 0 & e^{j2\pi\varepsilon.2} & \cdots & 0 \\ \vdots & \vdots & \ddots & \vdots \\ 0 & 0 & \cdots & e^{2j\pi\varepsilon.K} \end{bmatrix} \tag{3.98}$$

Eq. 3.90 can be stated as:

$$Y = AX + W \quad (4) \tag{3.99}$$

Based on the approach of Yu and et al. [57], X should be estimated by the LS method, and then CFO would be estimated by using ML function. With this technique, the estimation of CFO is achieved by the following steps:

By having X, the LS estimate of X is:

$$X_{LS} = (1/K)A^H Y \equiv A + Y \tag{3.100}$$

$(A)^H$ means Hermitian Operation. However by plugging X_{LS} into Eq. 3.99, we have:

$$\sum_n^{N-1} \|y(n) - AA + y(n)\|^2 = N\,.\,trace((I - AA^+)R_Y \tag{3.101}$$

I is the identity matrix and

$$R_Y = E[YY]^H \tag{3.102}$$

Considering [58], the pth and qth entry of R_Y is as follows:

$$(1/N)\sum_{n=0}^{N-1} y_p(n)y_q^*(n)\,,\ p,q \in [1,K] \tag{3.103}$$

However, in this technique, the equation for CFO estimation is as follows:

$$\hat{\varepsilon} = \arg\{min_\varepsilon\, trace\,((I - AA^+)R_Y)\} = arg\{Max_\varepsilon a^H R_Y a\} \tag{3.104}$$

where a is the vector that includes the diagonal elements of A, and $a^H R_Y a$ is [59]:

$$a^H R_Y a = \sum_{m=-(K-1)}^{k-1} b(m)e^{j2\pi m\varepsilon} \tag{3.105}$$

For getting the optimal of the CFO estimation, we need to take the derivative of Eq. 3.105 respect to ε and set it equal to zero, so we will have:

$$\sum_{m=1}^{K-1} mb(m)\,z^m = \sum_{m=1}^{K-1} mb(-m)\,z^{-m} \tag{3.106}$$

$$Im(\sum_{m=1}^{K-1} mb(m)\,z^m) = 0 \quad (8) \tag{3.107}$$

The role of the operator $Im()$ is isolating the imaginary part of the scalar value. Consider z as follows:

$$z = e^{j2\pi\varepsilon m} \tag{3.108}$$

The CFO estimation based on Yu and et al. [57] can be obtained as:

$$\hat{\varepsilon} = \frac{1}{j2\pi}\ln(\hat{z}) \tag{3.109}$$

$\hat{z}$ is as:

$$\hat{z} = \arg\{\max_{z\in\Omega}(A(z))\} \quad \text{and} \quad |\hat{z}| = 1 \tag{3.110}$$

As is obvious from Eq. 3.107, it needs the root finding procedure. Although this method has good performance, since it needs to go through the root finding procedure, it has computational complexity.

To solve the problem in the Yu and et al. method, Hung-Tao Hsieh and et al. [60] proposed an approximation method for finding ε as follows:

$$\hat{\varepsilon} = -\frac{\sum_{p=1}^{K-1}\sum_{q>p}^{K}|\gamma_{pq}|(q-p)\angle\gamma_{pq}}{2\pi\sum_{p=1}^{K-1}\sum_{q>p}^{K}|q-p|^2|\gamma_{pq}|} \tag{3.111}$$

where:

(3.112)

$$\gamma_{pq} = e^{j2\pi\varepsilon(p-q)}\sum_{n=0}^{N-1}|x_1(n)|^2 + \sum_{n=0}^{N-1}w_p(n)w_q^*(n) + e^{2j\pi\varepsilon(pN+P)}\sum_{n=0}^{N-1}x_1(n)w_q^*(n) + e^{j2\pi\varepsilon(pN-q)}\sum_{n=0}^{N-1}x_1^*(n)w_q(n)$$

$$\gamma_{pq} = \sum_{n=0}^{N-1}y_p(n)y_q^*(n) \qquad (q \geq p \quad abd\ o \geq 1) \tag{3.113}$$

$$\angle\gamma_{pq} \approx 2\pi\varepsilon(p-q) \tag{3.114}$$

However according to Eq. 3.113, the accuracy of CFO estimation in this technique depends on the level of the signal-to-noise ratio, and the result can be good if $\left|\angle\gamma_{pq} < \pi\right|$. Generally, we can say the estimation range in this method is:

$$|\varepsilon| \leq \frac{1}{2(q-p)} \tag{3.115}$$

3.31 Investigating of the estimation Technique using Cyclic Prefix (CP)

This technique uses the length of Cyclic Prefix (CP) to compensate the effect CFO [61]. Consider the signal of the transmitter as follows:

$$S_i(n) = \frac{1}{\sqrt{N}} \sum_{k=0}^{N-1} b_i(k) e^{j2\pi k/N} \tag{3.116}$$

where $-N_g \leq n \leq N-1$

N is the Inverse Fast Fourier Transform (IFFT) block length and N_g is length of Cyclic Prefix (CP).

The signal received by receiver can be stated as:

$$r(n) = \sum_{i=0}^{I-1} x_i(n-d_i) e^{j(\epsilon_i n+\varphi_i)} + v(n) \tag{3.117}$$

where d_i is propagation delay and φ_i is initial phase, ϵ_i is CFO and $v(n)$ is Additive White Gaussian Noise (AWGN).

In receiver side, the OFDM demodulator removes the CP and considers the sample vector as:

$$r(0) = \sum_{i=0}^{I-1} e^{j\varphi_i} E_i(0) H_i(0) S_i(d_i) + V(0) \tag{3.118}$$

where $S_i(d_i)$ is a symbol vector, $E_i(0)$ is CFO matrix, and $H_i(0)$ is the channel matrix. By switching the column of $H_i(0)$, we can state Eq. 3.118 as:

$$r(0) = \sum_{i=0}^{I-1} e^{j\varphi_i} E_i(0) H_i S_i + V(0) \tag{3.119}$$

Here the goal is to exploit the redundancy of Cyclic Prefix (CP) on Eq. 3.119. An equation similar to Eq. 3.119 can be stated as follows:

$$r(m) = \sum_{i=0}^{I-1} e^{j\varphi_i} E_i(m) H_i S_i + V(m) \tag{3.120}$$

$E_i(m)$ is:

$$E_i(m) = \begin{bmatrix} 0_{(m|N)\times(N-m|N)} \\ diag\left\{e^{j\epsilon_i(-m+m|N)}, \dots, e^{j\epsilon_i(N-m-1)}\right\} \\ diag\left\{e^{j\epsilon_i(-m)}, \dots, e^{j\epsilon_i(-m-1+m|N)}\right\} \\ O_{(N-m|N)\times(m|N)} \end{bmatrix} \tag{3.121}$$

Considering Equations 3.119 and 3.120, we can construct the following equation:

$$\begin{bmatrix} r(0) \\ \vdots \\ r(M-1) \end{bmatrix} = \sum_{i=0}^{I-1} e^{j\varphi_i} \begin{bmatrix} E_i(0) \\ \vdots \\ E_i(M-1) \end{bmatrix} H_i S_i + \begin{bmatrix} V(0) \\ \vdots \\ V(M-1) \end{bmatrix} \tag{3.122}$$

For the sake of simplicity, Eq. 3.122 can be stated as follows:

$$y = \sum_{i=0}^{I-1} e^{j\varphi_i} A_i H_i S_i + u \tag{3.123}$$

The goal is to design a CFO mitigation matrix X as follows:

$$XA_i = I_N \quad \rightarrow \quad X = I_N E_i(m) \tag{3.124}$$

In Eq. 3.121, consider $0 \leq p \leq N-1$ and $0 \leq l \leq N-1$. Therefore, this equation can be defined as follows:

$$[E_i(m)]_{p,l} = \begin{cases} e^{j\epsilon_i(p-m)} & if \quad p = (l+m)|N \\ 0 & Otherwise \end{cases} \tag{3.125}$$

Since all $r(m)$ does not have to be used, we select Q vector among them, where:

$$0 \leq m_0 \leq m_1 \leq \cdots \leq m_{Q-1} \leq M-1 \tag{3.126}$$

For $0 \leq i \leq I-1$, the CFO matrices are $E_i(m_0), \ldots, E_i\big(m_Q - 1)\big)$. In this case, Eq. 4.25 will be altered to search for a $N \times NQ$ CFO mitigation matrix X as follows:

$$X \begin{bmatrix} E_i(m_0) \\ \vdots \\ E_i(m_Q - 1) \end{bmatrix} = I_N \tag{3.127}$$

where $0 \leq i \leq I-1$

In this technique, first by using Eq. 3.126, you choose appropriate parameters, and, by using of ϵ_i and Eq. 3.124, you calculate X, and then finally by using Eq. 3.122, you can get a sample vector for the OFDM block. By using these results you can compensate the effect of the CFO. This method is efficient and a linear complexity, since $I \ll N$ and, for the whole OFDM block, we only need to determine X one time. Therefore, the computational complexity of this method is linear which makes it an

effective technique. But the CFO estimation technique using CP is only good when$-0.5 \leq \varepsilon \leq 0.5$.

3.32 Proposed Algorithm

Due to the weakness of the CFO estimation using CP, and to improve it for the amounts of ε which are greater than the mentioned values, we offer using training symbols. Before we start, first a signal model needs to be selected. Thus the first step in our algorithm is selecting a signal model. The general models that have been used for the received signal can be considered as follows:

$$x(n) = e^{j2\pi n\delta}s(n) + \omega(n) \tag{3.128}$$

where $\omega(n)$ is Gaussian noise and δ is Carrier Frequency Offset (CFO), $s(n)$ can be defined as follows:

$$S(n) = \sum_{k=0}^{L-1} h(K)a_{n-k} \quad n = 0,1,2,\dots,N-1 \tag{3.129}$$

Consider an OFDM-MIMO system, like figure 3.22 with n_i transmitter and n_r receiver antennas as follows:

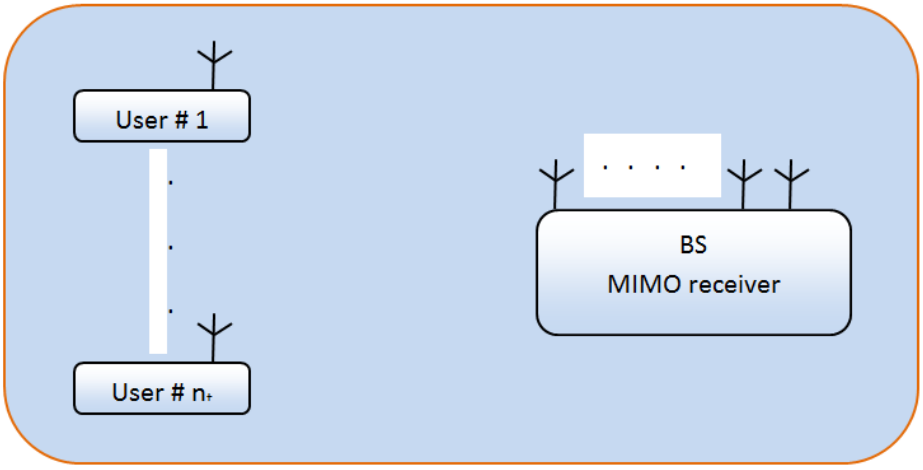

Figure 3.22 Multi-user MIMO-OFDM systems diagram

Here the channel is $n_r \times n_t$ matrix.

$$\begin{bmatrix} r_1 \\ \vdots \\ r_{n_r} \end{bmatrix} = \begin{bmatrix} H_{1,1} & \cdots & H_{1,n_t} \\ \vdots & \ddots & \vdots \\ H_{n_r,1} & \cdots & H_{n_r,n_t} \end{bmatrix} \begin{bmatrix} s_1 \\ \vdots \\ s_{n_t} \end{bmatrix} + \begin{bmatrix} n_1 \\ \vdots \\ n_{n_r} \end{bmatrix} \tag{3.130}$$

The received signal vector form can be written as follows:

$$h = [h(0), h(1), h(2), \dots, h(L-1)]^T \tag{3.131}$$

This is a vector containing $T_s - spaced$ samples. The symbol $[\,]^T$ means vector transpose and the training symbols are a_n with the condition:

$$-L + 1 \leq n \leq -1 \tag{3.132}$$

Eq. 3.129 can be written as:

$$x = \Gamma(\delta)Ah + \omega \tag{3.133}$$

However, this is the general model that they usually consider for investigating. For simplicity, in our algorithm consider one transmit antenna for each user, which in general denotes it by n_t , and consider the number of antenna for the Base Station by n_r

with this condition that n_r always is bigger or equal to n_t $(n_r \geq n_t)$. With this assumption, the received signal at any receiver antenna can be stated as:

$$r_i(k) = \sum_{m=1}^{n_t}(e^{j\delta_m k}\sum_{d=0}^{L-1} h_{i,m}(d)\, S_m(k-d)) + n_i(k) \tag{3.134}$$

where:

$h_{i,m}(d)$ Channel impulse response

S_m Transmitted signal from m[th] user

n_i Additive white Gaussian noise (AWGN)

As Eq. 3.134 states, the CFO should be calculated for each of the n_t. After removing the CP in receiver, Eq. 3.134 can be presented in matrix form as follows:

$$r_i = \sum_{m=1}^{n_t} E(\delta_m) S_m h_{i,m} + n_i \tag{3.135}$$

So we consider our signal model as Eq. 3.135. The second step in algorithm is using the training symbols. Consider that the transmitter is sending the training symbols with a repetitive pattern that is being called D. It is worth mentioning that these training symbols can be generated by taking the IFFT of the signal in frequency domain. Therefore:

$$X_l[D] = \begin{cases} A_m & if \quad K = D.i \\ 0 & otherwise \end{cases} \tag{3.136}$$

Here A_m is an M-array symbol. The receiver, by using the following Eq., can estimate the CFO:

$$\hat{\varepsilon} = \frac{D}{2\pi} arg\{\sum_{n=0}^{N/D-1} y_l^*[n] y_l[n+N/D]\} \tag{3.137}$$

where N/D is an integer. Here the range is:

$$-\frac{D}{2} \leq \varepsilon \leq \frac{D}{2} \tag{3.138}$$

By considering the average, Eq. 4.39 can be stated as:

$$\hat{\varepsilon} = \frac{D}{2\pi} arg\left\{\sum_{m=0}^{D-2} \sum_{n=0}^{N/D-1} y_l^*[n + mN/D] y_l[n + (m+1)\, N/D]\right\} \tag{3.139}$$

As it is obvious from Eq. 3.139; by increasing the repetitive pattern (D), the range for (ε) increases. Figure 3.23 illustrates the result of the simulation of the suggested algorithm.

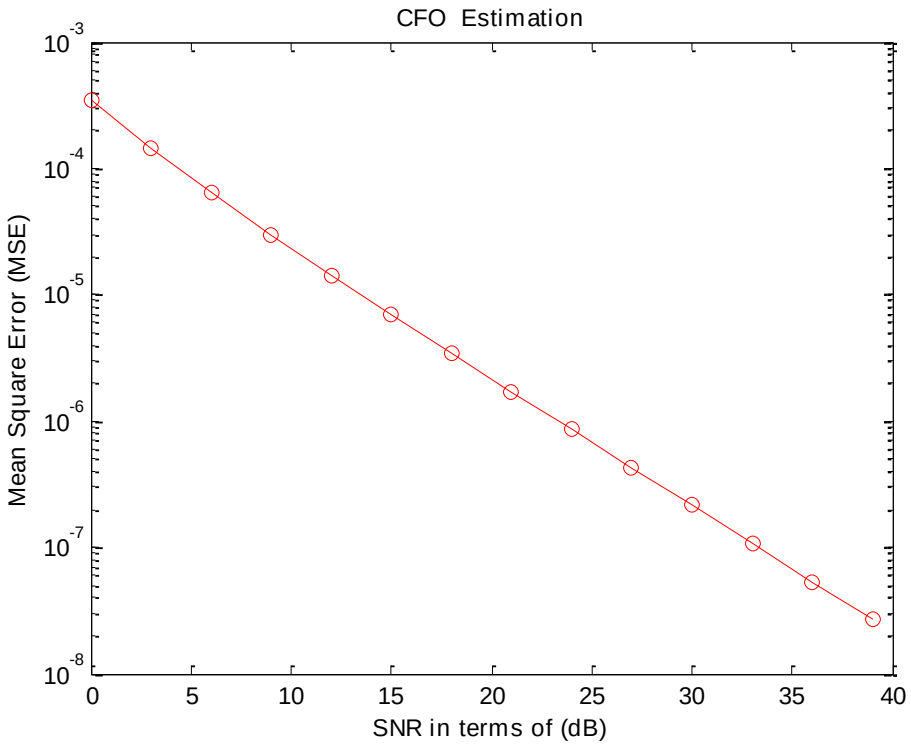

Figure 3.23 CFO Estimation

Another suggested frequency offset estimation works on the base of using training sequences. As we know the training symbols are positioned at the start of each frame as a preamble which is used for finding out the timing metric in the receiver.

This method includes the following units: Data Timing Detector (DTD), Timing Estimator (TE), and Fine Frequency Finder (FFF) (the schematic diagram for this method can be found in Chapter 6, Section 6.3).

The output of the FFT unit in this schematic is as follows:

$$F_k = \sum_{n=0}^{N-1} (r_n A_n)\, e^{-j2\pi nk/N} \tag{3.140}$$

where $0 \leq k \leq N-1$, A_n and r_n in order are the conjugate of the training sequence and useful portion of the received training symbols.

f_{corse} is defined as follows:

$$f_{corse} = \frac{k_{max}}{NT_s} \tag{3.141}$$

T_s is sample interval

Eq. 3.140 give us the exact frequency, only when the biggest amount of $|F(K_{max})|$ is at the center. But since this is most of the time, an offset due to the noise and Doppler Effects effects the output of the Eq. (16) and it is not going to be correct. Below shows the offset in the right and left side of the center as follows:

$$|F(K_{max}+1)|$$

$$|F(K_{max}-1)|$$

To fix the output of the Eq. (16), define β as follows:

$$\begin{cases} if|F(k_{max}-1)| > |F(k_{max}+1)| & \rightarrow \quad \beta = -1 \\ if|F(k_{max}-1)| \leq |F(k_{max}+1)| & \rightarrow \quad \beta = 1 \end{cases} \tag{3.142}$$

Therefore we can state:

$$f_e = f_{fine} + f_{corse} \tag{3.143}$$

$$f_{fine} = \frac{\beta}{NT_s F(k_{max})/(k_{max}+\beta)+1} \tag{3.144}$$

$$f_e = \frac{1}{NT_s}\left(k_{max} + \frac{\beta}{F(k_{max})/(k_{max}+\beta)+1}\right) \tag{3.145}$$

The schematic diagram of this method and result can be found in Chapter 6, Section 6.3.

Figure 3.25 shows the BER VS Eb/N0 for QPSK modulation for theoretical and simulated.

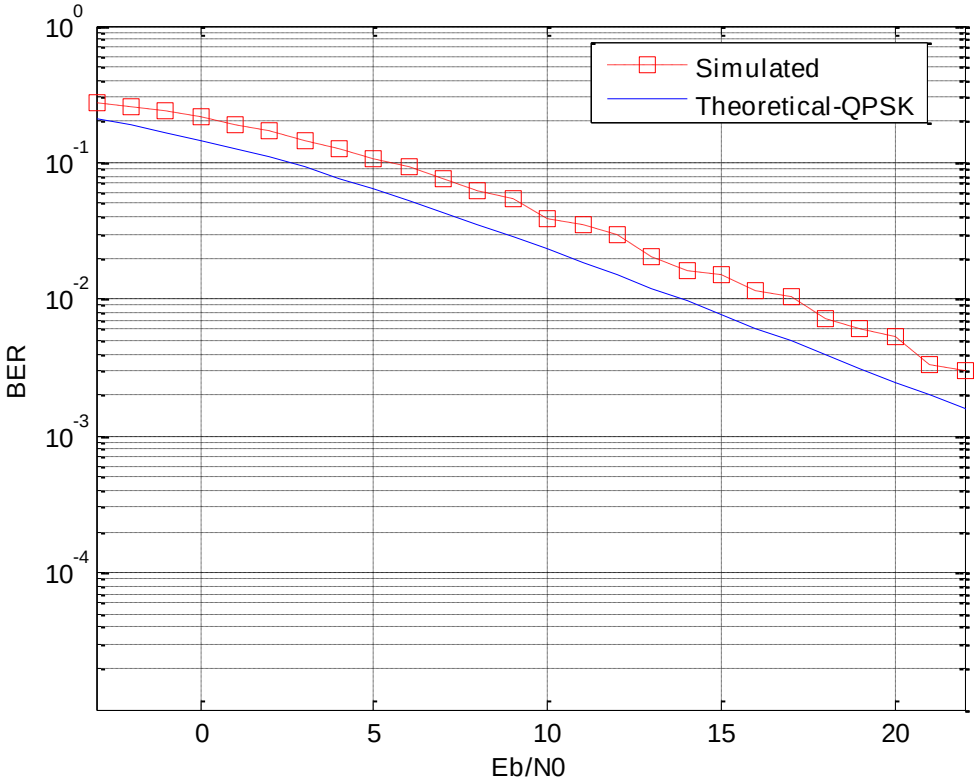

Figure 3.24 BER VS Eb/N0

Chapter 4

Peak to Average Power Ratio

4.1 Introduction

In this section, the various PAPR reduction techniques are reviewed and studied and then our algorithm for PAPR reduction is proposed. The comparison of different PAPR reduction algorithms is based on their performance, bandwidth (BW) expansion, and computational complexity. This chapter ends with Path loss, which after investigating the indoor and outdoor path, our proposed algorithm for predicting the indoor and outdoor path loss is presented.

4.2 Peak to Average Power Ratio (PAPR)

High Peak to Average Power Ratio (PAPR) for OFDM system is still a demanding area and difficult issue. The radio transmitter stations have to use a High Power Amplifier (HPA) to get enough transmission power for coverage in their desired areas. On the other hand, in order the HPA have the most output power efficiency, it must be designed to work close to the saturation region. Therefore, due to the high PAPR of input signals, a factor which is called memory-less nonlinear distortion will come into the communication channels. We know the OFDM receiver's efficiency is sensitive to the

HPA. If the high power amplifier does not work in a linear region it can cause the out-of-band power to be kept under the specified limits. This condition can cause inefficient amplification and expensive transmitters. Thus, it is necessary to investigate PAPR reduction techniques for the OFDM system.

4.3 Techniques for reduction PAPR

In order to reduce the PAPR of a transmitted signal, various techniques have already been explored and investigated. The most approaches which have been used to reduce PAPR are: clipping [62,63], Selective Mapping (SLM) [64,66], coding schemes [65,67], nonlinear compounding transforms [68,69], Partial Transmission Sequence (PTS), Tone Reservation (TR), and Tone Injection (TI) [70,71]. These techniques can be divided into three main categories:

1. Selecting mapping and Partial Transmission Sequence (PTS)
2. Clipping and Filtering (CAF)
3. Coding techniques

4.4 Selecting Mapping (SLM)

In the Selecting Mapping (SLM) technique, the multiple transmit signals that are generated by the multiplication of the different phase vectors with OFDM symbols, are taken and the one that produces the least PAPR will be selected. Naturally, when the receiver receives these signals and wants to recover the phase information, it needs to know which phase vector has been used in transmitter. That is why, in this technique for

letting the receiver know which phase vector has been selected, sending a separate control signal is necessary. Figure 4.1, shows the block diagram of the SLM technique.

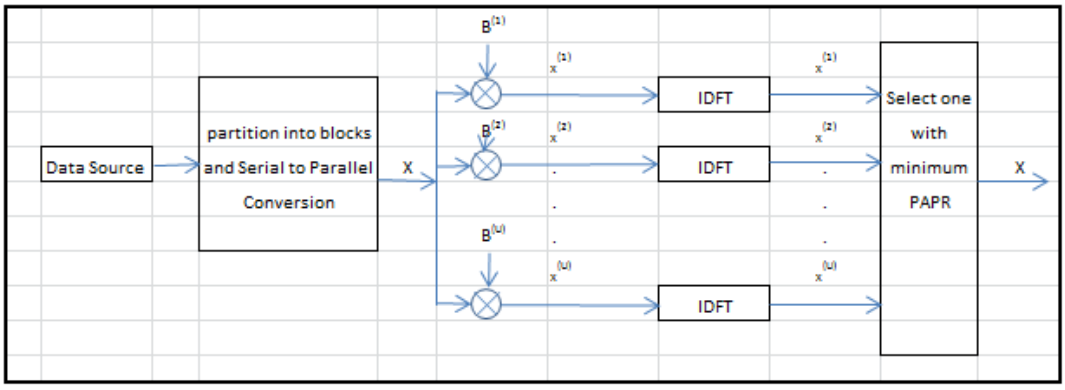

Figure 4.1 Block diagram of the SLM technique [72]

4.5 Partial Transmission Sequence (PTS)

In the Partial Transmission Sequence technique, the data block to be transmitted is partitioned into disjoint sub-blocks and the sub-blocks are combined using phase factors to minimize PAPR [73].

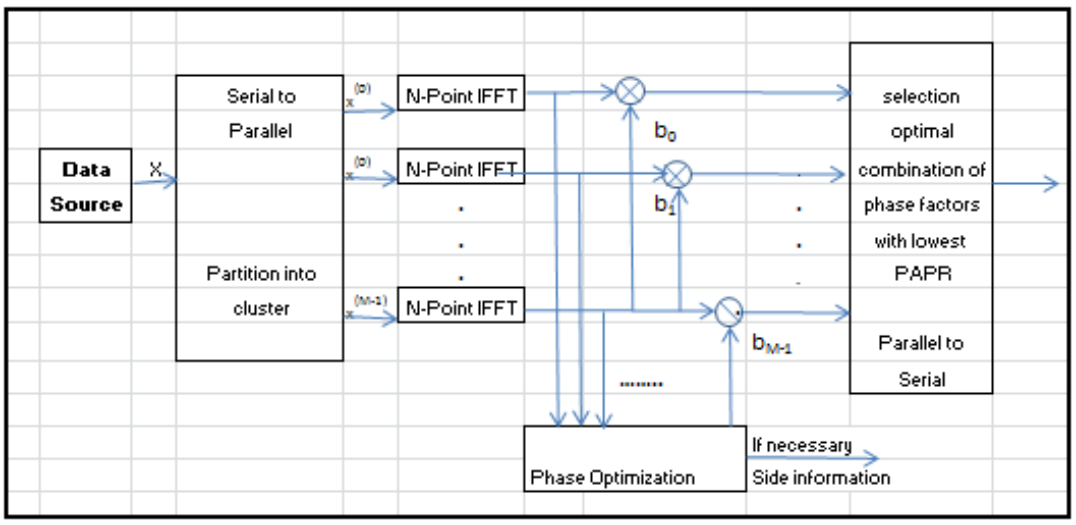

Figure 4.2 Block diagram of partial transmission sequence (PTS) approach [74]

Figure 4.2 shows the block diagram of the partial transmission sequence (PTS) approach. As can be seen from figure 4.2, PTS requires M IFFT operations for each data block, and the number of the required side information bits is $\lfloor \mathrm{Mlog}_2^{\mathrm{M}} \rfloor$ where ⌊x⌋denotes the smallest integer that does not exceed. Considering the method that PTS technique uses to reduce the PAPR reduction, two important issues come to the table. First consider the high computational complexity for searching the optimal phase factors, and then sending the information that the receiver must have in order to be able to do the correct decoding of the bit sequence that is transmitted. Obviously complexity will be the main point of view. In short, PTS in comparison with SLM has less computational complexity and has a better PAPR reduction. But SLM needs less bits of side information.

4.6 Clipping and Filtering (CAF)

This technique, by assigning a set point level, clips the time domain signal to the pre-assigned set point level. (See figure 4.3) Among the techniques that have been used for reducing PAPR, the most common and easiest technique is clipping and filtering (CAF). In this technique, the part of the signal that is not in the permitted region will be clipped. Clipping and filtering happens on the transmitter side, but in order for the receiver will be able to compensate, it needs to know two parameters, size of the clipping and its location.

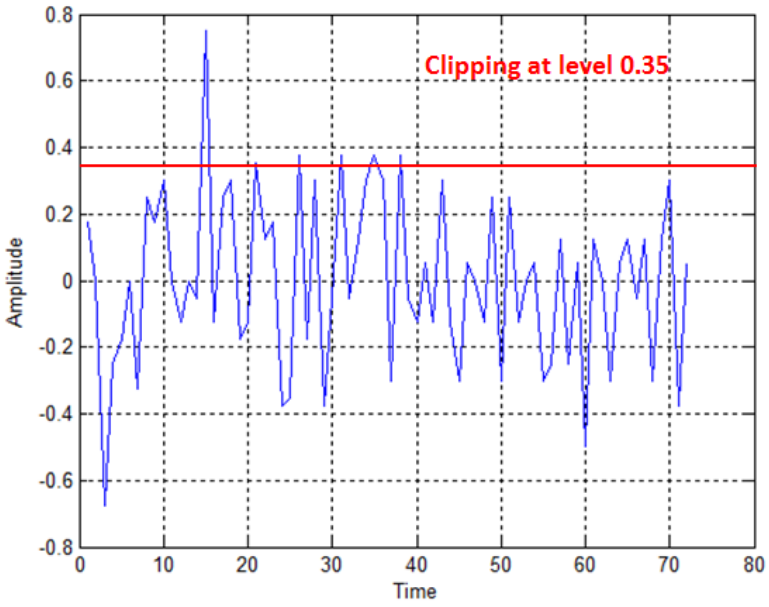

Figure 4.3 Time domain OFDM signal

It was shown that the CAF of amplitude would lead to the expense of in-band distortion and out-of-band radiation [62], which causes degradation of the system's performance. One way of reducing the out-of-band radiation is to apply filtering after clipping. Since the out-of-band can interfere with the communications in an adjacent frequency band, out-of-band is more critical. Among the methods, the clipping and filtering-based method is very powerful from the viewpoint of the tradeoff between the PAPR reduction and error rate. Figure 4.4 illustrates the OFDM transmitter using clipping scheme.

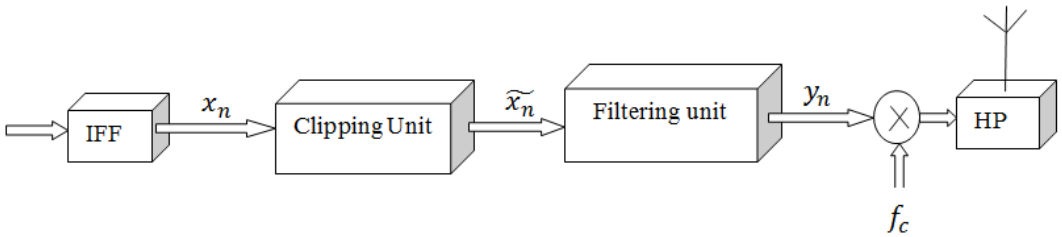

Figure 4.4 OFDM transmitter using clipping and filtering

4.7 Types of Clipping Techniques

There are four clipping techniques for PAPR reduction. These four techniques can be compared with each other regarding their PARA reduction, average power variation and total degradation. These techniques are:

1. Classical-Clipping (CC)
2. Heavy side-Clipping (HC)
3. Deep- Clipping (DC)
4. Smooth-Clipping (SC).

The clipped signal $\tilde{x}_n$ is expressed as [75]:

$$\tilde{x}_n = f(x_n)e^{j\varphi_n} \tag{4.1}$$

where the $f(r)$ is the clipping function. The clipping functions for CC, HC, DC, and SC clipping techniques in order are defined as follows [75]:

$$f(r) = \begin{cases} r & , \quad r \leq A \\ A & , \quad r > A \end{cases} \tag{4.2}$$

$$f(r) = A, \quad \forall r \geq 0 \tag{4.3}$$

$$\begin{cases} r & , \quad r \leq A \\ A - \alpha(r - A) & , \quad A < r < \frac{1+\alpha}{\alpha}A \\ 0 & , \quad r > \frac{1+\alpha}{\alpha}A \end{cases} \tag{4.4}$$

$$\begin{cases} r - \frac{1}{b}r^3 & , \quad r \leq \frac{3}{2}A \\ a & , \quad r > \frac{3}{2}A \end{cases} \tag{4.5}$$

Where in these functions, the clipping level is A, the clipping depth factor is α, and $b = \frac{27}{4}A^2$. Figure 4.5 shows the clipping on base of the mentioned clipping function.

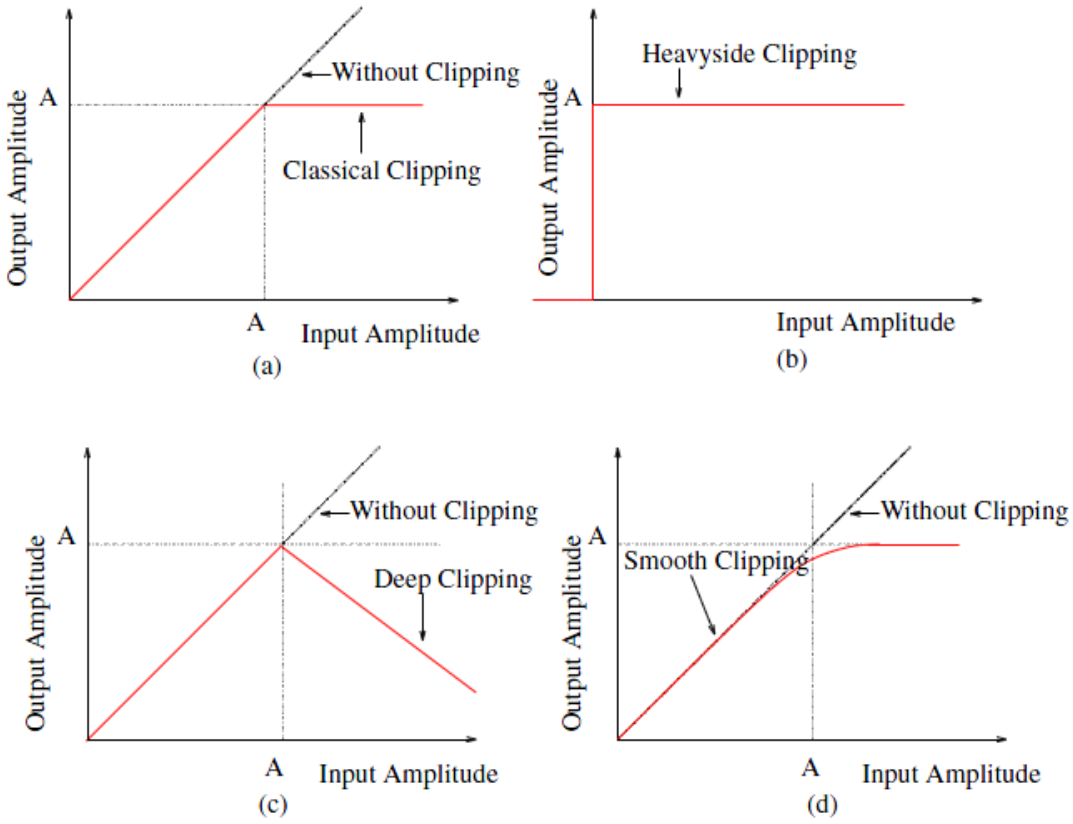

Figure 4.5 Functions-based clipping for PAPR reduction for

(a) Classical-Clipping (b) Heavy side-Clipping
(c) Deep Clipping (d) Smooth-Clipping [75]

Figures 4.6 and 4.7 shows side by side simulation results for the average power performance, BER performance, and PAPR reduction for the mentioned techniques.

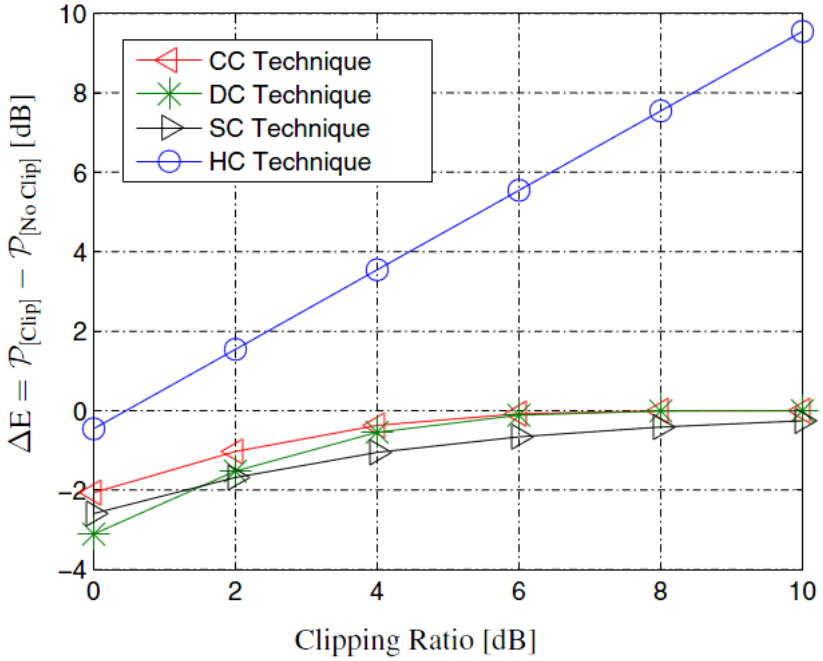

Figure 4.6 (a) Average Power Performance [75]

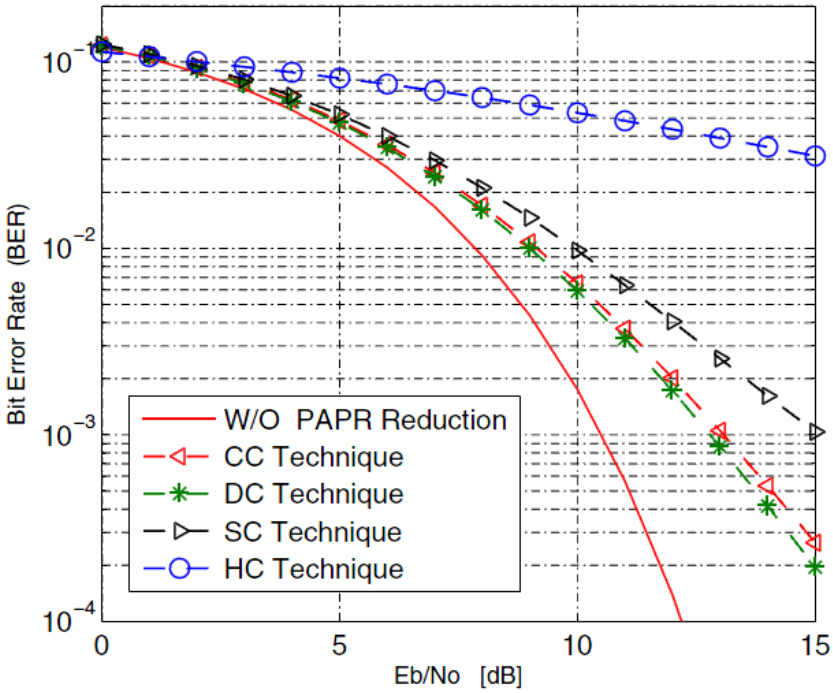

Figure 4.6 (b) BER Performance [75]

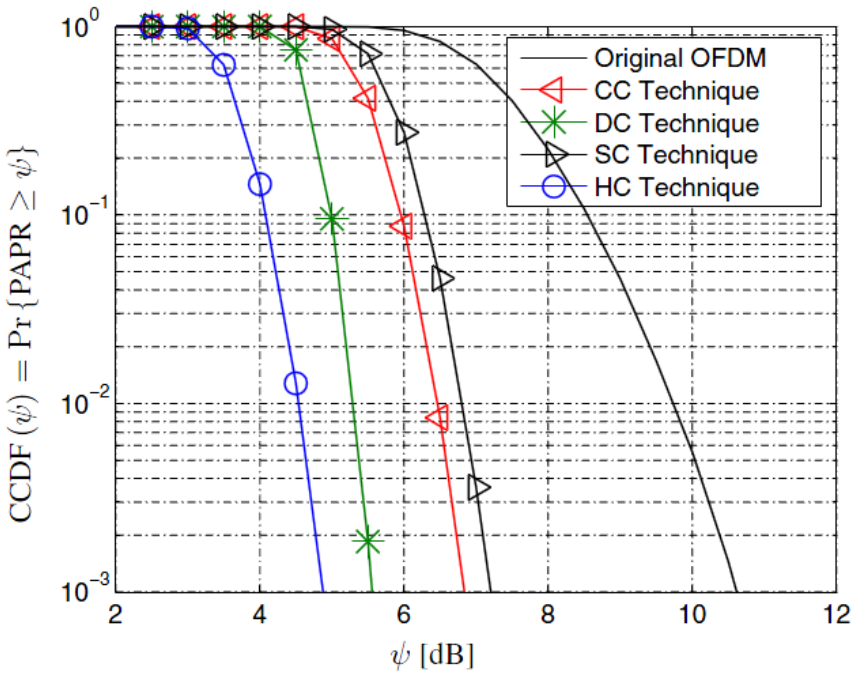

Figure 4.7 PAPR Reduction Performance [75]

Figure 4.6 is the simulation results for the average power performance, BER performance and PAPR reduction. Consider the results for CC, HC, DC, and SC clipping technique. HC is the worst technique among the four. The others are almost the same, so it is very hard to say which of these three one is the best.

However, even though the clipping is the simplest method, clipping can produce some peak re-growth., This peak re-growth shows itself after the clipping and filtering and can cause the signals to exceed from the set point of clipping in some spots. The offered solution for this problem in some papers is to repeat the clipping and filtering. Although this solution fixes the re-growth problem, it will increase the cost of computational complexity.

4.8 Coding techniques

Coding techniques work on the base of finding the code words among a set of code words that produce the lowest PAPR and then using them for mapping the input data. In this technique, if the number of subcarriers (N) is small, the lookup table has to be considered to be used.

A.E. Jones [67] in his paper “Block coding scheme for reduction of peak to mean envelope power ratio of multicarrier transmission schemes” offered the idea of mapping three bits data into 4 bit code word. The added bit is the odd parity code which is added to the last bit across the channel. The big drawback of this method is that it is only good for reducing the PAPR for a 4 bit code word. Later, in the publication “Multicarrier transmission peak-to-average power reduction using simple block code”. S**.** Fragiacomo, C. Matrakidis and J.J. O'Reilly suggested a very simple but efficient block code for reducing PAPR. In their technique, a simple added bit code applies across the channels of a multicarrier system for reducing the PAPR [76]. Even though this reduction achieves the minimum increase in complexity, but it is done at the expense of reducing bandwidth. If the frame size gets large, the proposed technique will not be effective. However, Tao Jiang and Guangzi Zhu [77] proposed a new coding scheme as Complement Block coding (CBC) for deleting the frame size problem in Fragiacomo’s method. They claimed it would reduce the PAPR with no restriction for frame size. The proposed method has a lower complexity than the other scheme even when the frame size is large. The flexibility in coding rate choice and low complexity of this technique with large frame sizes and high coding rates can make it a good candidate for an OFDM system.

Table 4.1 is shows the PAPR reduction for different coding techniques. In this table, CBC stands for Complement Block coding, SBC stands for Simple Block Coding, MSBC stands for Modified SBC, SOPC stands for simple odd parity code, and CC stands for Cyclic Coding.

N	n	r	PAPR (dB)				
			CBC	SBC	MSBC	SOPc	CC
4	1	3/4	3.56	3.56	3.56	3.56	3.56
8	1	7/8	2.59	2.52	2.52	2.52	3.66
8	2	3/4	2.67	3.72	2.67	1.18	3.66
16	1	15/16	2.74	1.16	1.16	1.18	3.742
16	2	7/8	2.74	2.52	2.49	1.18	3.742
16	3	13/16	2.74	——	——	1.18	3.742
16	4	3/4	2.74	2.98	3.12	1.18	3.742
32	1	31/32	2.74	0.55	0.55	0.58	——
32	2	15/16	1.16	1.16	1.16	0.58	——
32	3	29/32	1.16	——	——	0.58	——
32	4	7/8	2.5	2.51	2.51	0.58	——
32	5	27/32	2.75	——	——	0.58	——
32	8	3/4	2.75	3	3.69	0.58	——

Table 4.1 PAPR reduction comparison [78]

T. Jiang and G. X. Zhu [79], proposed a new block coding scheme with low complexity called Sub-Block Complement Coding (SBCC). This is similar to the Fragiacomo's method, with almost the same advantages. At the end of coding techniques, we can conclude that simplicity and the abilities of this technique make it a good candidate for use in OFDM systems. The only disadvantage that can be mentioned is getting a worthy performance of PAPR reduction is at the price of coding rate loss. Table 4.2 illustrates the comparison for the three discussed major reduction techniques.

	Complexity for implementation	Bandwidth Expansion	Bit Error Rate Degradation	Power Increase
Selecting Mapping / Partial Transmission Sequence	HIGH	YES	NO	NO
Clipping and Filtering	LOW	NO	Yes	NO
Coding	LOW	YES	NO	NO

Table 4.2 Comparison for reduction technique

4.9 Proposed algorithm for reducing PAPR

OFDM is a multiplexing technique that divides the bandwidth into multiple frequency sub-carriers. It uses multiple sub-carriers which are closely spaced to each other without causing interference. As illustrated in figure 4.8, carrier centers are in orthogonal frequencies and there is an orthogonality relationship between signals. In this figure, the peak of each signal coincides with the trough of the other signals, and, since there is $1/T_s$ space between the subcarriers (SCs), the subcarriers are orthogonal. Orthogonality between two signals lets the multiple information signals be transmitted and detected without a glitch and interference.

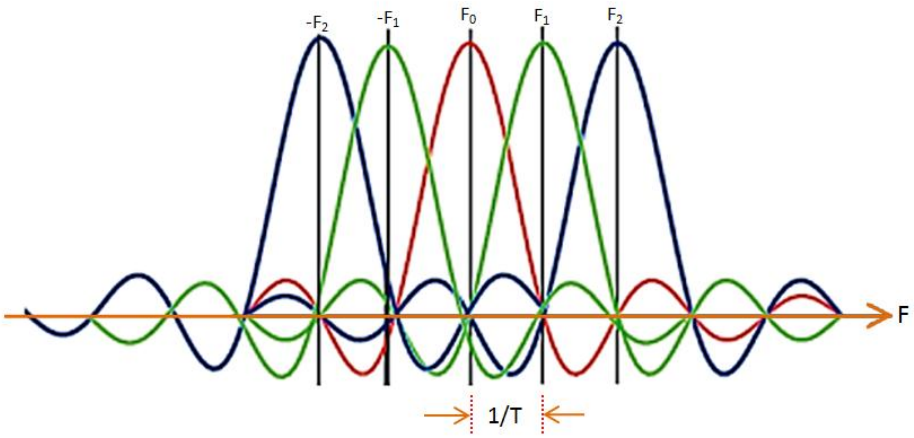

Figure 4.8 Space between subcarriers ($1/T_s$)

For designing an OFDM system, it is very useful to be able to apply a mathematical expression for calculating PAPR distribution. On the other hand, by having PAPR distribution, we can use it to calculate Bit Error Rate (BER). Depending on the type of model and technique used, we have a different expression for PAPR. However, PAPR is calculated from the peak-amplitude of the waveform divided by the average value of the waveform

$$PAPR = \frac{max_n\{|x[n]|^2\}}{E\{|x[n]|^2\}} \tag{4.6}$$

The amplitude of x[n] has a Rayleigh distribution, while the power has a central chi-square distribution with two degrees of freedom. The distribution of PAPR, in terms of a Complementary Cumulative Distribution Function (CCDF), can be given as follows [80]:

$$F_x(\propto) = Pr\left(\frac{|x[n]|^2}{E\{|x[n]|^2\}} < \propto\right) = 1 - e^{-\propto} \tag{4.7}$$

The probability that PAPR will be above a certain threshold point ($PAPR_0$) is [80]:

$$\Pr(PAPR > PAPR_0) = 1 - F(PAPR_0)^N = 1 - (1 - e^{-PAPR_0})^N \tag{4.8}$$

The decibel form for Eq. (3.8) is as follows:

$$PAPR_{dB} = 10log_{10}(PAPR) \tag{4.9}$$

As has been mentioned previously, there is $1/T_s$ space between the subcarriers and OFDM uses multiple sinusoidal, which can be defined as follows:

$$s(t) = a_0 g_0(t) + \ldots\ldots\ldots\ldots\ldots\ldots\ldots + a_{k-1} g_{k-1}(t) = \sum_0^{k-1} a_k g_k\,(t)$$

$$s(t) = \textstyle\sum_0^{k-1} a_k g_k\,(t) \tag{4.10}$$

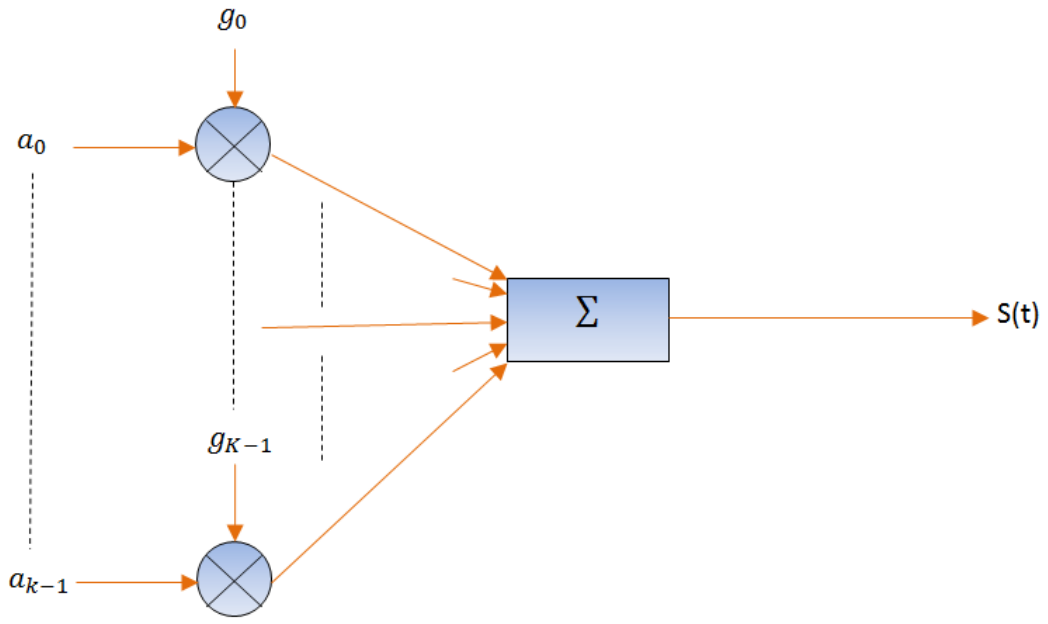

Figure 4.9 Illustration for Eq. (4.10)

where

$$g_k(t) = \frac{1}{\sqrt{T}} e^{\frac{2\pi ktj}{T}} \omega(t) \tag{4.11}$$

where $\omega(t) = u(t) - u(t-T), \qquad [0 \;\; T)$

By substituting Eq. (4.11) for Eq. (4-10) we get:

$$s(t) = \frac{1}{\sqrt{T}} \sum_0^{K-1} a_k \, e^{\frac{2\pi ktj}{T}} \, \omega(t) \tag{4.12}$$

where the a_k is information signal and $g_K(t)$ is corresponding carrier signal.

The simulation in figure 4.10 shows the reduction of PAPR of about 0.2 dB therefore the performance of reducing PAPR. This is the advantage of this method.

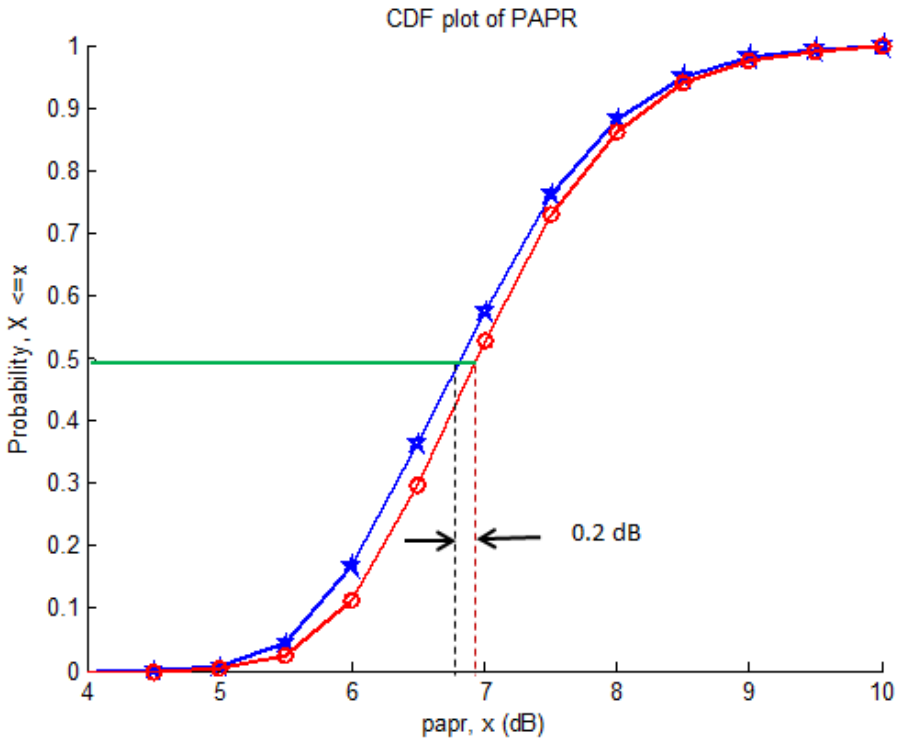

Figure 4.10 Reduction of PAPR is about 0.2 dB

Chapter 5

Path Loss

5.1 Introduction

In wireless communication, the radio propagation investigates the behavior of radio waves when they are transmitted from one point to another point. Radio propagation can be affected by numerous factors and understanding them has several practical benefits. When propagation is considered in an outdoor environment, one is primarily interested in three types of areas: urban, suburban, and rural areas. Of course, the presence of trees, buildings, moving cars, and other obstacles need to be considered also. The presence of objects in a channel can cause the channel to lose its free space classification. When this happens, various methods of propagation occur. These can be classified into four main propagation mechanisms: direct propagation, reflection, diffraction, and scattering. Generally speaking, radio waves can usually be affected by reflection, diffraction, and scattering whose intensity depends on the environment. Direct propagation is the Line Of Sight (LOS) signal component. Therefore, it can be considered as the free space propagation. The phenomena of reflection and scattering are functions of the wavelength and object dimensions. If the wave length is smaller than the dimension of the object, the phenomenon of reflection takes place. If the dimensions of

the object are smaller than the wavelength, the phenomenon of scattering happens. Reflection and scattering are the source of multipath in a channel which can change the signal amplitudes, signal phases, and times of arrival signals at the receiver antenna. Other terms that describe the multipath characteristics of a channel are delay spread, angle spread, and power delay. The change of signal amplitude over the time and frequency is called fading. Signal fading can be produced by various signal components (LOS and/or multipath propagation) or it can be caused by shadowing from an obstacle. In the former it is called multipath fading, and in the latter it is called shadow fading. Basically, fading can be categorized into two major kinds, Small Scale Fading (SSF) and Large Scale Fading (LSF). Small Scale Fading (SSF) happens when there is a rapid change in the signal levels. In a short distance, these changes in the signal level occur while the mobile station is in motion. In this case, the interference of the multiple signal paths is the factor that causes the rapid variation in the signal level. On the other hand, the Large Scale Fading (LSF) refers to average path loss and shadowing. Figure 5.1 is a brief graphic illustration of the different types of fading channel and table 5.1 shows the channel environment classification.

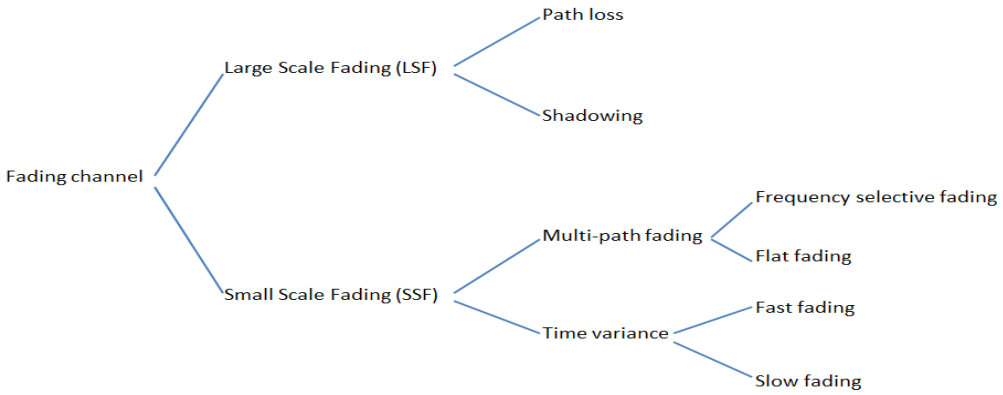

Figure 5.1 Types of various fading channel

Category	Objects in Channel	LOS / NLOS	Fading
Free space	No	LOS	Flat fading
LOS Multipath Environment	Yes	LOS + NLOS	Flat fading / Frequency selective
LOS Multipath + LOS interference	Yes	LOS + NLOS	Flat fading / Frequency selective
NLOS Multipath	Yes	NLOS	Flat fading / Frequency selective

Table 5.1 Classification of the channel environments

The radio channel is known by the amount of the Inter Symbol Interference (ISI). The movement of the transmitter and receiver, the presence and the type of the objects, and changing the weather conditions can cause the channel to vary over the time. All of the above mentioned issues and some other issues are factors that are considered in wireless system design and development. Figure 5.2 illustrates the LOS and multipath channel environment.

What makes the exact analysis of the wireless channel difficult is the dynamic environment between the transmitter antenna and receiver antenna. Optimization of the wireless communication systems is getting more and more critical due to the growth of the broad band mobile communication. Propagation models are usually used to predict the received signal strength at a certain distance from the transmitter. Propagation models are very useful for estimating the coverage area of the transmitter. This can help a radio service provider plan efficient radio coverage. Moreover propagation models are useful for predicting signal attenuation or path loss [82].

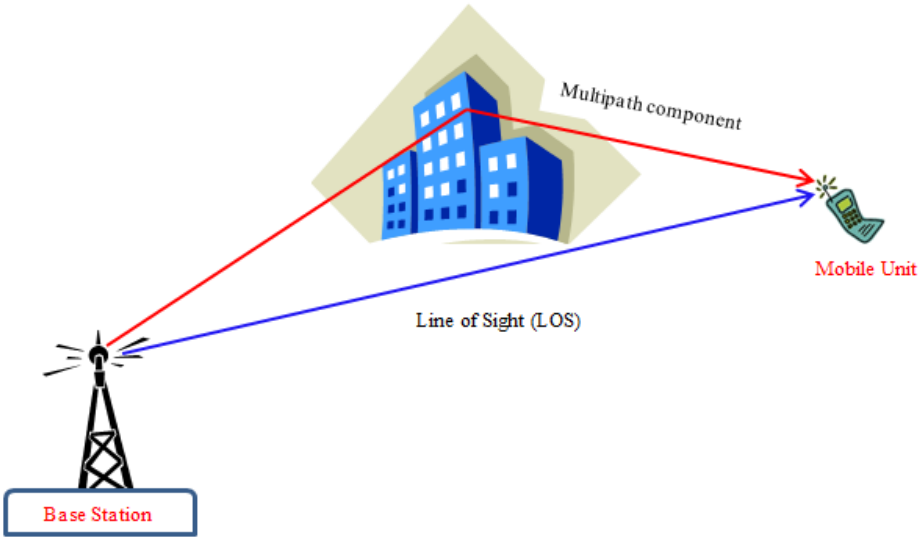

Figure 5.2 LOS, Multipath channel environment

5.2 Path loss models

There are different empirical and statistical models that can be used for outdoor and indoor environments. In the following section, we investigate some of the outdoor and indoor models which can be used as propagation models.

5.3 Free–Space model

This model is an analytical model in which the electromagnetic signals that radiate from transmitter antenna is a function of the inverse square of the distance(i.e. $1/d^2$) . This model is generally good for the satellite communication where the signals actually travel through the free space. This model is not an adequate model for precisely predicting the path loss for mobile communication systems where there are additional losses such as terrestrial obstacles, reflections, etc., Therefore, to construct a

more generalized model we need to consider the parameter in actual environments. The Friis equation [83] is the equation that is used for a free-space propagation model. This model is applicable for predicting the strength of the received signal where there is no obstacle between the transmitter antenna and receiver antenna, and the transmitter and receiver antenna are in line-of-sight (LOS). Figure 5.3 illustrates the free space model.

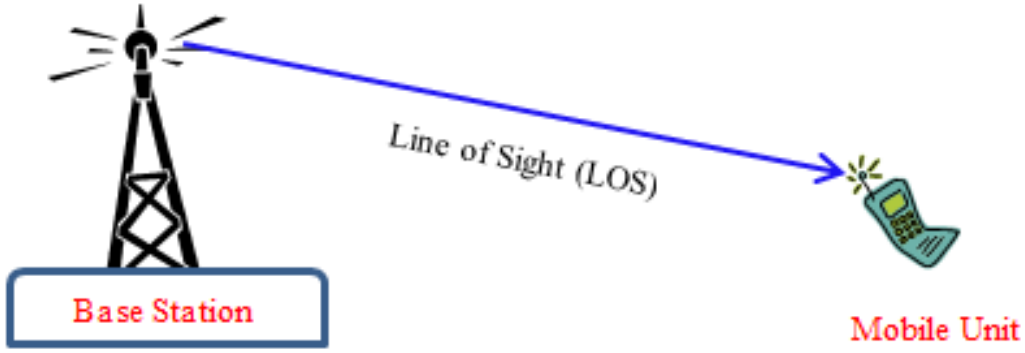

Figure 5.3 Free space model

The Friis equation is as follows:

$$P_r(d) = \frac{P_t G_t G_r \lambda^2}{(4\pi)^2 d^2 L} \tag{5.1}$$

where P_r is received power, P_t is transmitted power, G_t is transmitted gain, G_r is received gain, λ^2 is wavelength of the radiation, d is distance, and L is hardware system loss factor. Eq. (5.1) shows that the received power has an exponential relationship with the distance d, which it means it exponentially decreases by increasing the distance and it increases by increasing the antenna gains. The free space path loss, $PL_F(d)$, in dB can be stated as:

$$PL_F(d) = 10log\left(\frac{P_t}{P_r}\right) \tag{5.2}$$

$$PL_F(d) = -10log\left(\frac{G_t G_r \lambda^2}{(4\pi)^2 d^2 L}\right) \quad (5.3)$$

Since the actual environment has a direct effect on the received signal, to construct a more generalized model for path loss we need to consider it. The Log distance path loss model $PL_{LD}(d)$ is:

$$PL_{LD}(d) = PL_F(d_0) + 10log\left(\frac{d}{d_0}\right)^n \quad (5.4)$$

$$PL_{LD}(d) = PL_F(d_0) + 10nlog\left(\frac{d}{d_0}\right) \quad (5.5)$$

where d_0 is the reference distance and its value depends to the propagation environments, n is called path loss exponent and its value also depends toon the propagation environment (for free space $n = 2$). Since the surrounding environment depends on the location of the receiver and can vary, every path can have different path loss. To consider such a condition, a model called log normal shadowing is used. This model allows the receiver to have different path loss at the same distance from the receiver. This model is stated as follows:

$$PL(d) = \overline{PL}(d) + X_\sigma \quad (5.6)$$

$$PL(d) = PL_F(d_0) + 10log\left(\frac{d}{d_0}\right)^n + X_\sigma \quad (5.7)$$

Here X_σ is a Gaussian random variable with standard deviation of σ.

5.4 Plane-Earth Model

In this model the path loss is more than the free space. The received signals to the receiver antenna are a combination of the signals that come from the direct path and the

indirect path. The direct path is considered as the Line of Sight (LOS) signal and the signal that comes from the reflection form objects are considered as No Line of Sight (NLOS). This model is called the Plane-Earth model since it considers the reflection from the ground that is flat, not curved. The equation that is used for this analytical model is:

$$L_p = a\frac{h_r^2 h_t^2}{d^4} \tag{5.8}$$

or

$$L_p = 10\log a + 20\log h_t + 20\log h_r - 40\log d \tag{5.9}$$

where a is called correction factor and its value depends on the carrier frequency. h_r and h_t are the height of the receiver antenna and transmitter antenna, and d is the distance between transmitter antenna and receiver antenna, with this assumption that $d \gg h_t \; and \; d \gg h_r$.

5.5 Multipath Fading

There are short periods where there is no line of sight signal (NLOS) path between the transmitter antenna and receiver antenna. In this instance, the received signal in the receiver comes from the reflections from the different objects (see figure 5.4). Therefore, these reflected received signals have different amplitude, different phase and, to some extent, different times. These occurrences can cause the received power to the receiver to go up and down. This effect, which occurs over a short distances, is called fast fading. Since the Rayleigh distribution refers to the variations on the received power in

the absence of the existence of the line of sight (LOS) between the transmitter antenna and receiver antenna, the fast fading is also called Rayleigh fading. This is verified both experimentally and theoretically that it is a Rayleigh distributed [84]. The received signal envelope in a complex form can be stated as Eq. 5.10.

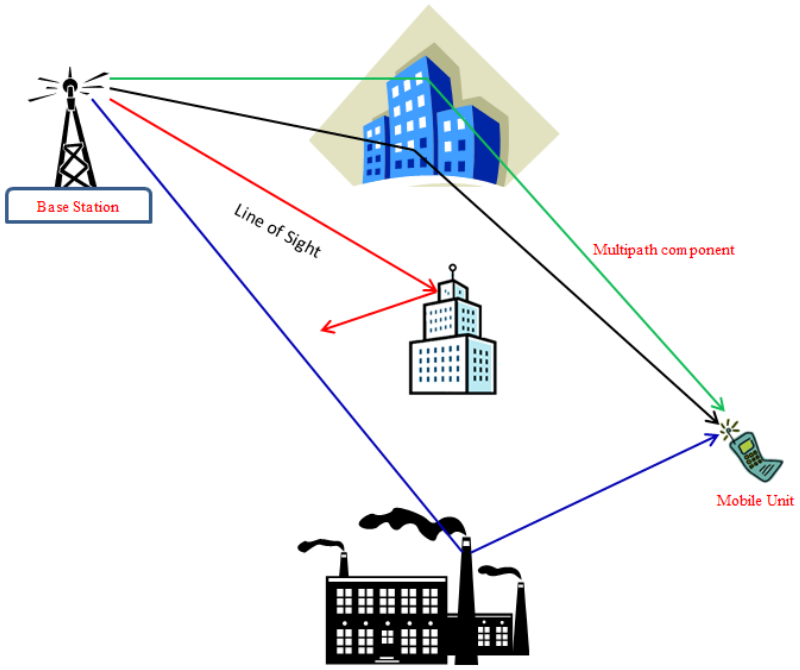

Figure 5.4 No LOS channel

$$S = \sum_{n=1}^{N} S_n e^{j\theta_n} \tag{5.10}$$

Here θ_n is the phase and S_n is the amplitude and $S = S_r + jS_i$

where the amplitude is:

$$S = \sqrt{S_r^2 + S_i^2} \tag{5.11}$$

It is necessary to mention that the term Fast Fading does not always refer to the movement for the transmitter, the receiver, or both of them. It only implies that the distance between continuous fades are to some extent small. Undeniably, it is obvious that if the transmitter, the receiver, or both of them are in motion, the chance of successive fades occurring will increase at that time.

5.6 Delay spread

In multipath there are different path lengths from the transmitter antenna to the receiver antenna. Therefore, different signals from different paths hit the receiver antenna at different times. Comparing with symbol period, when the maximum time difference (τ_{MAX}) between the first arriving signal and last one is big enough, the receiver experiences the Inter Symbol Interference (ISI). In time domain, delay spread is directly related to coherence bandwidth W_c in frequency domain. The relation between delay spread and coherence bandwidth is [85]:

$$W_c \approx \frac{1}{\tau_{MAX}} \tag{5.12}$$

If $W\tau_{MAX} \geq 0.1$, then the channel is considered as frequency selective and if $W\tau_{MAX} < 0.1$ then the channel is considered as frequency flat [86, 87]. To show that the channel is not flat, consider figure 5.5 with two signal paths and with the equal amplitude A. One of them hits the receiver antenna with delay.

In this model, the received signal can be written as:

$$r(t) = As(t) + As(t - \tau_{MAX}) \tag{5.13}$$

Take the Fourier transform

$$R(f) = AS(f) + AS(f)e^{-j2\pi f\tau_{MAX}} \tag{5.14}$$

$$R(f) = AS(f)\left[1 + e^{-j2\pi f\tau_{MAX}}\right] = AS(f)H(f) \tag{5.15}$$

where the transfers function $H(f)$ and its magnitude $|H(f)|$ can be stated as follows:

$$H(f) = 2e^{-j2\pi f\left(\frac{\tau_{MAX}}{2}\right)} cos\left[2\pi f\left(\frac{\tau_{MAX}}{2}\right)\right] \tag{5.16}$$

$$|H(f)| = cos\left[2\pi f\left(\frac{\tau_{MAX}}{2}\right)\right] \tag{5.17}$$

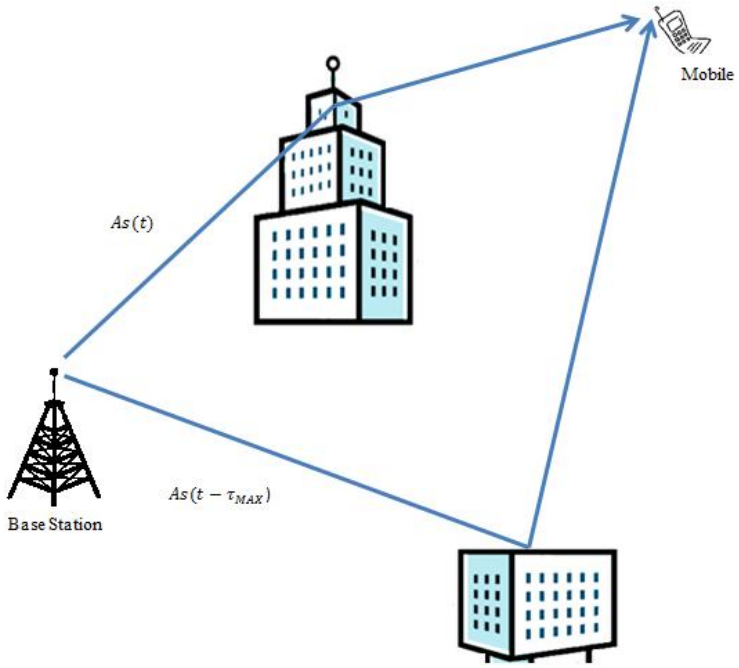

Figure 5.5 Two multipath components

5.7 Okumura-Hata (OH) Model

The Okumura-Hata model [88] is a usual propagation model that can be used for an urban area, a suburban area and an open area. Okumura/Hata is the most common model that is applied for path loss. The Okumura model is the model that has been gained after doing numerous experiments [89]. It is one kind of model that is used for predicting

the path loss in urban areas for mobile communication systems [90]. For determining the path loss, the OH model uses empirical data. According to the OH model, the path loss (L_{OH}), in terms of dB for different environments, is as follows [88]:

$$L_{OH} = A + B.\log_{10}(d) + CA \tag{5.18}$$

where L_{OH} is the path loss for Okumura-Hata model and d is the distance of the Base Transceiver Station to Mobile Station in terms of meters which sometimes is shown as d_{BTS-MS}. A. B depends on the antenna height and frequency and is defined as follows:

$$A = 69.55 + 26.16\log_{10}(f) - 13.82\log_{10}(h_b) - a(h_m) \tag{5.19}$$

$$\mathrm{B} = 44.9 - 6.55\log_{10}(h_b) \tag{5.20}$$

Where f is the frequency in terms of MHz, $a(h_m)$ is called the correction factor for the Mobile Station antenna (MS-antenna) with the height h_m in terms of meters, and h_b is the BTS-MS distance in terms of meters.

CA is the environmental correction factor and has a different value for urban, suburban and open areas as follows:

CA for open areas is:

$$CA = 4.78(log_{10}(f))^2 + 18.33\log_{10}(f) - 40.94 \tag{5.21}$$

CA for suburban areas is:

$$CA = -2(log_{10}(f/28))^2 - 5.4 \tag{5.22}$$

CA in dB for urban areas which can be considered as:

For a large city:

$$a(h_m) = 8.29(\log_{10} 1.54.h_m)^2 - 1.1 \qquad for\ f \geq 400\ MHz \tag{5.23}$$

For a medium to small city:

$$a(h_m) = (1.1\log_{10}(f) - 0.7).h_m - (1.56\log_{10}(f) - 0.8) \tag{5.24}$$

The environmental correction factor for an urban area that is considered small can be considered as zero (CA=0). Figure 5.6 show the free space propagation path loss versus the Okumura Hata (OH) model for an open area, an urban area and a suburban area. In figure 5.6, the values of the parameters are as follows: $h_m = 1.5\,meter$, $h_b = 25\,meters$ and $f = 900\,MHz$.

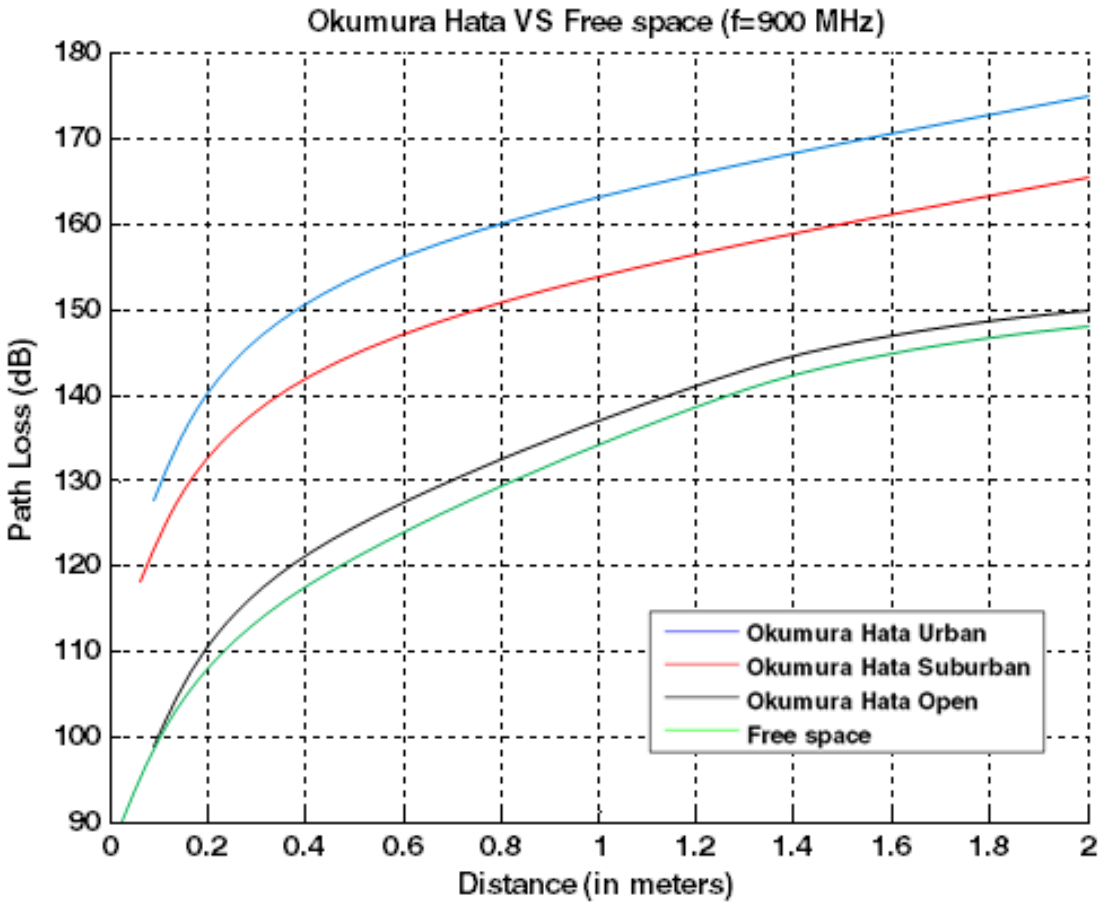

Figure 5.6 OH model VS free space path loss

Figure 5.7 shows the path loss in an urban zone versus a plain zone for this model. As expected, due to the obstructions that can be found in an urban zone, the path loss is much larger than in the open zone.

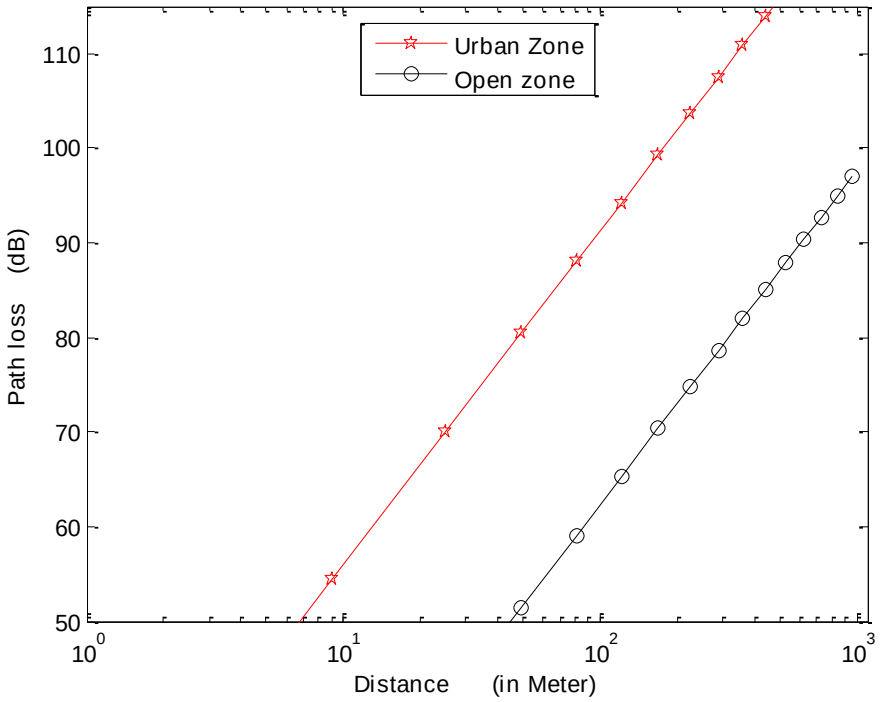

Figure 5.7 Path loss in urban zone versus open zone

The Okumura-Hata (OH) model has some limitations. Since the signal level can be severely affected by both Line Of Sight (LOS) and Non-Line Of Sight (NLOS) signal paths in the distances less than one kilometer [91], Okumura-Hata is not suitable for the personal communication systems that are under a circular area with a one kilometer radius. There is also a limitation for the range of the h_m, h_b and f as follows:

$$150\ MHz \leq f \leq 1500\ MHz$$

$$1\ meters \leq h_m \leq 10\ meters$$

$$30\ m \leq h_m \leq 200\ m$$

5.8 COST-231 Model

This model is the extension of thr Okumura-Hata model. The COST-231 model gives us more freedom in frequency range by extending the frequency bound to 2 GHz. The frequency range in this model is:

$$150\ MHz \leq f \leq 1500\ MHz$$

The path loss (L_{C-231}) for COST-231 is given as follows [92, 93]:

$$L_{C-231} = A_{C-231} + B.\log_{10}(d) + C_{C-231} \tag{5.25}$$

$$L_{C-231} = 46.3 + 33.9\log_{10}(f) - 13.82\log_{10}(h_b) - a(h_m) + \tag{5.26}$$

$$[44.9 - 6.55\log_{10}(h_b)]\log_{10}(10) + C_{C-231}$$

Since this is the extended model for the Okumura-Hata model, the $a(h_m)$ is the same as mentioned in Equations (5.22), (5.23), and (5.24). The values of (C_{C-231}) depends to the dimensions of the city. For instance, for small to medium cities it can be considered zero ($C_{C-231} = 0$) and for big cities it can be considered 3 dB ($C_{C-231} = 3\ dB$).

5.9 Dual Slope Model

As previously mentioned, another weakness of the Okumura-Hata model is that it is not suitable for the zones which are under a circular area with less than a one kilometer radius. The Dual Slope model can be used for extending the Okumura-Hata model to cover less than one kilometer as follows:

$$L_{Near} = L_{OH}(L_{BP}) + slope_L[\log_{10}(d) - \log_{10}(d_{BP})] \tag{5.27}$$

d_{BP}, $slope_L$ and d respectively is: break point distance which is 1 kilometer, path loss slope for near area and BTS-MS distance in Kilometers. The $Slope_L$ is given as follows [91]:

$$slope_L = \frac{L_{OH}(d_{BP})\log_{10}(d_{BP}) - L_{FS}(d_{20})\log_{10}(d_{20})}{\log_{10}(d_{BP}) - \log_{10}(d_{20})} \quad (5.28)$$

Here $d_{20} = 20\ meters$ and $L_{FS}(d_{20})$ which is called free space path loss is as follows:

$$L_{FS}(dB) = 3.24 + 20\log_{10}(f) + 20\log_{10}(d) \quad (5.29)$$

where f and d respectively are frequency in Mega Hertz and BTS-MS distance in meters.

5.10 Multi-Slope/Extended Hata model for urban zone

This model, which is actually an extended Hata model for urban areas, is an approach for path loss where the distance is from 0.1 kilometer to 20 kilometers ($0.1\ km \leq d \leq 20\ km$) [94]. This model divided the distance into three categories. For each category it proposes an equation. The equations for this model are [94]:

$for\ \ d < 0.4\ km$

$$L(d) = 32.4\log_{10}(f) + 10\log_{10}[d^2 + (H_b - H_m)^2/10^6] \quad (5.30)$$

$for\ \ d < 0.1\ km\ \ and\ d > 0.4\ km$

$$L(d) = L(0.04) + \frac{\log_{10}(d) - \log_{10}(0.04)}{\log_{10}(0.1) - \log_{10}(0.04)}[L(0.1) - L(0.04)] \quad (5.31)$$

$for\ \ d < 0.1\ km\ \ and\ d > 0.4\ km$

$$L(d) = 46.3 + 33.9\log_{10}(2000) + 10\log_{10}(f/2000) - 13.82\log_{10}(max\{30, H_b\})$$
$$+(44.9 - 6.55\log_{10}(max\{30, H_b\}))(\log_{10}(d)) - a(H_m) - b(H_b) \quad (5.32)$$

where

$$a(H_m) = (1.11\log_{10}(f) - 0.7)min\{10, H_m\} - (1.56\log_{10}(f) - 0.8)$$
$$+max\{0, 20\log_{10}(max\{H_m/10\})\} \quad (5.33)$$

$$b(H_b) = min\{0, 20\log_{10}(max\{H_b/30\})\} \quad (5.34)$$

Here $d\ and\ f$ are the distance between the transmitter and the receiver in terms of km. The carrier frequency in terms of MHz, H_b is the maximum height of the transmitter antenna and the receiver antenna in terms of km antenna. H_m is the minimum height of the transmitter antenna and the receiver antenna in terms of km. When the height of the antenna is very low for $b(H_b)$ the following equation should be used:

$$b(H_b) = (1.11\log_{10}(f) - 0.7)min\{10, H_b\} - (1.56\log_{10}(f) - 0.8)$$
$$+max\{0, 20\log_{10}(max\{H_b/10\})\} \quad (5.35)$$

Figure 5.8 [94] shows the mean path loss versus the distance between the transmitter antenna and the receiver antenna at 2.6 GHz for different distances.

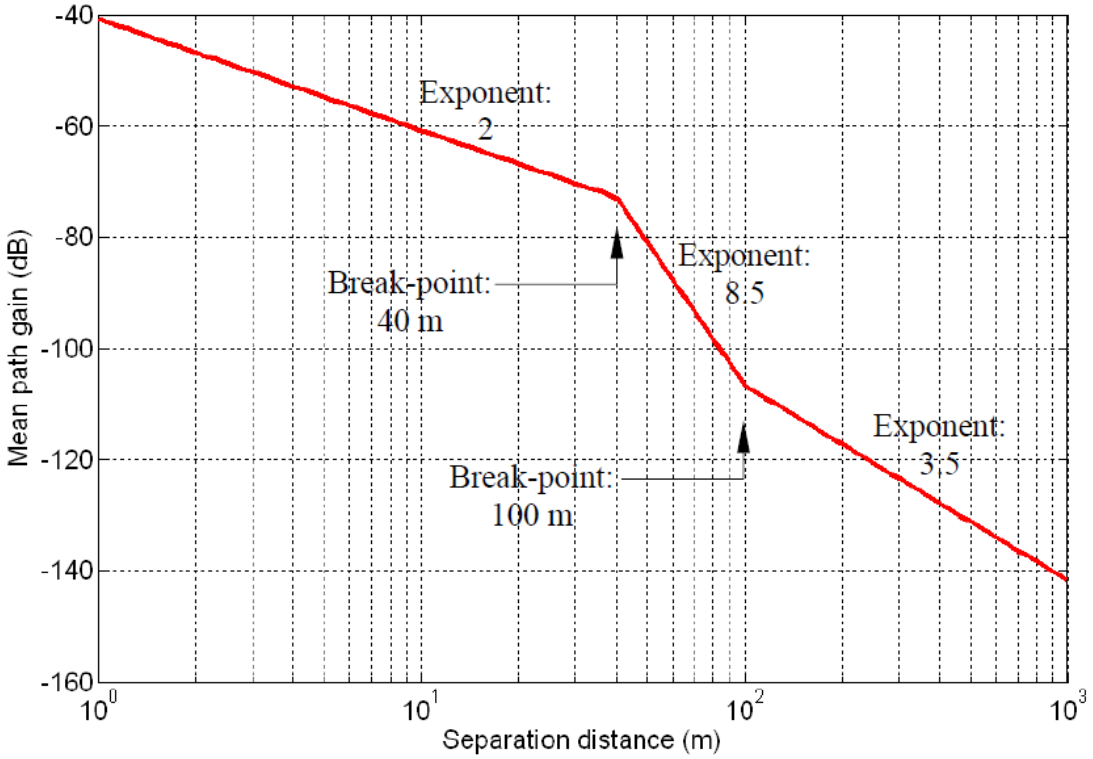

Figure 5.8 Mean path loss as the function of the distance between the transmitter and receiver antenna [94]

5.11 The other Models

There are different models [95, 96] that have recently been developed and used. Most of them come from the measurement for different situations and different cases and most of them also use different parameters for different conditions and cases.

5.12 Indoor path loss

Due to the increasing usage of the Personal Communication Systems (PCS), there is heightened interest in characterizing radio propagation inside buildings. Because of the refractions, reflections, and diffraction by the objects inside the malls or buildings, the signals that reach the receiver comes from a different path. Generally, the indoor

propagation is influenced by the layout of the building. Path loss between the transmitter and the receiver is the amount of average attenuation that the Radio Frequency (RF) experiences. This amount depends on whatever is between the transmitter antenna and the receiver antenna. This path loss in dB is defined by [97]:

$$PL(dB) = 10log\frac{P_t}{P_r} \tag{5.36}$$

where P_r is received power and P_t is transmitted power.

5.13 Indoors Propagation

Considering the growth of the OFDM mobile communication system, the size of a cell is getting smaller and smaller; from Macro-cell to the Pico-cell. Therefore, the services should include both indoor and outdoor environments.

The differences of the indoor mobile channel to the outdoor mobile channel can be summarized as follows:

i. The distance covered in an indoor environment is considerably smaller;

ii. The indoor environment has more variability;

iii. Due to the nature of the structures of the buildings, or malls, and the materials that have been used to construct them, the indoor propagation inside the malls and buildings has a more complex multipath structure.

5.14 Building propagation

The propagation of waves inside the malls and buildings has a complex mechanism which governs by some detailed parameters. These parameters depend on the

following criteria: building layout, structure of the building, type of the walls and windows (which specifies the wave penetration), and propagation inside the building and between the interior walls and roofs.

5.15 Wall Penetration

The amount of path loss during the penetration of the waves inside the buildings depends on:

(i) the wall dielectric coefficient;

(ii) the thickness of the wall;

(iii) the direction of the wave incident;

(iv) the polarization of the waves.

There is another loss for the waves that passes through the walls. This loss is called Ohmic loss. The amount of Ohmic loss depends on the type of the material that is used for building the walls and its moisture content.

5.16 Window Penetration

The windows of the building are considered as receiving apertures. All the plane waves that hit the windows can penetrate through the windows without any attenuation to the depth of $(\frac{S^2}{4\lambda})$. Figure 5.9 illustrates the passage of wave through the window. Any diffusion inside the building can happen when the wave is diffracted by the objects and bounced from the interior walls. The other diffraction that can be considered is that from

the windows' edges. These diffractions can affect the plane wave that goes through the window.

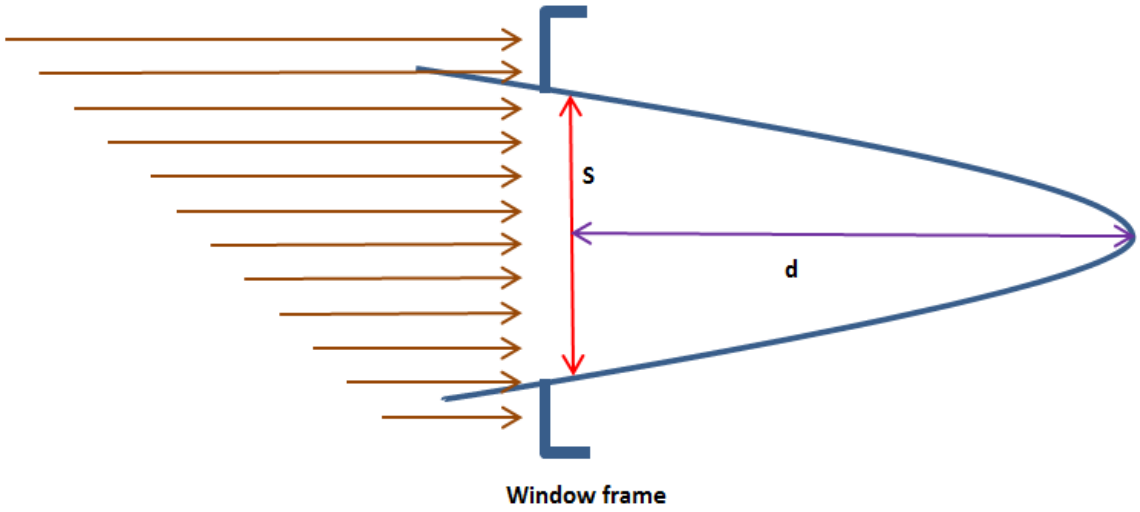

Figure 5.9 Passage of wave through the window

5.17 Indoors Propagations

Indoor propagations include floor propagation and interior propagation. Since the floor is usually built with reinforced steel grid, the usual loss can be considered from 10 to 20 dB/F (dB per floor). The interior of the building varies from big open spaces (such as spaces in the malls) to dense spaces (such as crowded offices).

5.18 Indoor model

Because of the increased usage of mobile systems inside malls, buildings, airports, and train stations [98], the indoor propagation prediction is getting increasingly more important for OFDM mobile systems. There are different approaches to model

indoor propagation. A good approach can be based on the empirical propagation model combined with an electromagnetic theory such as Uniform Theory of Diffraction (UTD). As previously discussed, for indoor path loss walls and floors need to be considered. Depending on the type of the walls and floors, each has an attenuation factor [99, 97]. Wall attenuation is a function of the angle of incident. Wave incident to the wall partially reflects and partially penetrates.

Considering Snell's law of refraction (Eq. 5.37), the reflection and transmission between two media depends on the dielectric constant of the media and the incident angle of the wave.

$$\frac{Cos\theta_1}{Cos\theta_2} = \sqrt{\frac{\varepsilon_2}{\varepsilon_1}} \tag{5.37}$$

where ε_1, ε_2 are dielectric constant, θ_1, θ_2 are angle of incident and reflation.

Figure 5.10 illustrates the wall attenuation for two different wall structures [100]. Floor attenuation also depends on floor structure.

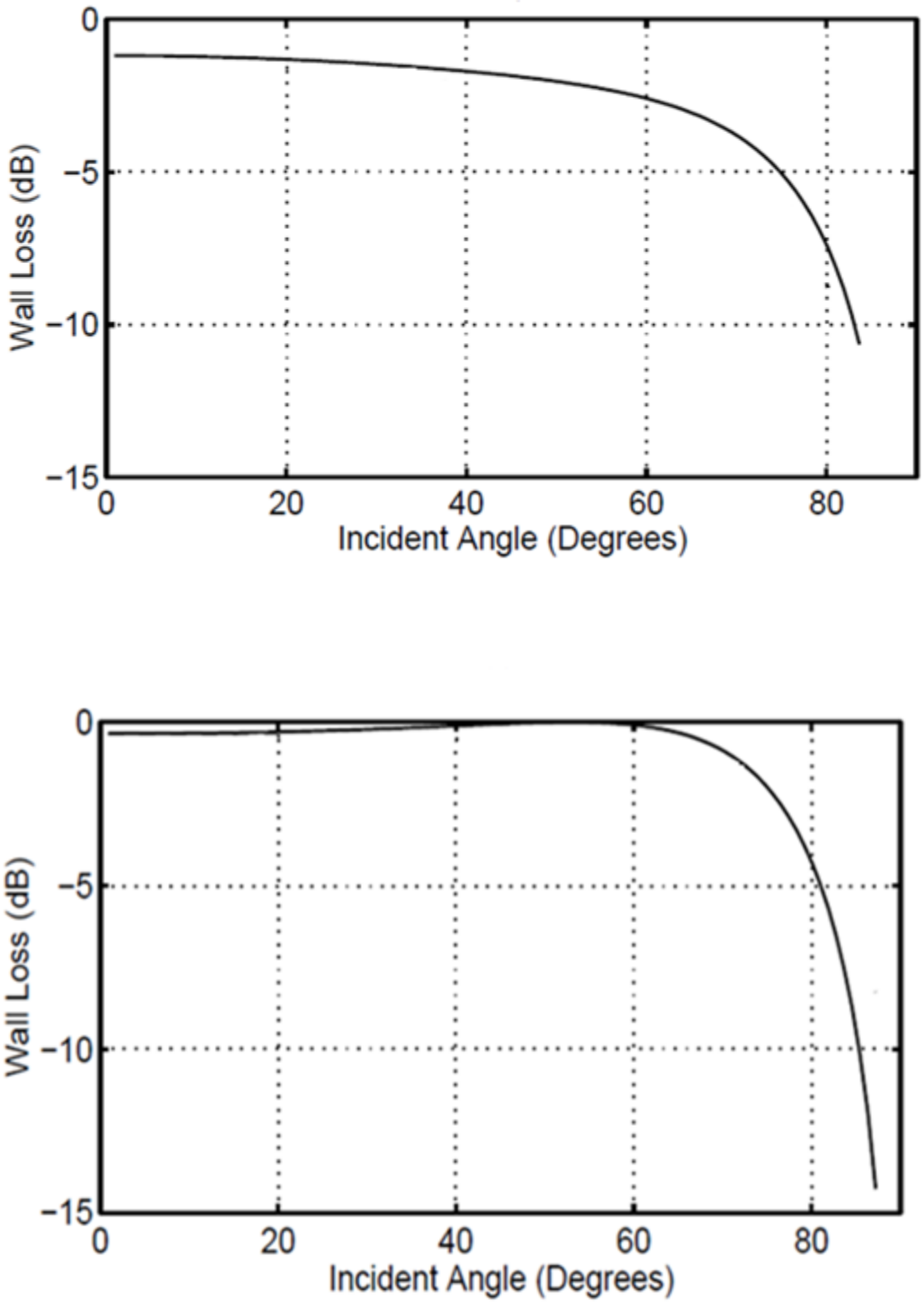

Figure 5.10 Wall attenuation for two different wall structures [100]

Table 5.2 shows the floor attenuation for two different buildings [101].

Office Building #1		
Location	**FAF (dB)**	**PL (dB)**
Through 1 floor	12.9	7
Through 2 floor	18.7	2.8
Through 3 floor	24.4	1.7
Through 4 floor	27	1.5

Office Building #2		
Location	**FAF (dB)**	**PL (dB)**
Through 1 floor	16.2	2.9
Through 2 floor	27.5	5.4
Through 3 floor	31.6	7.2

Table 5.2 The average floor attenuation for two different building [101]

On the other hand, the distance of the building from the transmitter antenna is an important factor. The distance inside the buildings or malls where considerable attenuation starts to occur is called Break Point (BP) [102]. This break point depends on the location, the structure of the buildings, and their distance from the transmitter antenna. The distance of break point (d_{BP}) can be calculated by using the size of first Fresnel zone [22]. The model for indoor path loss can be considered as [99, 97]:

$$PL_{BP}(d) = 10\log\left(\frac{d}{d_0}\right)^{n1} U(d_{BP} - d) + 10\left[\log\left(\frac{d_{BP}}{d_0}\right)^{n1} + \log\left(\frac{d_0}{d_{BP}}\right)^{n2}\right] U(d - d_{BP}) + \sum_{p=1}^{P} WAF(p) + \sum_{q=1}^{Q} FAF(q) \quad (5.38)$$

where WAF is wall attenuation factor, FAF is floor attenuation factor, P and Q are the number of walls and floors, n_1 and n_2 are path loss components, and $U(d_{BP} - d)$ is a

step function, when $d < 0$ the value of step function is 0, and when $d \geq 0$ the value of step function is 1.

When electromagnetic radiation is incident on a wall or a floor in an oblique fashion, less power will be transmitted through the wall than would happen at the normal incidence. In this case, the $WAF(P)$ term changes to $WAF(P)/cos\emptyset_p$ and the $FAF(q)$ term changes to $FAF(p)/cos\emptyset_q$ [103] where $\emptyset_p$ and $\emptyset_q$ are the angles of incidence of the signal on the walls and floors. Note that inside malls and buildings, the received signals to the mobile unit are the summation of the infinite number of the scatters. It is also worth mentioning that the indoor propagation, like outdoor propagation, can be subject to LOS or NLOS. The only difference is that the LOS environment follows Rician distribution while the NLOS environment follows Rayleigh distribution.

5.19 Proposed algorithm

The objective of channel characterization is its evaluation, at any point within the region and at any time, in terms of its effect on the performance of the wireless communications system.

In order for a channel model to be reliable for designing and system research of OFDM based systems, it should consider the following criteria:

i) it should be as close as it possible to the physical propagation phenomena for the desired environment;

ii) it should be as simple as it can be for simulation;

iii) it should be a comprehensive model for different case scenarios, not for a particular condition.

Considering [105-108], the IEEE is using the Eq. (5.39) to model the path loss. This model considers for $d > d_0$:

$$PL_{IEEE}(d) = PL_F(d_0) + 10\gamma \log_{10}\left(\frac{d}{d_0}\right) + C_f + C_{RX} \tag{5.39}$$

where d_0 is 100 meters. C_{RX}, which is related to the receiver antenna, is called the correlation coefficient for receiver antenna. C_f, and γ are defined as:

$$C_f = 6 \log_{10}\left(\frac{f_c}{2000}\right) \tag{5.40}$$

$$\gamma = a - bH_{TX} - \frac{c}{H_{TX}} \tag{5.41}$$

Here H_{TX} is the height of the transmitter antenna. Depending on the model, the parameters a, b, and c can get different values. The following values are the range of values that are considered in IEEE for different path loss models. Depending on the models, these values are: $3.6 \leq a \leq 4.6$, $0.007 \leq b \leq 0.005$, and $12.6 \leq c \leq 20$

For this model, d_0, which is considered as the initial or reference distance, causes a discontinuity at $d = 100$ meters. To fix this problem, a different reference distance, which is called d_{00}, should be defined [106, 107]. To find d_{00}, Eq. (5.3) is used as a reference. The proposed equation is as follows:

$$PL_T(d) = PL(d)_{|d_{00}} + PL_{BP}(d) + L_{OA} \tag{5.42}$$

In Eq. (5.42); $PL(d)_{|d_{00}}$ is the path loss with the new initial reference (i.e. d_{00}), $PL_{BP}(d)$ is break point path loss, and L_{OA} is the attenuation impact factor. The result of proposed method has been discussed in Chapter 6, Section 6.5.

Chapter 6

Results, Conclusion and future Work

6.1 Preface

The goal of this dissertation was to focus on the study of the effects of Carrier Frequency Offset (CFO) and frequency synchronization on OFDM wireless systems. Although we have targeted on the effect of CFO on OFDM wireless systems and have completely achieved this objective in Chapter 3, we have presented two independent pieces of work on PAPR and path loss for OFDM Wireless systems.

Since the high PAPR is another major drawback in OFDM wireless systems, we have decided to dedicate Chapter 4 to investigate PAPR. Since the path loss is the main reason for losing power between the transmitter and the receiver antenna in any wireless communication system, we have devoted Chapter 5 to investigating the indoor and outdoor path loss for OFDM wireless systems.

Please note that part of the work that has been presented in Chapters 3, 4, 5, and 6 of this dissertation have been published by us in journals (see the list of our publications in page 133).

6.2 Summary

In Chapter 1 of this dissertation, we have talked about five main elements that have been followed for our research. These five elements are: background, problem statement, objective, scope of research, and methodology. This chapter is followed by the chapter organizations section. This section includes the main titles that have been studied and reviewed in each of the individual chapters.

In Chapter 2 we have presented a short review on the history of OFDM and the concept of OFDM systems. We have talked about the advantages and disadvantages of OFDM wireless systems and we have gone through the pros, the cons, and the challenges that are inherent in OFDM wireless systems. We have also talked about modulation, path losses, and fading related to OFDM wireless systems. Finally, we have had a short discussion on the choice of the OFDM parameters and which is the most important of these to be considered. In short, this chapter has provided a brief but a good knowledge base on OFDM wireless systems.

In Chapter 3, which is the main chapter, the focus is on Carrier Frequency Offset (CFO). In this chapter, CFO has been discussed in detail. After discussing the sources of creating CFO, the effect of CFO and frequency synchronization on different parameters that are problematic in OFDM wireless systems have been reviewed and investigated from different aspects and in detail.

This chapter has also included a detailed discussion on CFO, frequency error, and frequency synchronization. The most important CFO estimation techniques and algorithms, such as blind and semi-blind algorithm, training based algorithm, periodic

preambles and cyclic preambles, have been studied, compared and covered in this chapter. Finally, we have proposed an algorithm for CFO estimation techniques which has lower computation complexity.

In Chapter 4, after explaining and reviewing the Peak to Average Power Ratio (PAPR), the causes of creating PAPR have been investigated. We have discussed the effect of PAPR on OFDM wireless systems in detail. We have also included a detailed discussion on PAPR reduction techniques and algorithms such as Selecting Mapping (SLM), Partial Transmission Sequence (PTS) and clipping and filtering techniques. Finally, we have presented our proposed technique for PAPR reduction.

In Chapter 5, we have presented a short investigation and overview of the behavior of the radio waves propagation. After a detailed discussion on the path loss models, we investigated the factors that cause indoor path loss and outdoor path loss. We also studied the indoor and outdoor propagation in detail. Finally, we have proposed a comprehensive algorithm that can be used to predict the path loss for indoors/outdoors in the usual urban area.

6.3 Carrier Frequency Offset (CFO)

In Chapter 3, we discussed the CFO and presented comprehensive literature for CFO and frequency synchronization. We analyzed the effects of CFO on different parameters on an OFDM wireless system.

As previously mentioned, CFO is called the most significant drawback in Orthogonal Division Multiplexing wireless systems. In this dissertation, we have

investigated and overviewed the frequency synchronization algorithms and methods that can be used to estimate the CFO for wireless communication OFDM systems. Our main goal was to find a technique that can set a fair balance between the computational complexity and good performance. During the investigation of the different CFO estimation techniques, we found out when CFO is very large, we will experience performance degradation. This degradation of performance is due to the approximation error.

In Chapter 3 we presented a comprehensive and detailed analysis of the effect of CFO on OFDM wireless systems. We studied the effect of CFO on different factors on OFDM wireless systems. As mentioned, one of the causes that creates CFO is the Doppler Effect (DE).

Doppler Effect, which is also called dynamic CFO, is the result of moving the receiver, the transmitter, or both.

Considering the tolerances that the electronic components have, there is always a difference between the carrier frequencies that the local oscillator creates in the receiver and the one that is created in the transmitter. Therefore:

$$f_r = f_c \pm f_{dif} \tag{6.1}$$

where f_r and f_c are respectively carrier frequency in the receiver and carrier frequency on the transmitter side, and f_{dif} is the difference between them.

The equation for the Doppler Effect is as follows:

$$f_d = \frac{v.f_c}{c} \tag{6.2}$$

Here f_d is Doppler Frequency, c is the speed of light, and v is the velocity of the moving receiver.

The maximum Doppler Frequency is defined as:

$$f_d = \frac{u}{\lambda} \tag{6.3}$$

u Relative speed between receiver and transmitter

λ Carrier wavelength

On the other hand, the amount of frequency offset depends to the angle of incident (AOI). Therefore, we have:

$$f = f_d cos\theta \tag{6.4}$$

According to the [110] the probability of the distribution of the AOI can be expressed as:

$$p(\theta) = \frac{e^{kcos(\theta-\alpha)}}{2\pi I_0(k)}, \quad and \quad \theta \in (-\pi, \pi] \tag{6.5}$$

α Angle between mobile and scattering

$I_0(k)$ Zero order Bessel function

k Directional scattering bandwidth (DSBW)

Figure 6.1 illustrates the relative location of the Base Station (BS) and a moving vehicle. This figure shows the Doppler frequency respect to angle of incident. What

reaches the receiver antenna is: $f \in [(f_d(cos\alpha - \emptyset), f_d cos\alpha]$ and $f \in [f_d cos\alpha, f_d \cos(\alpha + \emptyset)]$ where $\emptyset$ is the antenna beam width.

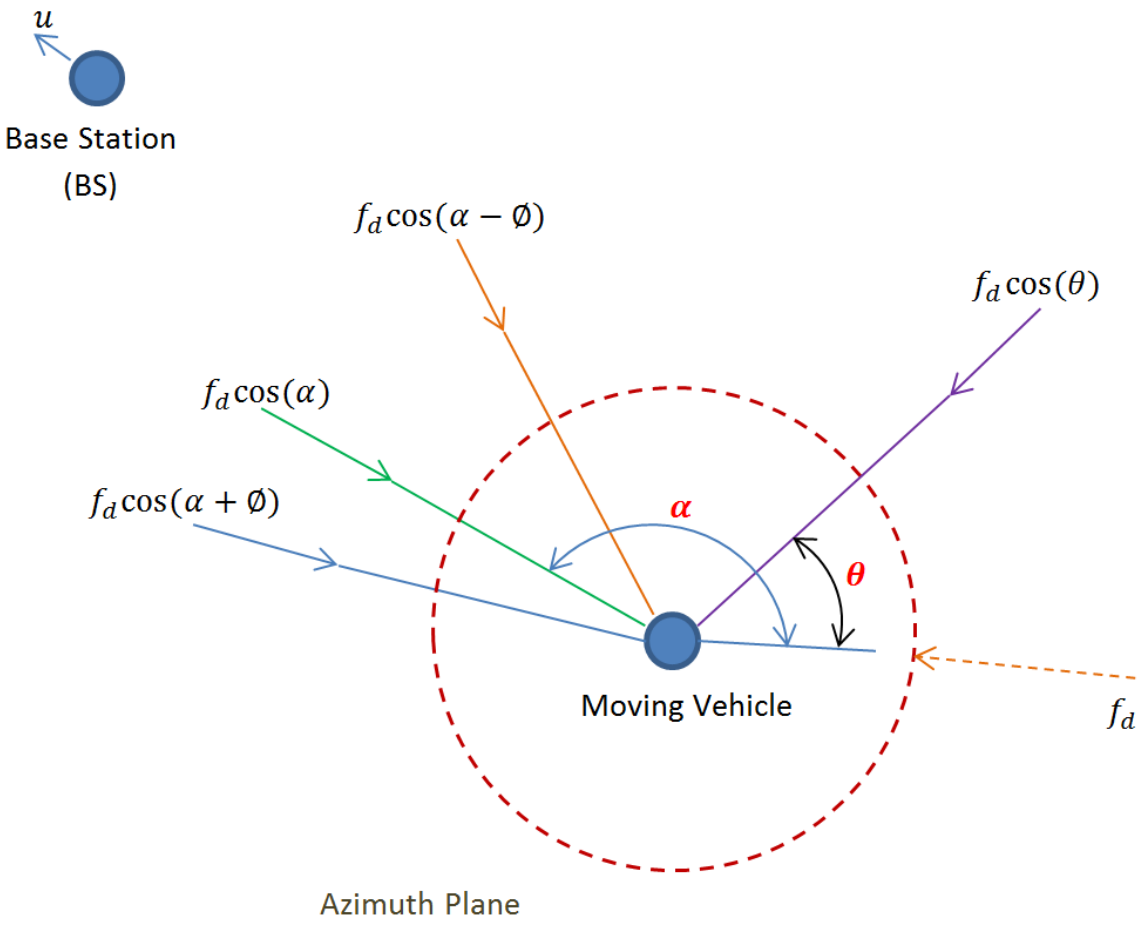

Figure 6.1 Doppler frequency respect to the angle of incident

As is obvious from the above discussion, the vehicle speed, the angle of the incident of the transmitted signal, and the direction of moving vehicle have serious effect on frequency offset. It is good to mention that the Vehicle Travel Direction (VTD) can vary from 0 to 2π. Figure 6.2 is an illustration of the moving component in wireless vehicle communication.

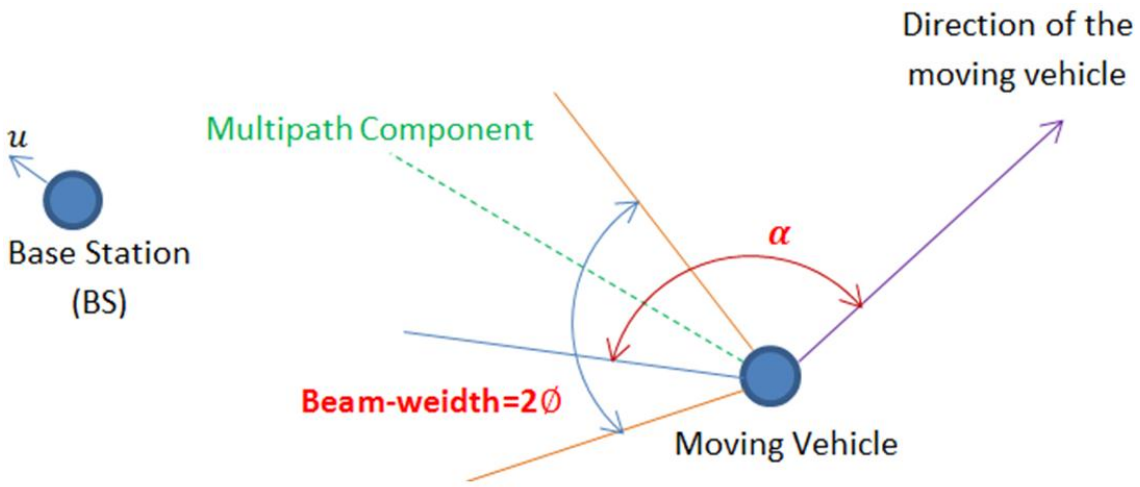

Figure 6.2 Illustration of moving component in wireless vehicle communication

Therefore, we can consider the following equation:

$$f = f_d cos\theta = f_c \frac{v}{c} cos\theta \tag{6.6}$$

where θ is the angle between two vectors, i.e. electromagnetic wave and velocity. The normalized Doppler frequency is defined as [111]:

$$\varepsilon_d = T f_c \frac{v}{c} cos\theta \tag{6.7}$$

As figure 6.3 [111] shows, by growing velocity, the normalized Doppler Frequency will be increased. On the other hand, the angle θ is the one that assigns its sign.

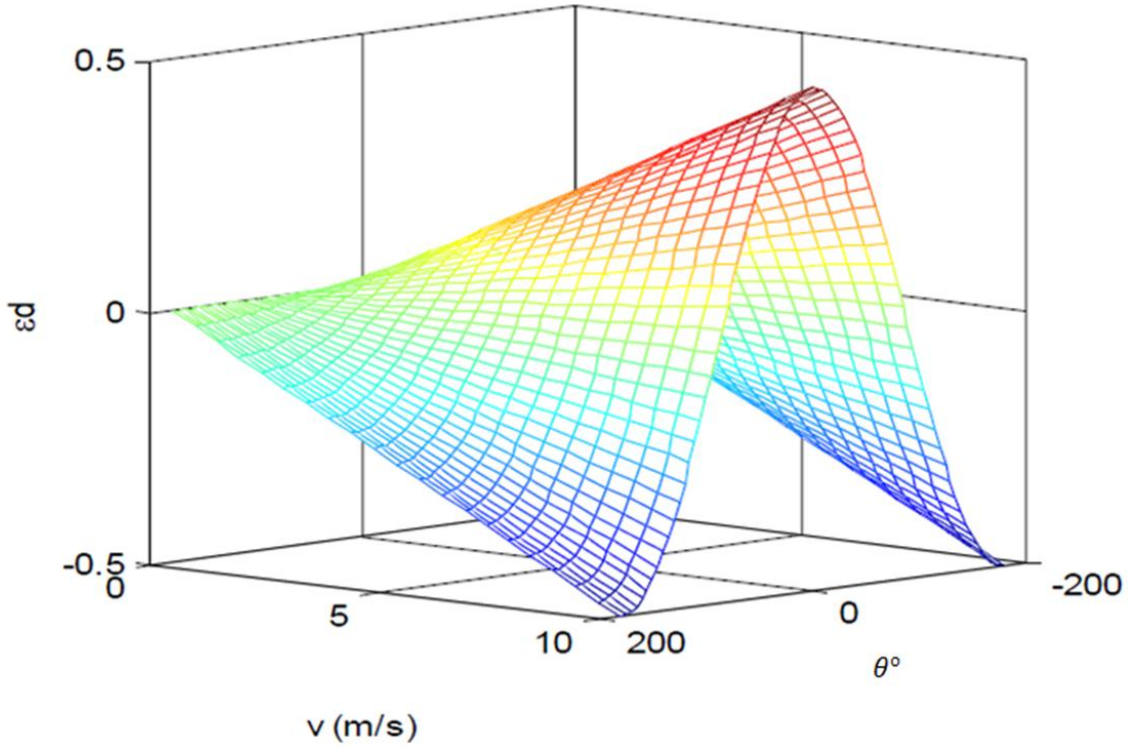

Figure 6.3 Normalized Doppler Frequency [111]

The figure 6.4 shows the BER for different values for SNR, considering the angle of arrival signal due to the Doppler Effect. As the figure 6.3 shows for the angle bigger than 90 degrees, the Doppler Effect is negative, but for the angle that is less than 90 degrees, the Doppler Effect is positive.

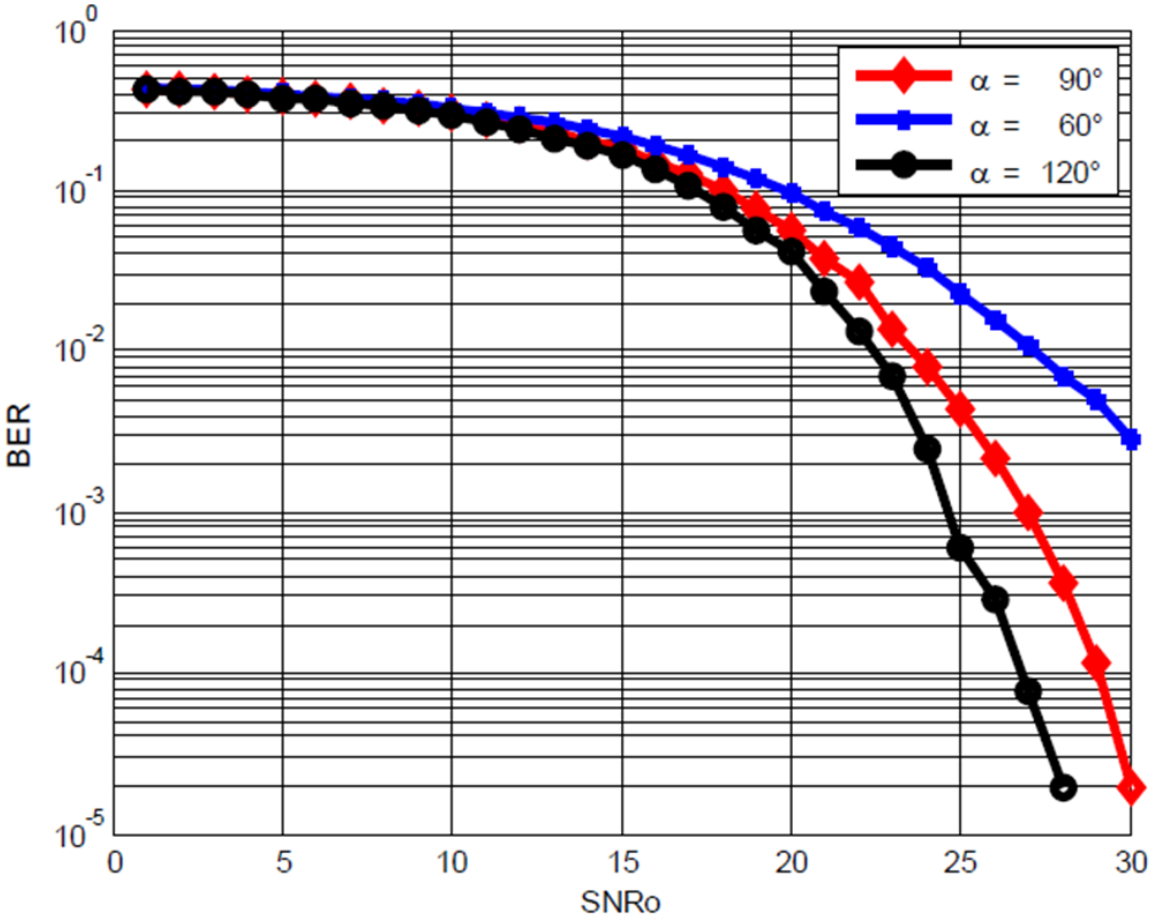

Figure 6.4 BER VS SNR for three different values for angles of incident [111]

As the investigation shows, the optimal frequency offsets for the lowest ICI is predicted by considering the Doppler power spectrum Density (D-PSD).

D-PSD refers to the power distribution of the signal frequency (in the wireless communication) by considering the Doppler Effects.

In OFDM mobile systems, the Doppler Effects give a certain span of the frequency offsets which are assigned with the Doppler PSD.

It is good to mention that there are two methods for getting the D-PSD. The first method is based on analytical predictions and the second method is based on experimental methods. However, the D-PSD for the direction scattering channel can be stated as [110]:

$$S_{\alpha}(f)=\begin{cases}\frac{1}{1+k}\frac{e^{kcos\alpha\frac{f}{f_d}cosh\left(ksin\alpha\sqrt{1-\left(\frac{f}{f_d}\right)^2}\right)}}{\pi I_0(k)\sqrt{1-\left(\frac{f}{f_d}\right)^2}}+\frac{k}{1+k}\delta(f-f_d sin\theta_0), & |f|\le f_d \\ 0 & Otherwise\end{cases} \tag{6.8}$$

θ_0 is the angle of mobile direction with LOS

k is called k-factor which is the ratio of LOS/NLOS

In OFDM mobile wireless systems used in High Speed Transportation (HST), the effect of Doppler spread can be respectively large. This can cause degradation of frequency alignment for Inter-Carrier-Interference (ICI) reduction.

In Quick Time-Varying OFDM (QTV-OFDM) wireless mobile systems, applying the suitable frequency alignment in the Receiver's Local Oscillator (R-LOSC) and using the directional antenna is a good solution for decreasing ICI. Therefore, to reduce Inter-Carrier Interference, we need to apply different rules for frequency alignments and beams-widths as the directional antenna. Figure 6.5 illustrates the results of applying these rules in the performance of BER, for different values of frequency alignment and beam-widths versus SNR.

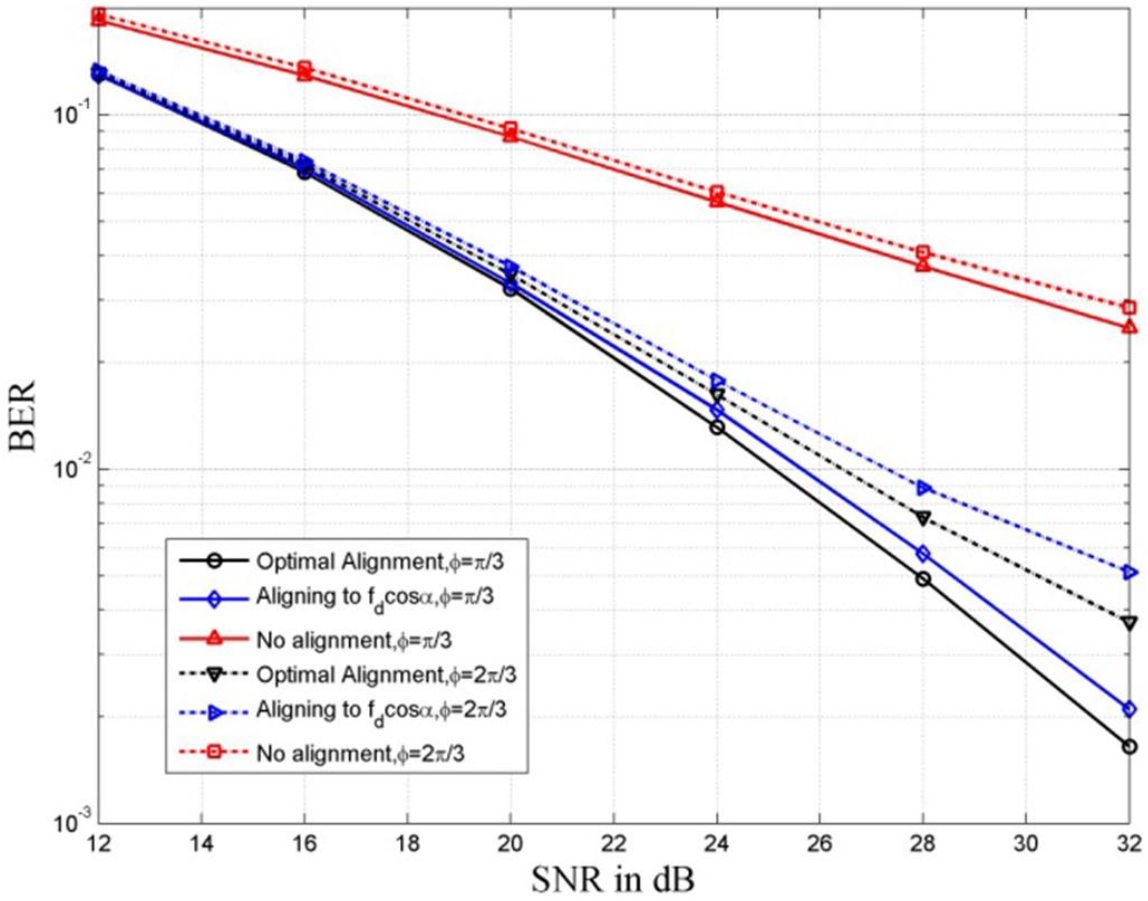

Figure 6.5 Performance of BER versus SNR considering the different values of beam-width and frequency alignment

As figure 6.5 illustrates, using the frequency alignment with using a direction antenna has a big impact on reducing the ICI.

As discussed in Chapter 3, the lack of orthogonality in the received signal to the OFDM receiver creates carrier frequency offset. CFO introduces the ICI in the system. As figure 6.6 illustrates, by increasing the frequency ICI increases are offset.

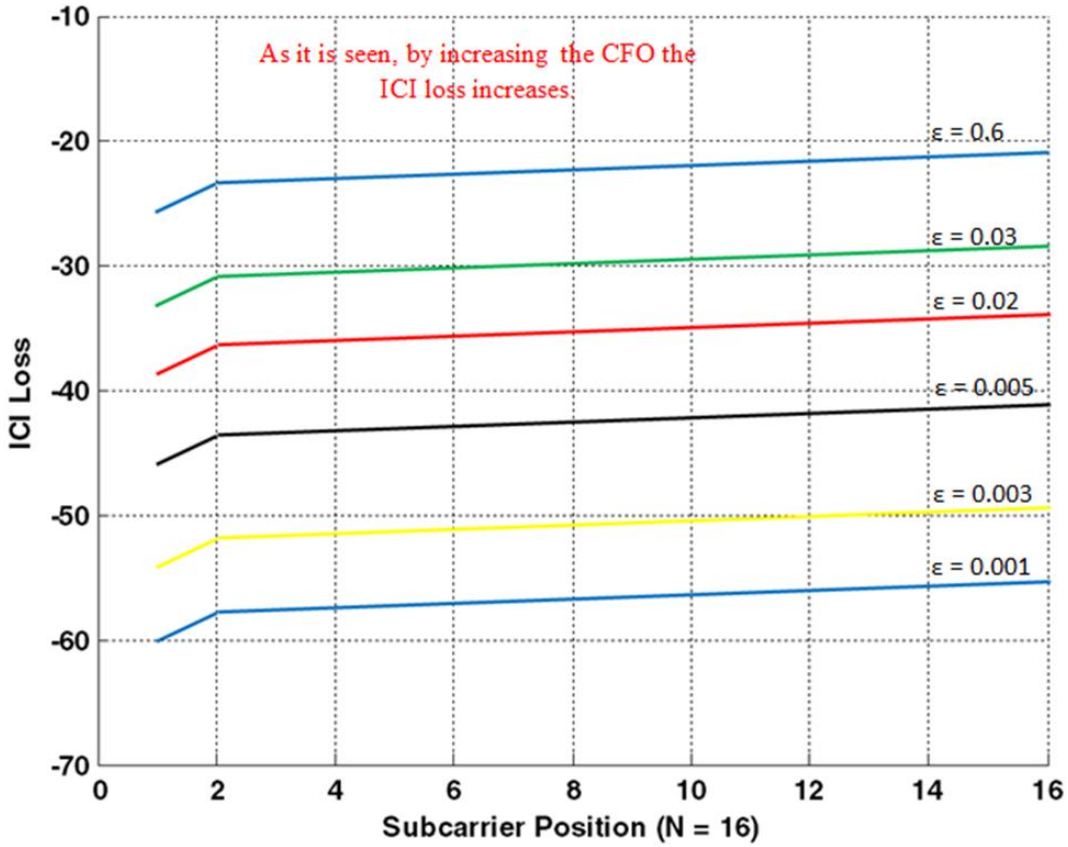

Figure 6.6 Effect of frequency offset on ICI loss

The other important CFO impact on OFDM wireless systems is the dependency of the SNR on the frequency offset.

Eq. 6.9 [112] shows the dependency of the SNR on the frequency offset.

$$SNR(\varepsilon) = \frac{f_N^2(\varepsilon) P_h \sigma_X^2}{\left(1 - f_N^2(\varepsilon)\right) P_h \sigma_X^2 + \sigma_Z^2} \tag{6.9}$$

P_h The total average power of the channel response

σ_X^2 Power of desired signal

σ_Z^2 Power of noise

ε Frequency offset

where $f_N(\varepsilon)$ is defined as follows:

$$f_N(\varepsilon) \triangleq \frac{\sin(\pi\varepsilon)}{N\sin(\pi\varepsilon/N)} \tag{6.10}$$

As is obvious from Eq. 6.1, the effect of frequency offset is to decrease the signal power by $f_N^2(\varepsilon)$. Since $f_N(\varepsilon)$ depends on N, the SNR also depends on the number of N. By increasing N, we can write:

$$\lim_{N\to\infty}(N\sin(\pi\varepsilon/N)) = \pi\varepsilon \tag{6.11}$$

Therefore we have:

$$\frac{sin(\pi\varepsilon)}{\pi\varepsilon} = sinc(\varepsilon) \tag{6.12}$$

By plugging this into Eq. 6.1 we have:

$$SNR(\varepsilon) = \frac{sinc^2(\varepsilon)P_h\sigma_X^2}{(1-sinc^2(\varepsilon))P_h\sigma_X^2+\sigma_Z^2} \tag{6.13}$$

So the SNR degradation due to the frequency offset can be stated as:

$$D(\varepsilon) \triangleq \frac{SNR(0)}{SNR(\varepsilon)} \tag{6.14}$$

$$D(\varepsilon) = \frac{1+(1-f_N^2(\varepsilon))\frac{P_h\sigma_X^2}{\sigma_Z^2}}{f_N^2(\varepsilon)} \tag{6.15}$$

Figure 6.7 illustrates the SNR degradation versus relative frequency offset for selected values (i.e. 5 dB, 10 dB, 15 dB, and 20 dB).

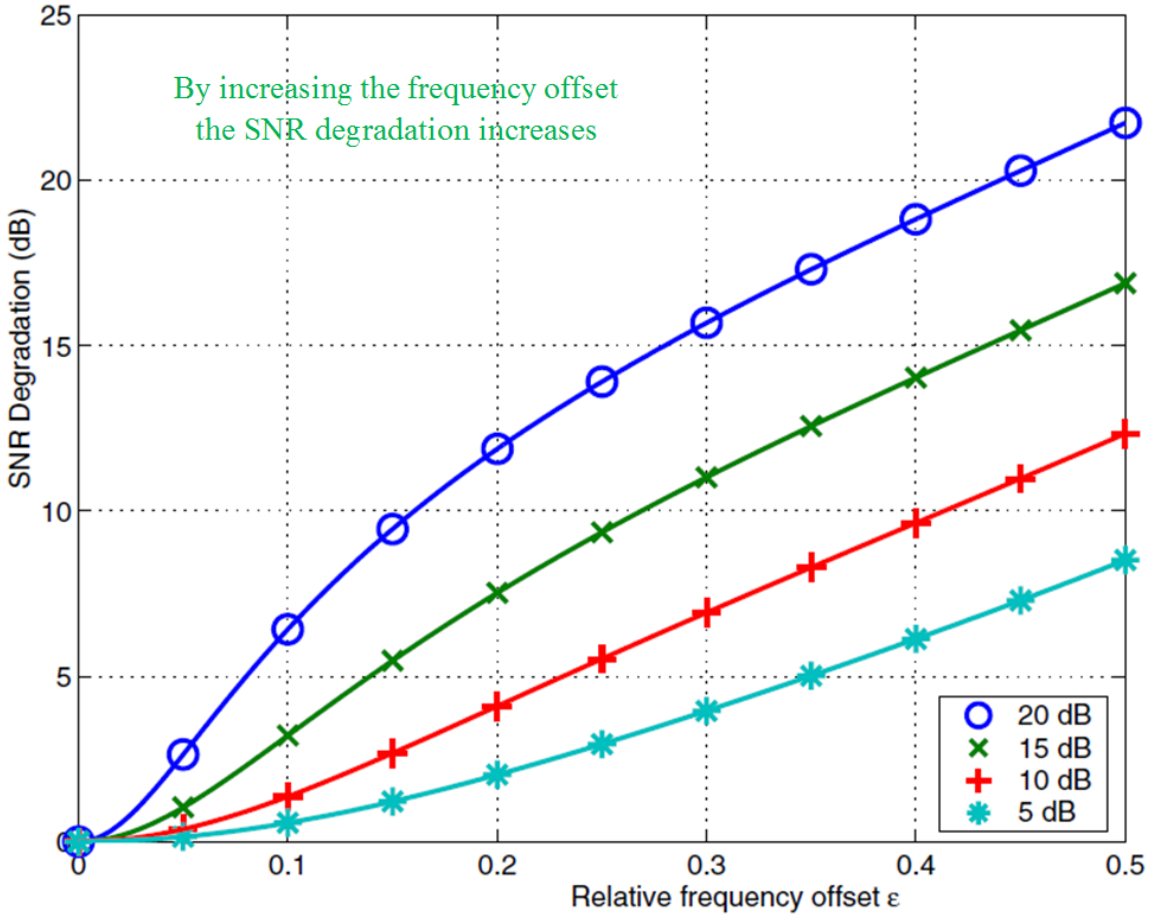

Figure 6.7 SNR degradation versus relative frequency offset [112]

In figure 6.7, the nominal SNR (i.e. $\frac{P_h \sigma_X^2}{\sigma_Z^2}$) is selected from 5 dB to 20 dB. As figure 6.7 shows, by increasing the frequency offset the SNR degradation grows.

On the other hand, CFO has an effect on phase shift. Figure 6.8 shows the effect of CFO on phase shift in time domain. For more details and discussion on the effect of frequency offset see Chapter 3.

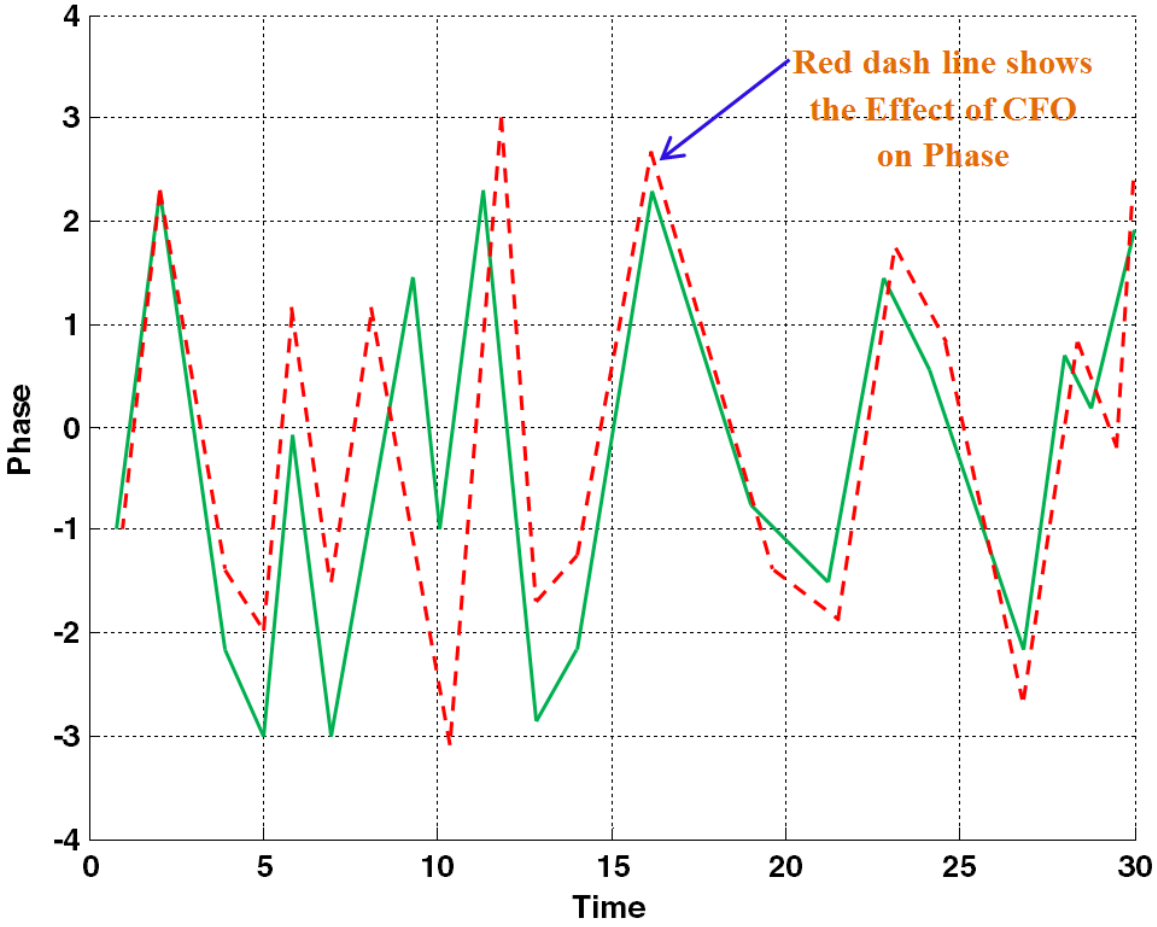

Figure 6.8 Effect of CFO on phase in time domain

As we have also discussed in Chapter 3, the algorithms that use Cyclic Prefix for estimating and compensating CFO only estimate the CFO in the limited ranges between -0.5 and 05 (i.e. $-\frac{1}{2} \leq \varepsilon \leq \frac{1}{2}$). To remove this limitation, the equation for estimating CFO

had to be modified. Eq. 3.139, brought in Chapter 3, give us more freedom in CFO estimation range. Considering Eq. 3.139 in Chapter 3, the range of CFO can be any integer number (i.e. $-\mathrm{D} \leq 2\varepsilon \leq \mathrm{D}$).

Although the result of the simulation confirms the gain in performance and we would be able to increase the range of CFO estimation, it costs in the degradation of the MSE performance. This can be seen in figure 6.9. However, figure 6.10 shows the comparisons between suggested and training base method.

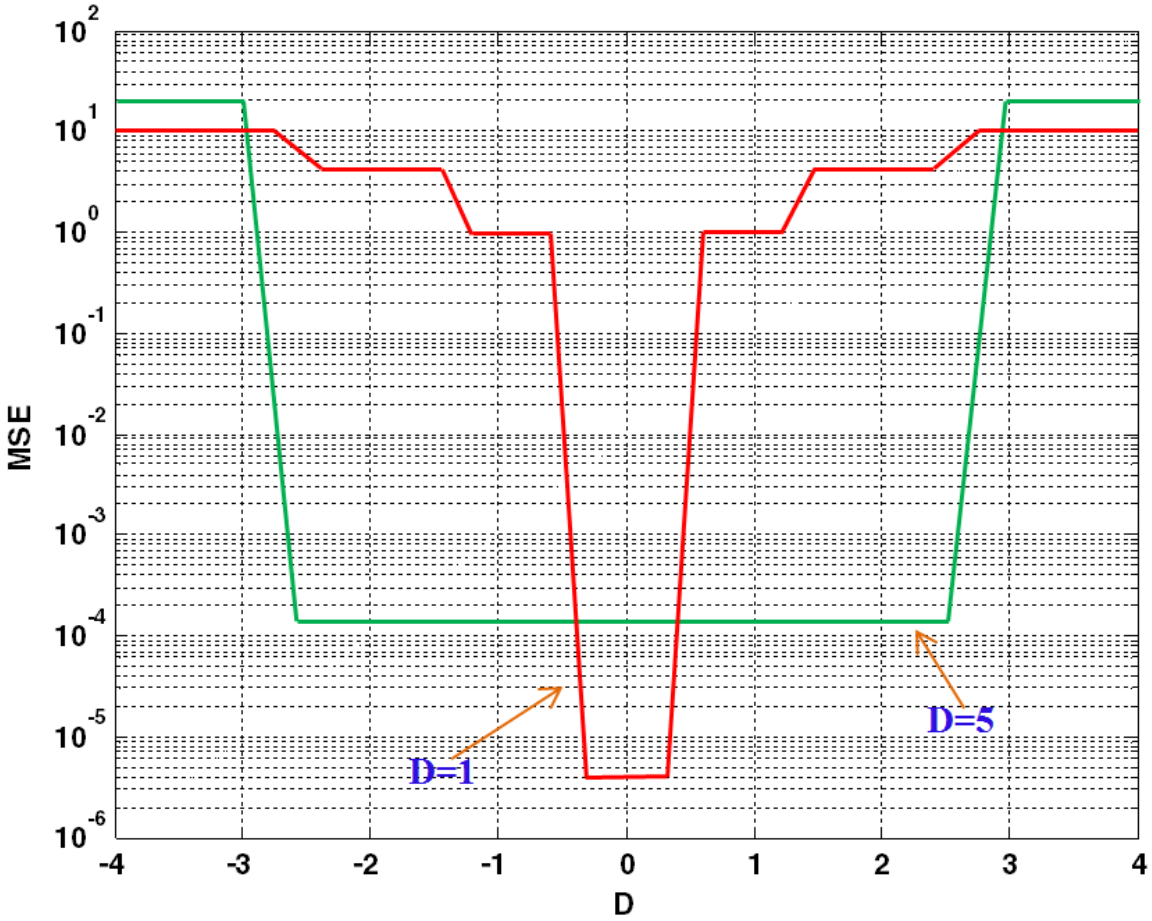

Figure 6.9 MSE versus D

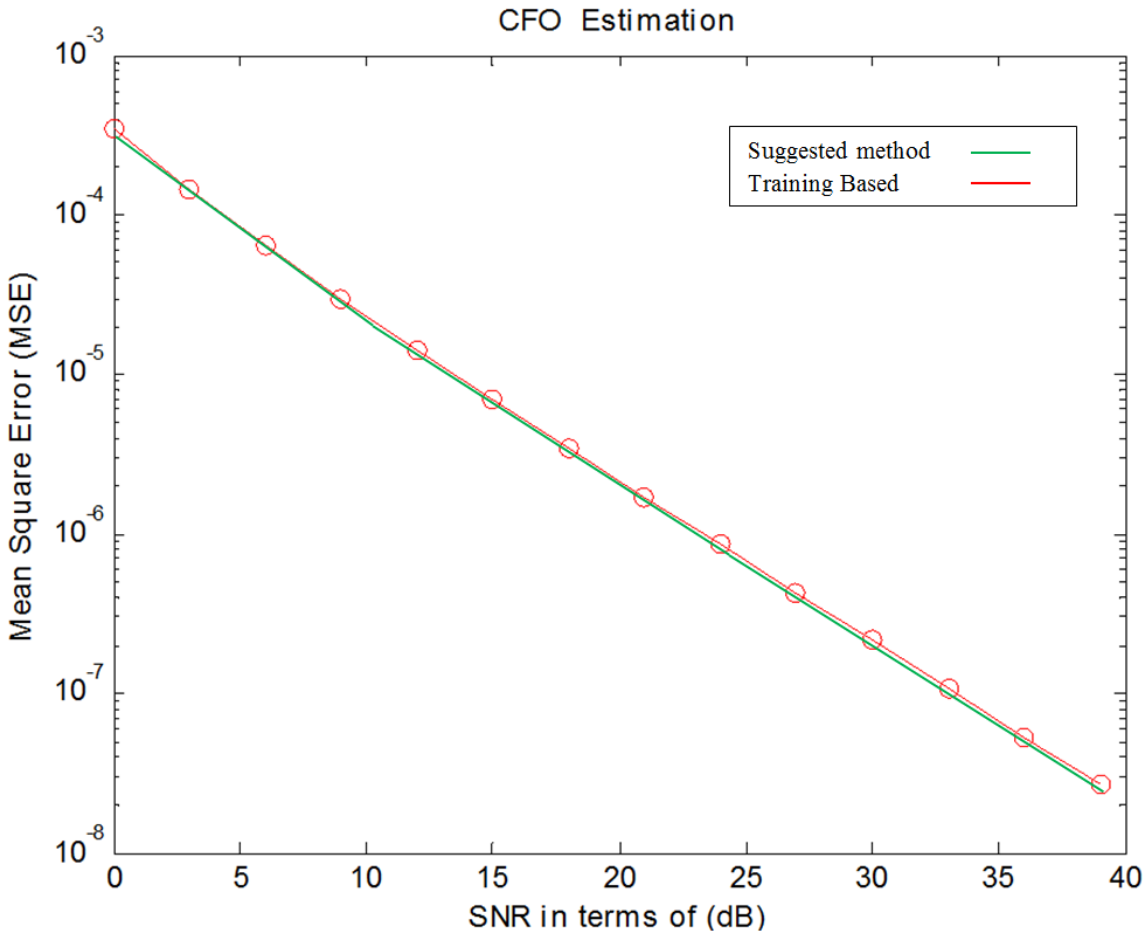

Figure 6.10 CFO Estimation

Figure 6.11 illustrates the block diagram of the other method that can be used for CFO estimation. DTD, TE and FFF in the diagram stand for Data Timing Detector (DTD), Timing Estimator (TE), and Fine Frequency Finder (FFF).

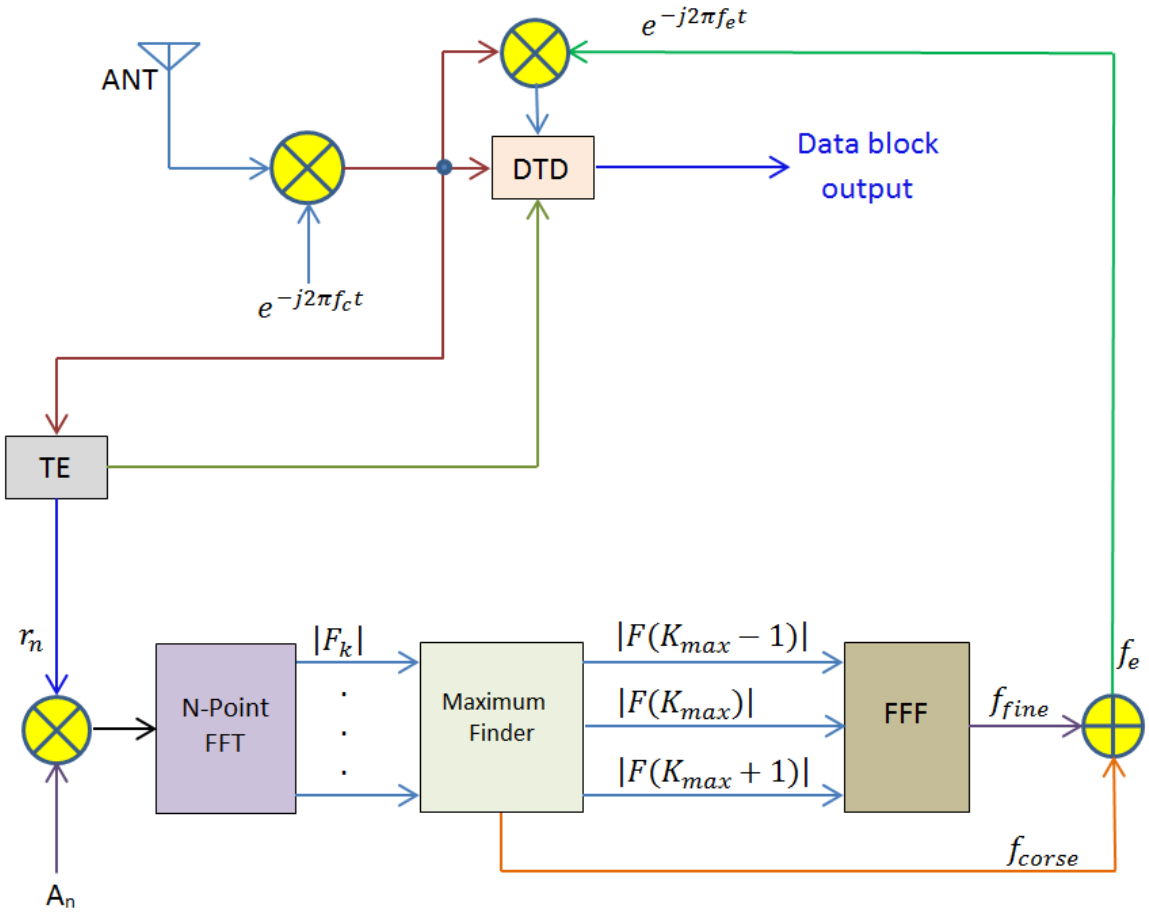

Figure 6.11 Schematic diagram of proposed method

The f_e *and* f_{fine} are as follows:

$$f_e = f_{fine} + f_{corse} \tag{6.16}$$

$$f_{fine} = \frac{\beta}{NT_s F(k_{max})/(k_{max}+\beta)+1} \tag{6.17}$$

$$f_e = \frac{1}{NT_s}\left(k_{max} + \frac{\beta}{F(k_{max})/(k_{max}+\beta)+1}\right) \tag{6.18}$$

Figure 6.12 illustrates the comparison of this method with Schmidle method. More discussion can be found in Chapter 3, Section 3.32.

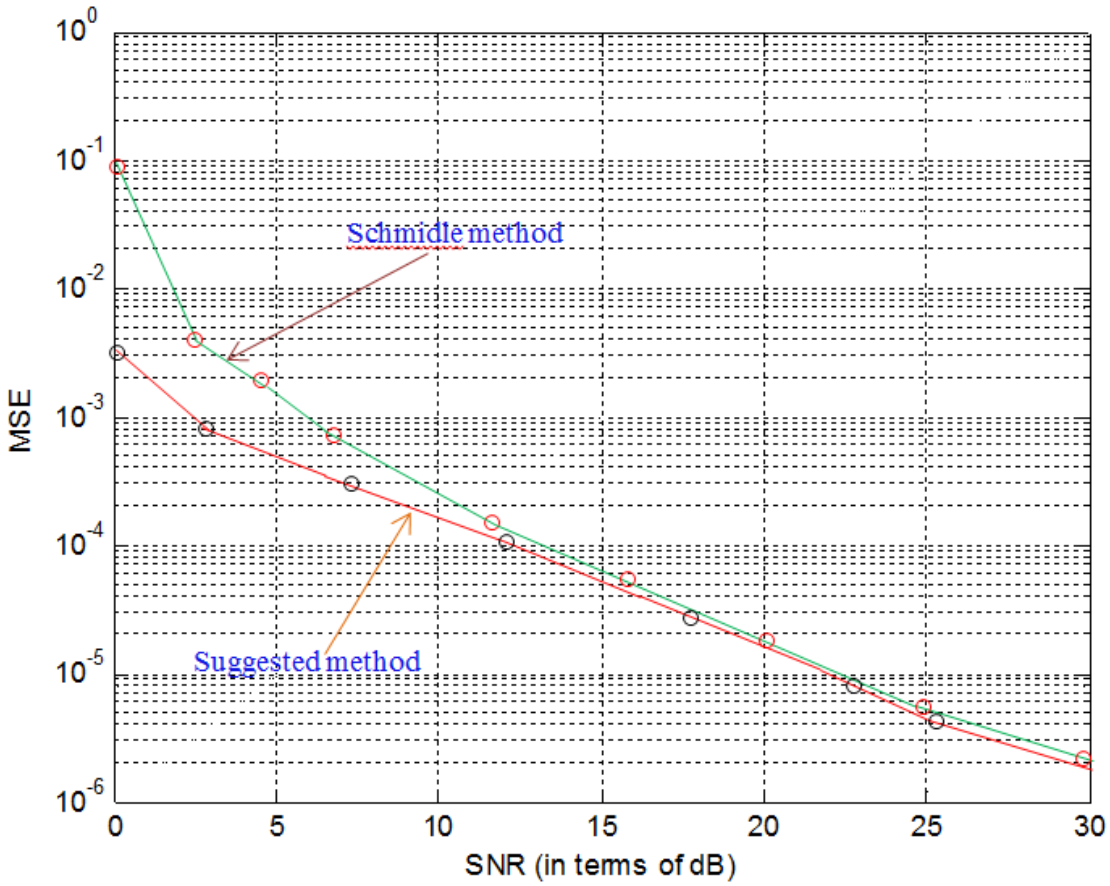

Figure 6.12 MSE versus SNR

As a result, we have shown that CFO has serious effect on different factors of OFDM wireless systems. Therefore, estimating and compensating for it has a high degree of importance. But it is good to mention that, in the real world, the frequency offset cannot perfectly be estimated for the OFDM wireless systems and it always impacts the performance of the OFDM systems. Nonetheless, we have an acceptable range of the carrier frequency offset (CFO). In that range, we can reach to our desired performance for the OFDM wireless system.

6.4 Peak to Average Power Ratio

In Chapter 4, we have studied the PAPR and techniques for reducing it. However, reducing PAPR is meant to decrease the distortion that is presented by nonlinearity. Therefore, as a result, PAPR reduction leads to a reduction of both out-of-band radiation and the BER degradation. In this dissertation, some of the important approaches, by focusing on PAPR reduction, have been discussed and a simple and effective method, combining clipping, filtering, and reducing the number of OFDM symbol, has been proposed.

Please note that PAPR is not unsolvable. The key is the complexity and the cost associated with the proposed schemes. Considering this, we came up with a solution that satisfies the above.

As we know, the average power ratio is defined as:

$$PAPR = 10log_{10}\left[\frac{P_{peak}}{P_{avg}}\right] \tag{6.19}$$

If we consider our signal tone as $r(t) = Acos(2\pi f_c t)$

$$P_{peak} = max\{|A^2cos^2(2\pi F_c t)|\} = A^2 \tag{6.20}$$

$$P_{avg} = F_c \int_0^T A^2cos^2(2\pi F_c)dt \tag{6.21}$$

We know $T_c = \frac{1}{F_c}$. Therefore:

$$P_{avg} = \frac{F_c}{2}\left\{\frac{A^2}{F_c} + \int_0^{1/F_c} A^2 \cos(4\pi F_c t)\, dt\right\} \tag{6.22}$$

Since: $\int_0^{1/F_c} A^2 \cos(4\pi F_c t)\, dt = 0 \Rightarrow \quad P_{avg} = \frac{A^2}{2}$ (6.23)

the PAR will be:

$$PAPR = 10log_{10}\left[\frac{P_{peak}}{P_{avg}}\right] = 10log_{10}\left[\frac{A^2}{A^2/_2}\right] = 3\ db \tag{6.24}$$

Now, consider a signal as:

$$r(t) = Acos(2\pi f_1 t) + Bcos(2\pi f_2 t) \tag{6.25}$$

To find its PAPR, first find its peak and its average.

Its peak can be found by raising it to the 2nd power, taking its derivative, and setting it equal to zero.

$$r^2(t) = \frac{A^2}{2} + \frac{B^2}{2} + \frac{A^2}{2}cos(2\pi f_1 t) + \frac{B^2}{2}cos(2\pi f_2 t) + ABcos(2\pi(f_1 - f_2)t) + ABcos((f_1 - f_2)t) \tag{6.26}$$

$$\frac{dr^2(t)}{dt} = 0 \tag{6.27}$$

$$max\left[\frac{dr^2(t)}{dt}\right] = r^2(0) = (A + B)^2 \tag{6.28}$$

The P_{avg} of Eq.1 will be as follows:

$$P_{avg} = \alpha f_0 \int_0^{1/\alpha f_0} [Acos(2\pi f_0 t) + Bcos(2\pi\alpha f_0 t)]^2 dt$$

$$= \frac{1}{2}(A^2 + B^2) \tag{6.29}$$

Therefore:

$$PAPR = 10log_{10}\left[\frac{P_{peak}}{P_{avg}}\right] = 10log_{10}\left[2 + \frac{4AB}{(A^2+B^2)}\right] \tag{6.30}$$

Consider two scenarios. First, the amplitude of A is equal to the amplitude of B and second, the amplitude of A is much bigger than B.

If $A = B$ then:

$$PAPR = 10log_{10}\left[\frac{P_{peak}}{P_{avg}}\right] = 10log_{10}\left[2 + \frac{4A^2}{(A^2+A^2)}\right] = 10log_{10}(4) \cong 6\ db \quad (6.31)$$

If $A \gg B$ then:

$$PAPR = 10log_{10}\left[\frac{P_{peak}}{P_{avg}}\right] = 10log_{10}(2) \cong 3\ db \quad (6.32)$$

To summarize of the above discussion:

1. the PAPR for the signal that is made of M signal with the same amplitude and the same phase is:

$$PAPR = 20log_{10}(M) \quad (6.33)$$

2. the amount of PAPR is ruled by the amplitude of the signal.

Now consider the signal as a complex sinusoidal signal with the period T, as follows:

$$r(t) = e^{\omega t} = e^{2\pi f t} \quad (6.34)$$

The PAPR is:

$$PAPR = \frac{Max[r(t)r^*(t)]}{\frac{1}{T}\int_0^T exp^{4\pi f t}dt} = \frac{1}{1} = 1 \quad (6.35)$$

Therefore, a complex sinusoidal tone has a PAPR equal to one.

Since the OFDM signal is the summation of multiple sinusoidal with the frequency separation equal to $1/T$, each of them is modulated with independent a_n. The mathematical form of such a signal can be stated as:

$$r(t) = \sum_0^{N-1} a_n e^{\frac{2\pi njt}{T}} \tag{6.36}$$

For simplicity, consider $a_n = 1$ so, in this case, the maximum expected PAPR for an OFDM signal with N subcarrier can be stated as follows:

$$PAPR = \frac{Max[r(t)r^*(t)]}{E[r(t)r^*(t)]} = \frac{N^2}{N} = N \tag{6.37}$$

The Eq. 2 is the max value of PAPR for an OFDM with N subcarrier if, and only if, all the subcarriers align in phase and are modulated similarly and equally.

In our suggested method comparing with conventional OFDM, the separation of subcarriers (SCs) will be fourth.

Thus, in each OFDM symbol, only the first $1 + N/4$ samples will be sent while the rest will be ignored. As we know, in order for the receiver to be synchronized, the rest of the samples by using the partial symmetry of Fourier transform and using Eq. 4.11(Chapter 4), will be constructed.

$$s(t) = \frac{1}{\sqrt{T}} \sum_0^{K-1} a_k \, e^{\frac{2\pi ktj}{T}} \, \omega(t) \tag{6.38}$$

As Eq. 6.38 shows, each of the information signals multiplied by the related sinusoidal (which its frequency is K/T) and then summed will be sent out as $s(t)$. However, the OFDM signal can be represented as follows [81]:

$$\mathrm{S_{tx}(t)} = \sum_{\mathrm{K}=-\infty}^{\infty} \sum_{\mathrm{n}=0}^{\mathrm{N}-1} \mathrm{a_{n,k} g_n(t - Kt)} \tag{6.39}$$

$$g_n(t) = \begin{cases} \frac{1}{\sqrt{T-T_{CP}}} e^{\frac{2n\pi t}{T-T_{CP}} j} & , \quad t \in [0, T] \\ 0 & , \quad t \notin [0, T] \end{cases} \tag{6.40}$$

where T is the period of each subcarrier, and 1/T is the space between the subcarriers. In our method for each OFDM symbol, only the first 1+N/4 sample will be sent. Therefore, the mathematical representation for our proposed scheme is as follows:

$$\mathrm{S_{tx}(t)} = \sum_{\mathrm{K}=-\infty}^{\infty} \sum_{\mathrm{n}=0}^{\mathrm{N}-1} \mathrm{a_{n,k} g_n(t - Kt)} \tag{6.41}$$

$$g_n(t) = \begin{cases} \frac{1}{\sqrt{T-T_{CP}}} \left(e^{\frac{n\pi t}{2(T-T_{CP})} j} \right) & , \quad t \in [0, T] \\ 0 & , \quad t \notin [0, T] \end{cases} \tag{6.42}$$

By using Eq. 6.42 and clipping and filtering techniques, we get a better performance comparing to [62] and [75]. Here, the complete relation between PAPR, CCDF and BER are used to determine the performance of the proposed method. The simulation results in figures 6.13, 6.14 and 6.15 show the reduction of PAPR.

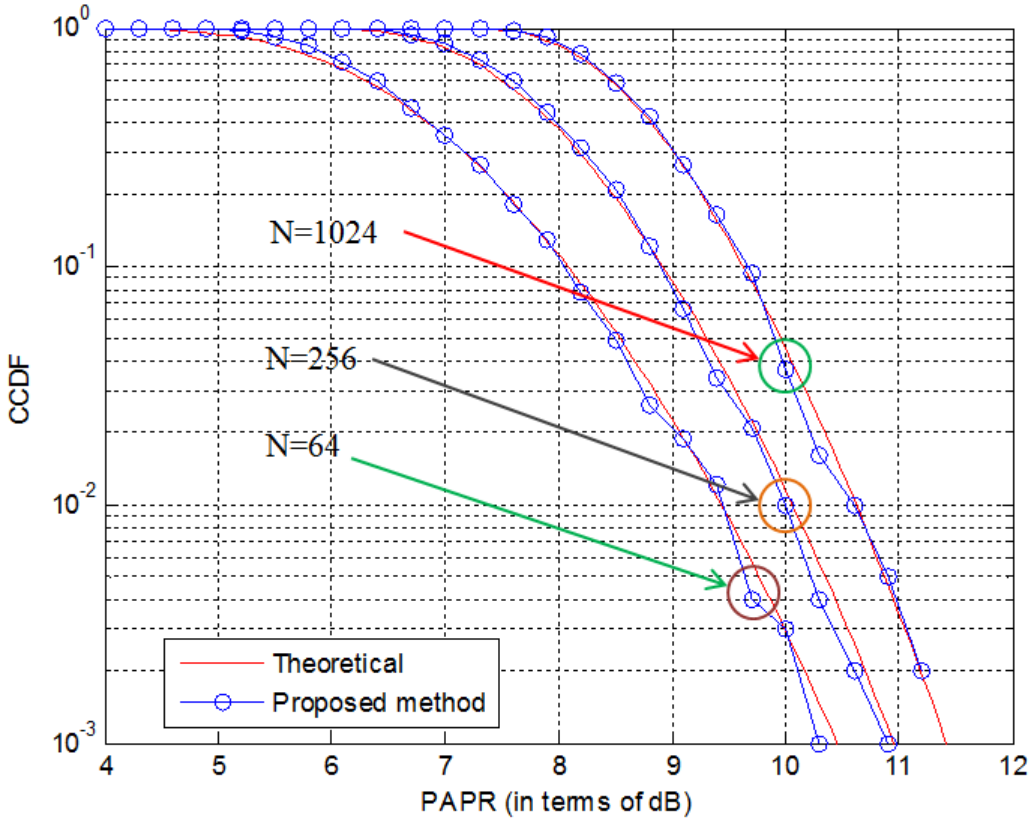

Figure 6.13 CCDF OF OFDM

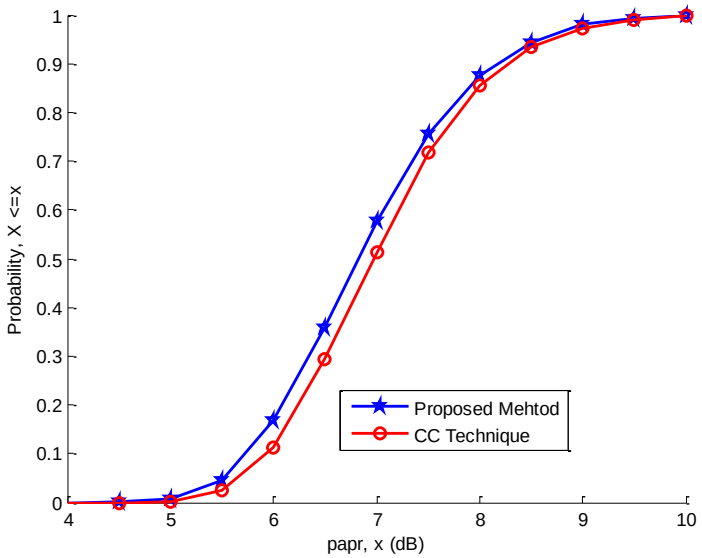

Figure 6.14 CDF Plot of PAPR

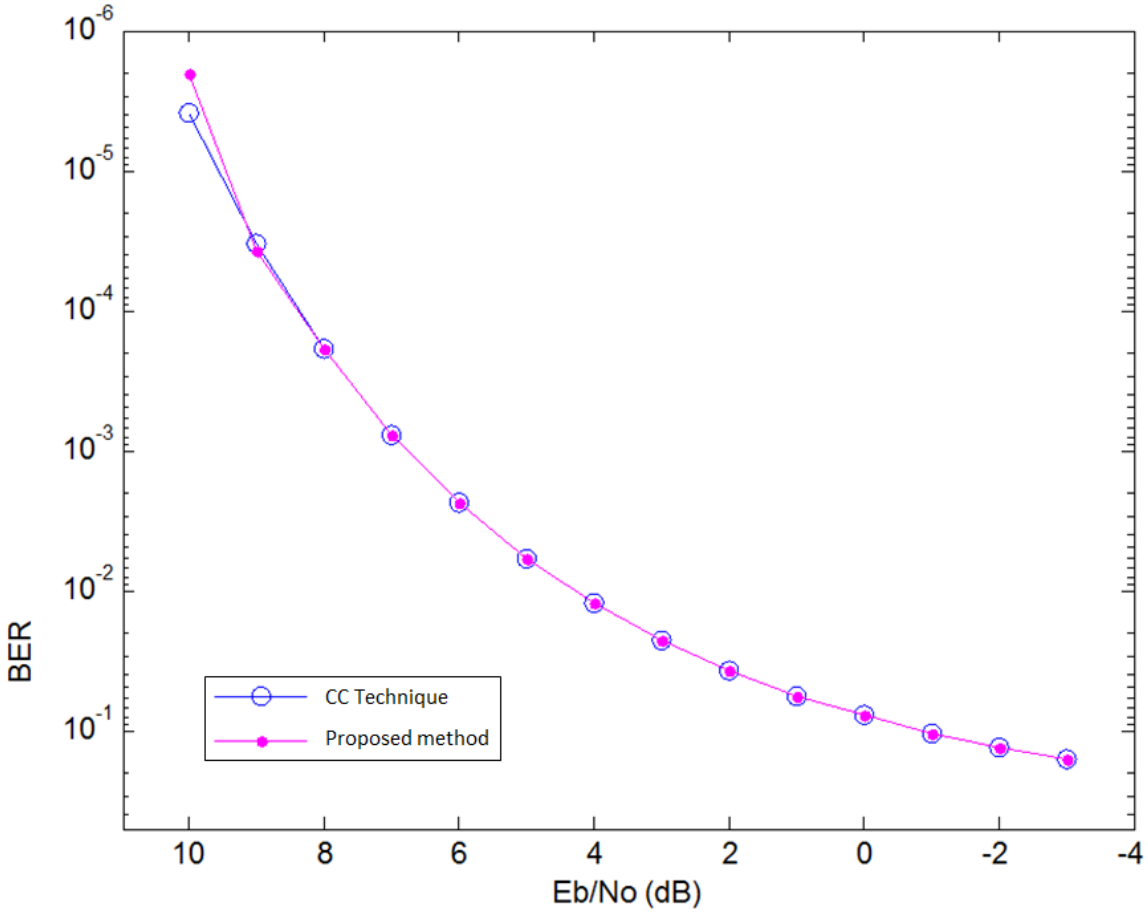

Figure 6.15 BER VS SNR

As figure 6.1 in Chapter 4 shows, compared with the clipping technique, our proposed method can obtain a better reduction of PAPR. For a detailed discussion, refer to Chapter 4 of this dissertation.

6.5 Path Loss

In Chapter 5, we presented a short overview of propagation channel characteristic and modeling. We also talked about different types of models for wireless channel systems. Distance dimension is one of the causes of path loss. Shadowing and multipath

fading is the cause of delay spread. We also talked about indoor environments and finally, proposed an equation for modeling outdoor and indoor environments.

AN indoor environment, due to the presence of different type of obstacles such as walls, furniture and etc., causes the radio wave to experience multiple reflections. Therefore, the waves that hit the receiver antenna come from different paths which lead to fading phenomena.

In a practical wireless communication system, the indoor propagation is more complex than the outdoor propagation. Objects that are in indoor environments can strictly affect the propagation characteristics of any wireless radio channel. The performance of indoor OFDM wireless systems can be limited by propagation characteristics. Therefore, it is very significant to know how the surrounding objects can impact the propagation. In another words, indoor propagation is complicated. Each indoor environment can be different. Eq. A large number of measurements are required for getting the coefficients for any equation that is offered for any model. These measurements can obtain statistical results that lead to the realistic values for different environments and can provide good estimates for both large scale and small scale indoor environments. With more measurements, it is likely that the models can be refined and accurately predict the path loss in many more different environments. However, the method, results, and conclusion are as follows.

As we mentioned in Chapter 5, d_0, which is considered as the initial or reference distance, causes a discontinuity at $d = 100$ meters. This can be seen in figure 6.16.

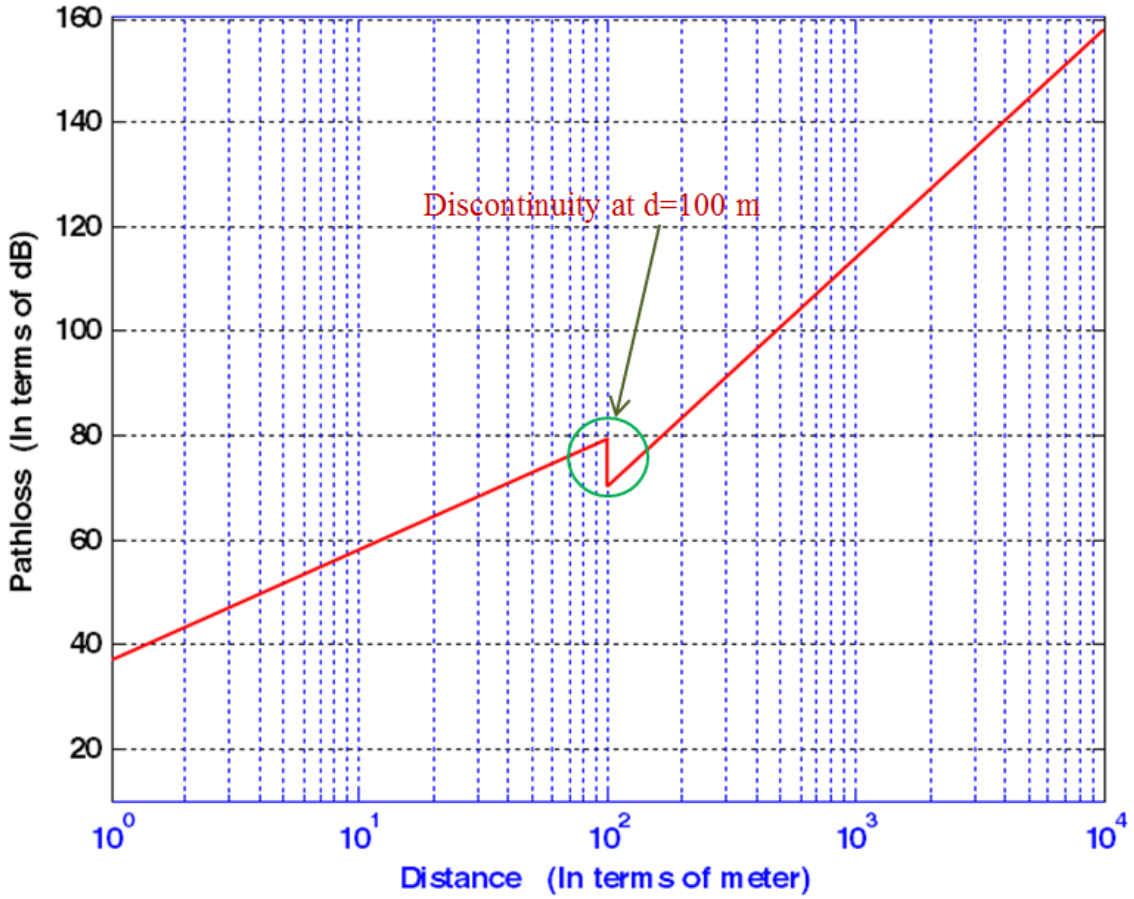

Figure 6.16 IEEE model for path loss with initial d_0

To fix this problem, a different reference distance called d_{00} is needed. For finding d00, in Eq. (5.3), consider $G_r = G_t = 1$ and L=1. Therefore, Eq. (5.3) can be written as:

$$PL_F(d) = -10log\left(\frac{1\times1\times\lambda^2}{(4\pi)^2 d^2\times1}\right) = 10log\left(\frac{\lambda}{4\pi d}\right)^{-2} \quad (6.43)$$

$$PL_F(d) = 20log\left(\frac{4\pi d}{\lambda}\right) \quad (6.44)$$

By putting d_{00} for d in Eq. (5.39) and Eq. (6.44) and then set it equal to each other we have:

$$PL_F(d_{00}) + 10\gamma \log_{10}\left(\frac{d_{00}}{d_0}\right) + C_f + C_{RX} = 20log\left(\frac{4\pi d_{00}}{\lambda}\right) \quad (6.45)$$

On the other hand, for finding $PL_F(d_{00})$, we put d= d_{00} in Eq. (6.44), so we have:

$$PL_F(d_{00}) = 20log\left(\frac{4\pi d_{00}}{\lambda}\right) \quad (6.46)$$

Put this value for $PL_F(d_{00})$ in Eq. (6.45), and:

$$20log\left(\frac{4\pi d_{00}}{\lambda}\right) + 10\gamma \log_{10}\left(\frac{d_{00}}{d_0}\right) + C_f + C_{RX} = 20log\left(\frac{4\pi d_{00}}{\lambda}\right) \quad (6.47)$$

Solving the Eq. (6.47) for d_{00} gives:

$$-10\gamma \log_{10}\left(\frac{d_{00}}{d_0}\right) = C_f + C_{RX} \quad (6.48)$$

$$\log_{10}\left(\frac{d_{00}}{d_0}\right) = -\frac{C_f + C_{RX}}{10\gamma} \quad (6.49)$$

$$d_{00} = d_0 10^{-\frac{C_f + C_{RX}}{10\gamma}} \quad (6.50)$$

So the new equations are:

$$PL(d)_{|d>d_{00}} = 20\log_{10}\left(\frac{4\pi d_{00}}{\lambda}\right) + 10\gamma \log_{10}\left(\frac{d}{d_0}\right) + C_f + C_{RX} \quad (6.51)$$

$$PL(d)_{|d\leq d_{00}} = 20\log_{10}\left(\frac{4\pi d}{\lambda}\right) \quad (6.52)$$

This is shown in figure 6.17. As can be seen in figure 6.17, there is no discontinuity at $d = 100$ meters.

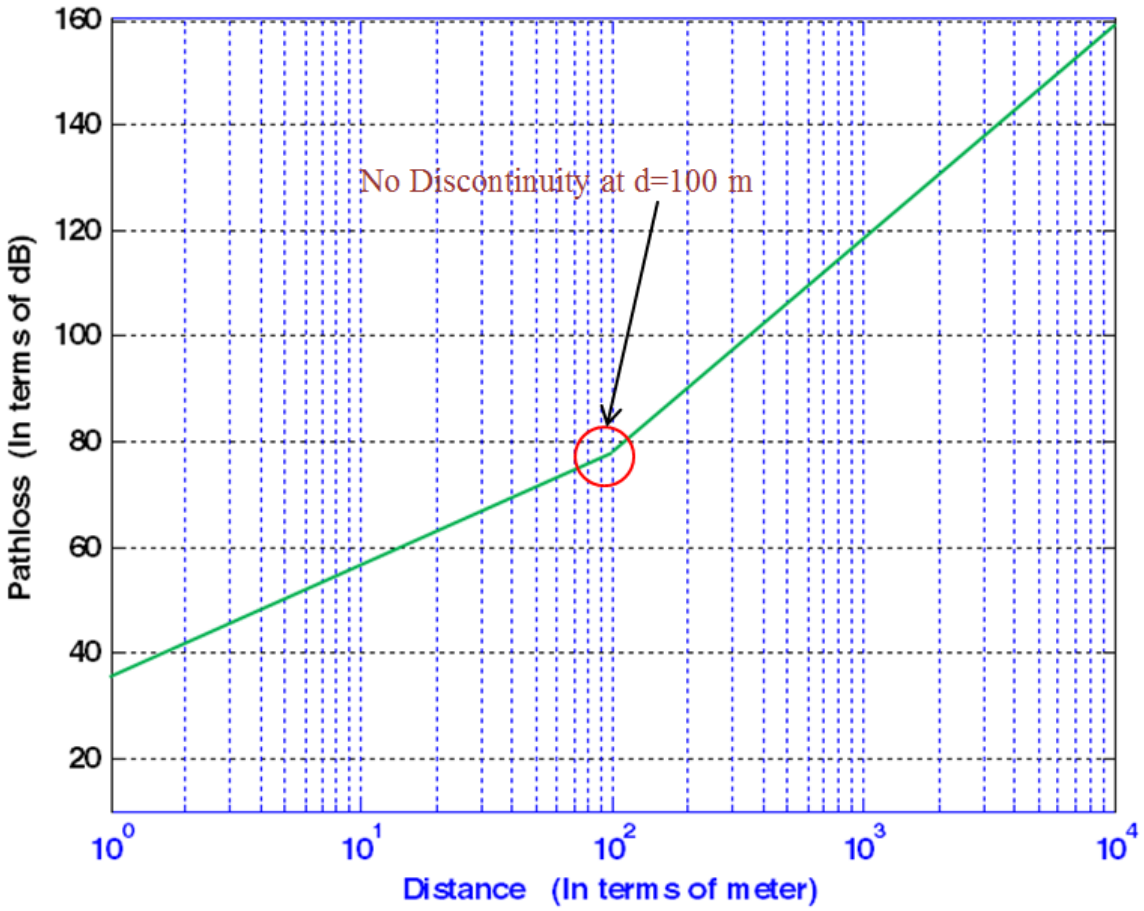

Figure 6.17 Path loss model with initial d_{00}

Now, recall Eq. (5.38) and consider the effect of the angles of incidence of the signal on the walls and floors [98, 104, 109] to get:

$$PL_{BP}(d) = 10\log\left(\frac{d}{d_0}\right)^{n1} U(d_{BP}-d) + 10\left[\log\left(\frac{d_{BP}}{d_0}\right)^{n1} + \log\left(\frac{d_0}{d_{BP}}\right)^{n2} U(d - d_{BP})\right] + \quad + \sum_{p=1}^{P}\left(\frac{WAF(p)}{cos\emptyset_p}\right) + \sum_{q=1}^{Q}\left(\frac{FAF(q)}{cos\emptyset_q}\right) \tag{6.53}$$

By contributing the indoor path loss Eq. (6.53) with Eq. (6.51), the total path loss $PL_T(d)$ will be the sum of the outdoor plus the indoor path loss.

$$PL_T(d) = PL(d)_{|d_{00}} + PL_{BP}(d) \tag{6.54}$$

If $d < d_{BP}$ therefore $PL_{BP}(d) = 0$ then the total path loss is

$$PL_T(d) = PL(d)_{|d_{00}} \tag{6.55}$$

Since the surrounding objects, medium and different electromagnetic fields from different sources in a desired area, have an attenuation impact on the received signal to the receiver, we add L_{OA} (in term of dB) to Eq. (6.54) which is for the impact of these factors. This attenuation impact factor varies with different environments and can only be found by taking a large number of onsite measurements.

$$PL_T(d) = PL(d)_{|d_{00}} + PL_{BP}(d) + L_{OA} \tag{6.56}$$

Figure 6.18 shows the result of path loss for a typical urban area with normal density of the obstacles by using the suggested method and a common urban method. Since the method considers all the mentioned factors for predicting the path loss, it looks more comprehensive and more close to the real area that can be considered.

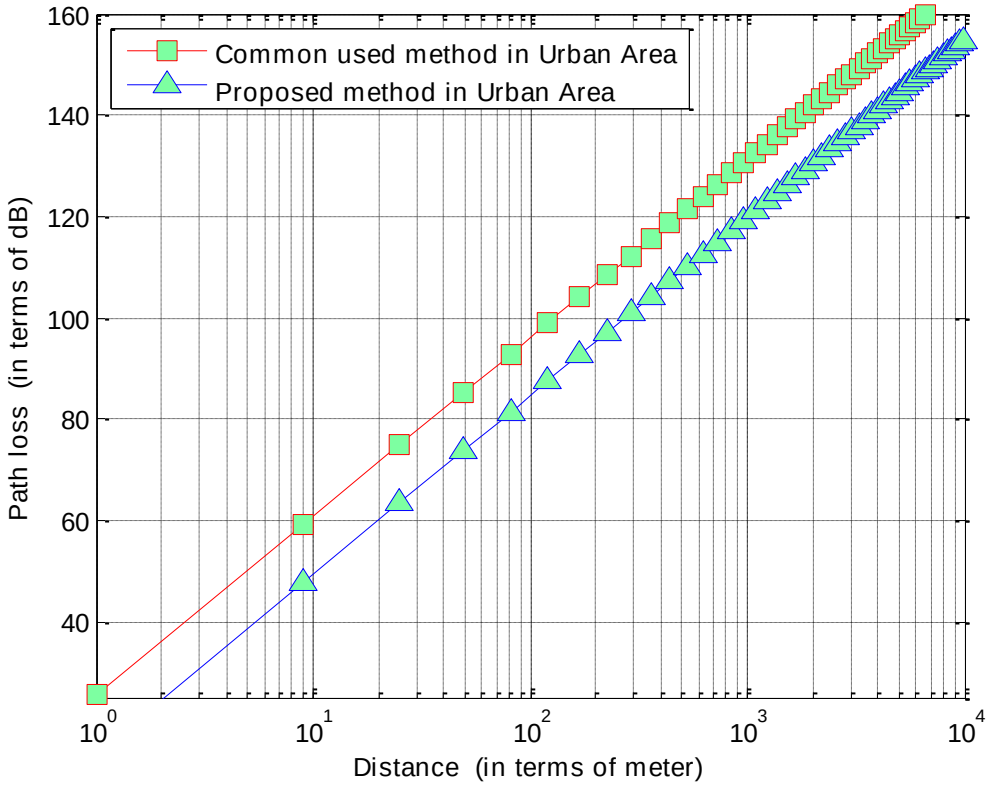

Figure 6.18 Proposed method VS common model

At the end of this discussion it is necessary to mention that any model has its own limitation for the prediction of path loss such as accuracy. The model's accuracy compared to the field measurements varies. That is why they do the custom calculations for their models in industry by taking the field measurements and using the results. It is worth mentioning that, despite the huge efforts to date, much work remains in understanding and predicting the exact characteristics of mobile communications channels.

6.4 Future work

In OFDM wireless communication systems, the pilots that are used for channel estimation are also used for synchronization. On the other hand, the cyclic prefix is used by the synchronizer for synchronization. Therefore, for creating the better performance for OFDM systems and avoid redundancy, future work can be done on the basis of combing these two factors. On the other hand, future work can be beyond the current idea of the CFO estimation algorithms. The future CFO estimation algorithm can work on the basis of the Q-learning algorithm. Of course, such an algorithm needs to have a low and tolerable penalty for its weak estimations.

Considering what we have covered in Chapter 5 and Chapter 6 for PAPR and path loss, future work for them can be stated as follows.

All the algorithms and techniques that are used for reducing PAPR are applied after detecting the high PAPR signals. Future work can be done on the basis of predicting and preventing the creation of PAPR.

By increasing the velocity of the mobiles and transportation systems, we will experience more time varying effects on the received signals to the OFDM wireless systems. Therefore, future work for prediction the path loss should give more attention to this fact.

Bibloiography

[1] Lee, Doelz, M.L.; Heald, E.T; Matin, D.L.; "Binary Data Transmission Techniques for Linear Systems" Proceeding of the IRE, Volume 45, pages 656-661; May 1957.

[2] R.W. Chang; "Orthogonal Frequency Division Multiplexing", U.S. Patent 3,488,455, filed 1960's issued Jan, 1970.

[3] Weinstein, S. B., and P. M. Ebert, "Data Transmission of Frequency Division Multiplexing Using the Discrete Frequency Transform" IEE Transaction on Communications, Volume 19, No. 5, pp 628-634 (in Ch. 1), October 1971.

[4] William Shieh, Ivan Djordjevic; "OFDM for Optical Communications" Academic press, Elsevier, 2010.

[5] Weinstein, S., Ebert, P.,"Data Transmission by Frequency-Division Multiplexing Using the Discrete Fourier transform," IEEE Transactions on Communications, vol. 19, no. 5, pp. 628–633, October 1971.

[6] Nick LaSorte, W. Justin Barnes, Hazem H. Refai, "The History of Orthogonal Frequency Division Multiplexing" IEEE, 2008.

[7] The history of orthogonal frequency-division multiplexing [History of Communications], IEEE Communications Magazine, 2009.

[8] 3GPP TR 25.814 V7.1.0, 3rd Generation Partnership Project; Technical Specification Group Radio Access Network; Physical layer aspects for evolved Universal Terrestrial Radio Access September 2006.

[9] Nick LaSorte, W. Justin Barnes, Hazem H. Refai, Member, IEEE; "The History of Orthogonal Frequency Division Multiplexing" 2008.

[10] Figure 2.3, comes from "OFDM" Presentation by Dennis Harding, 2009.

[11] A. Peled and A. Ruiz, "Frequency domain data transmission using reduced computational complexity algorithms", Processing of the IEEE International Conference Acoustics, Speech and Signal Processing, Denver Colorado, pp 946-968, 1980.

[12] Haykin S., "Communication Systems", Published by John Wiley & Sons, Printed: 1994.

[13] Samuel C Yang; "OFDMA System Analysis and Design" mobile communication series, Artech house, 2010.

[14] Rappaport, Theodore S., "Wireless Communications: Principles and Practice", 2nd Edition, page 76, 2002.

[15] IEEE Standards Association; http://standards.ieee.org/about/get/802/802.11.html, http://standards.ieee.org/getieee802/download/802.11-2012.pdf (Access January, 2012).

[16] "LTE the UMTS Long Term Evolution from Theory to Practice", Edited by: Stefania Sesia, Issam Tujik, Matthew Baker, 2009.

[17] T. Keller and L. Hanzo, "Adaptive multi-carrier modulation: A convenient framework for time-frequency processing in wireless communications," vol. 88, no. 5, pp. 611–640, May 2000.

[18] Mohseni S. and Matin M. A., "Study of the estimation techniques for the Carrier Frequency Offset (CFO) in OFDM systems", International Journal of Computer Science and Network Security, Vol. 12 No. 6, pp 73-80, 2012.

[19] Mohseni S. and Matin M. A., "Investigating the effect of the Carrier Frequency Offset (CFO) and Frequency synchronization on the performance of the OFDM Wireless systems", International Journal of Computer Science and Network Security, Vol. 12 No. 12, pp: 85-92, 2012.

[20] P. H. Moose, "A technique for orthogonal frequency division multiplexing frequency offset correction", IEEE Transaction on Communications, volume 42, issue 10, pp 2908-2914, 1994.

[21] J. G. Proakis, Digital communications, 4th ed. McGraw-Hill, 2001

[22] Patrick Robertson, Stefan Kaiser "the Effects of Doppler Spreads in OFDM (A) Mobile Radio Systems" Institute for Communications Technology, German aerospace Center (DLR), 2010.

[23] Muschallik, C "Influence of RF oscillator on an OFDM signal" IEEE Transaction, volume 41, issue 3, pp: 592–603, 1995.

[24] Minn, H., Zeng M., and Bhargava V. K., "On Timing Offset Estimation for OFDM Systems", IEEE Transaction Communication Volume 4, No. 7, 2000.

[25] Mohseni S. and Matin M. A., "Study of the Sensitivity of the OFDM wireless systems to the Carrier Frequency OFFSET (CFO)", International Journal of Distributed and Parallel Systems (IJDPS) Vol. 4, No. 1, pp 73-80, 2013.

[26] POLLET, T., Van Blade, M., and Moeneclaey, "BER sensitivity of OFDM systems to Carrier Frequency Offset and Wiener phase noise" IEEE Transaction on Communication, VOL. 43, NO. 2/3/4, Feb/Mar/April 1995.

[27] IEEE PES Technical Committee Meeting, Montreal 2006.

[28] Mathecken, P. Riihonen, T. Werner, and S. Wichman, "Performance Analysis of OFDM with Wiener Phase Noise and Frequency Selective Fading Channel" IEEE Transaction Communication, volume 59, Pages: 1321-1331, 2011.

[29] Pollet, T., Spruyt, P., and Moeneclaey, M. "The BER performance of OFDM systems using non-synchronized sampling," IEEE, Conference Publications, Volume 1, pp 253-257, 1994.

[30] Richard Van Nee and Ramjee Prasad, OFDM for Wireless Multimedia Communica-tions, The Artech House Universal Personal Communications, Norwood, MA, 2000.

[31] Sang Hyun Do ; Hong Bae Cho ; Hyung Jin Chol ; Ki Bum Kim " A new joint algorithm of symbol timing recovery and sampling clock adjustment for OFDM Systems" IEEE Volume: 44 Issue: 3, pp 1142-1149, 1998.

[32] Speth M., Dacke D., and H. Meyr, "Minimum overhead burst synchronization for OFDM broadband transmission" Global Telecommunications Conference, IEEE, Volume 5, pp 2777-2782, 1998.

[33] Pollet, T., Spruyt, P., and Moeneclaey, M. "The BER performance of OFDM systems using non-synchronized sampling," IEEE, Conference Publications, Volume 1, pp 253-257, 1994.

[34] S. Halford, and K. Halford, "implementing OFDM in Wireless" Intersil corporation, www.intersil.com, 2001 (Access January 2011).

[35] Michael Speth, Student Member, IEEE, Stefan A. Fechtel, Member, IEEE, Gunnar Fock, and Heinrich Meyr, Fellow, "Optimum Receiver Design for Wireless Broad-Band Systems Using OFDM" part I, IEEE transactions on communications, VOL. 47, NO. 11, November 1999.

[36] Pollet, T., Van Bladel, M., Moeneclaey, M. "BER sensitivity of OFDM systems to carrier frequency offset and Wiener phase noise" IEEE transactions on communications, VOL. 43, NO. 12, November 1995.

[37] A. Tarighat and A. H. Sayed, "Joint compensation of transmitter and receiver impairments in OFDM systems," IEEE Transaction,. Wireless Communication 2007.

[38] D. Tandur and M. Moonen, "Joint adaptive compensation of transmitter and receiver IQ imbalance under carrier frequency offset in OFDM based systems," IEEE Trans. Signal Processing, vol. 55, pp. 5246-5252, Nov. 2007.

[39] J. Tubbax, B. Come, L. V. der Perre, S. Donnay, M. Moonen, and H. D. Man, “Compensation of transmitter IQ imbalance for OFDM systems,” in Proc. IEEE Intl. Conf. Acoustics, Speech and Signal Process., May 2004.

[40] H. Lin and K. Yamashita, “Subcarrier allocation based compensation for carrier frequency offset and I/Q imbalances in OFDM systems,” IEEE Trans. Wireless Commun., vol. 8, no. 1, pp. 18–23, Jan. 2009.

[41] G. Xing, M. Shen, and H. Liu, “Frequency offset and I/Q imbalance compensation for direct-conversion receivers,” IEEE Trans. Wireless Commun., vol. 4, no. 2, pp. 673–680, Mar. 2005.

[42] H. Minn, M. Zeng, and V. K. Bhargava, “On timing offset estimation for OFDM systems,” IEEE Commun. Lett., vol. 4, no. 7, pp. 242–244, Jul. 2000.

[43] Schmidl, T.M., Cox, D.C. “Low-overhead, low-complexity [burst] synchronization for OFDM”, IEEE, Communications, ICC '96, Conference Record, Converging Technologies for Tomorrow's Applications, 1996 volume 3, pp 1301-1306, 1996.

[44] Schmidl, T.M. and Cox, D.C. (1997) “Robust frequency and timing synchronization for OFDM” IEEE Transaction on Communication, vol. 45, pp 1613–1621, 1997.

[45] Van de beek, J. , M. Sandell, M. Isaksson, and P. O. Borjesson, “Low-Complex Frame Synchronization in OFDM Systems”, Proceedings of International Conference on Universal Personal Communications ICUPC, 95, 1995.

[46] Sandell M., J. van de beek, and P. Borjesson, “Timing and Frequency Synchronization in OFDM systems Using the Cyclic Prefix”, Proceedings of International symposium On Synchronization, Germany, 1995, pp 16-19, December 14-15, 1995.

[47] P. H. Moose, “A technique for orthogonal frequency division multiplexing frequency offset correction” IEEE Transactions on Communications, vol. 42, no. 10, pages: 2908–2914, 1994.

[48] T. Schmidl and D. Cox, “Robust frequency and timing synchronization for OFDM," IEEE Trans. Commun., vol. 45, no. 12, pp. 1613{1621, 1997.

[49] Yonghong Zeng, A. Rahim Leyman, and Tung-sang Ng,“Joint Semi-blind Frequency Offset and Channel estimation for Multiuser MIMO-OFDM Uplink” IEEE Transaction on Communications, Vol. 55, No. 12, 2007.

[50] Ufuk Tureli, Hui Liu, and Michael D. Zoltowski, “OFDM Blind Carrier Offset Estimation: ESPRIT”, IEEE Transactions on communications, Volume 48, 2000.

[51] Hui Liu, and Ufuk Tureli, “A High-Efficiency Carrier Estimator for OFDM Communications”, IEEE communications Letters, Volume 2, No. 4, 1998.

[52] D. Huang and K. Letaef, “Carrier frequency offset estimation for OFDM systems using null subcarriers,” IEEE Transaction Communication, Volume 54, No. 5, pp 813–823, 2006.

[53] P. Moose, “A technique of orthogonal frequency division multiplexing frequency offset correlation”, IEEE Transaction Communication, Volume 42, pp 2908-2914, 1994.

[54] M. Morelli, and U. Mengali, “An improved frequency offset estimator for OFDM applications” IEEE Communication Letter, Volume 3, pp 75–77, 1999.

[55] H. Minn, P. Tarasak, and V Bhargava, “OFDM frequency offset estimationmethods based on BLUE principle” IEEE Vehicle Technology Conference, Vancouver, Canada, pp 1230–1234, 2002.

[56] J. Li, G. Liu, and G. Giannakis, “Carrier frequency offset estimation for OFDM-based WLANs” IEEE Signal Processing Letter, Volume 8, pp 80–82, 2001.

[57] J. H. Yu and Y. T. Su, “Pilot-assisted maximum-likelihood frequency offset estimation for OFDM systems,” IEEE Transaction Communication, volume 52, No. 11, pp 1997–2007, 2004.

[58] S. Tretter, “Estimating the frequency of a noisy sinusoid by linear regression”, IEEE Transaction Information Theory, Volume IT-31, Pp 832–835, 1985.

[59] P. Stoica and A. Nehorai, “MUSIC, maximum likelihood, and Cramer–Rao bound,” IEEE Transaction Acoustic, Speech, and Signal Processing, Volume 37, pp 720–741, 1989.

[60] Hung-Tao Hsieh, anWen-Rong Wud, “Maximum Likelihood Timing and Carrier Frequency Offset Estimation for OFDM Systems with Periodic Preambles”, IEEE Transactions on Vehicular Technology, Volume 58, 2009.

[61] Xiaohua (Edward) Li and Fan Ng, “Carrier Frequency Offset Mitigation in Asynchronous Cooperative OFDM Transmissions” IEEE Transactions on Signal processing, VOL. 56, No. 2, 2008.

[62] R. O’Neill and L. B. Lopes; “Envelope Variations and Spectral Splatter in Clipped Multicarrier Signals”, University of Leeds, United Kingdom. IEEE Conference, 1995.

[63] G. Ren, H. Zhang, and Y. L. Chang, “A complementary clipping transform technique for the reduction of peak-to-average power ratio of OFDM system,” IEEE, 2003.

[64] S.H. Muller and J.B. Huber, “OFDM with reduced peak-to-average power ratio by optimum combination of partial transmit sequences,” IEEE Conference, 1997.

[65] S. B. Slimane, “Reducing the peak-to-average power ratio of OFDM signals through precoding,” IEEE vol. 56, 2007.

[66] R. W. Bauml, R. F. H. Fisher, and J. B. Huber, “Reducing the Peak-to- Average Power Ratio of Multicarrier Modulation by Selected mapping,” IEE Electronics Letters, vol. 32, no. 22, pp. 2056–2057, 1996.

[67] A. E. Jones, T. A.Wilkinson, & S. K. Barton, “Block coding scheme for reduction of peak-to-average envelope power ratio of multicarrier transmission systems,” IEE Electronics Letters, vol. 30. 1994.

[68] Xianbin Wang, T. T. Tjhung, and C. S. Ng, “Reduction of Peak-to-Average Power Ratio of OFDM System Using A Companding Technique,” IEEE Trans. Broadcasting, vol. 45, no. 3, pp. 303–307, 1999.

[69] T. G. Pratt, N. Jones, L. Smee, and M. Torrey, “OFDM link performance with companding for PAPR reduction in the presence of nonlinear amplification,” IEEE Conference, 2006.

[70] J. Tellado, “Peak to Average Power Ratio Reduction for Multicarrier Modulation”, University of Stanford, 1999.

[71] S. Yoo, S. Yoon, S. Y. Kim, and I. Song, “A Novel PAPR Reduction scheme for OFDM systems: Selective Mapping of Partial Tones (SMOPT),” IEEE Trans. Consumer Electronics, vol. 52, 2006.

[72] S. H. Müller and J. B. Huber, “A Comparison of Peak Power Reduction Schemes for OFDM,” IEEE Conference, 1997.

[73] S. H. Han and J. H. Lee, “PAPR Reduction of OFDM Signals Using a Reduced Complexity PTS technique,” IEEE Signal Processing Letters, vol. 11, no. 11, 2004.

[74] Tao Jiang, Weidong Xiang, Paul C. Richardson, Jinhua Guo, and Guangxi Zhu, “PAPR Reduction of OFDM Signals Using Partial Transmit Sequences With Low Computational Complexity,” IEEE Trans. Broadcasting, vol. 53, no. 3, pp. 719–724, 2007.

[75] Désiré GUEL and Jacques Palicot "Analysis and Comparison of Clipping Techniques for OFDM Peak-To-Average Power Ration reduction", IEEE Trans. Broadcasting, Vol 53, no. 3, pp 719-724, 2007.

[76] S. Fragicomo, C. Matrakidis, and J. J. OReilly, "Multicarrier transmission peak-to-average power reduction using simple block code," IEE Electronics Letters, vol. 34, no. 14, 1998.

[77] Tao Jiang and Guangxi Zhu, Huazhong University of Science and Technology, "Complement Block Coding for Reduction in Peak-to-Average Power Ratio of OFDM Signals," IEEE Communications Magazine, 2005.

[78] Seung Hee Han, Stanford University, Jae Hong Lee, Seoul National University, Peak to Average Power Ration Reduction techniques for Multicarrier Transmission., IEEE Communication Magazine, 2005.

[79] Tao. Jiang and Guangxi Zhu, "OFDM Peak-to-Average Power Ratio Reduction by Complement Block Coding Scheme and Its Modified Version," IEEE Vehicular Technology Conference 2004.

[80] "LTE the UMTS Long Term Evolution from Theory to Practice", Edited by: Stefania Sesia, Issam Tujik, Matthew Baker, 2009.

[81] D. Karampatsis, M.R.D. Rodrigues and I. Darwazeh, "Implications of linear phase dispersion on OFDM and Fast-OFDM systems," London Communications Symposium UCL, pp 117-120, London, UK, 2002.

[82] Jalel Chebil, Ali K. Lwas, Md. Rafiqul Islam and Al-Hareth Zyoud "Comparison of Empirical Propagation Path Loss Models for Mobile Communications in the Suburban Area of Kuala Lumpur" 4th International Conference on Mechatronics (ICOM), 17-19 May 2011, Kuala Lumpur, Malaysia, 2011.

[83] Friis, H.T. "A note on a simple transmission formula". Proc. IRE, 34(5), 254–256, 1946.

[84] Jakes, W.C. "Microwave Mobile Communication" Wiley, IEEE Press, 1994.

[85] Rappaport, T.S., "Wireless Communications: Principles and Practice", Upper Saddle River, NJ: Prentice-Hall, 2002.

[86] Paularaj, A.J., et al., "an Overview of MIMO Communications, A Key to Gigabit Wireless," Proceedings of the IEEE, vol. 92, No. 2, pp. 198-218, 2004.

[87] Goldsmith, A. "Wireless Communications, Cambridge", U.K.: Cambridge University Press, 2005.

[88] HATA, M., "Empirical formula for propagation loss in land mobile radio services", IEEE Transaction on Vehicular Technology, vol. 29, No. 3, pp 317 – 325, 1980.

[89] Okumura, Y., Ohmori, E., Kawano, T., and Fukuda, K., "Field strength and its variability in VHF and UHF land mobile radio service". Rev. Elec. Communication. Lab., 16, 825–873, 1968.

[90] Hata, M. "Empirical formula for propagation loss in land mobile radio services". IEEE Trans. Veh. Technol., 29(3), 317–325, 1980.

[91] Rahnema, M. UMTS Network Planning, and interoperation with GSM Wiley and Sons Ltd. 2009.

[92] Goldsmith Andrea, "Wireless Communications" Cambridge University Press, 2005.

[93] V.S. Abhayawardhana, I.J. Wassel, D. Crosby, M.P. Sellars, M.G. Brown "Comparison of empirical propagation path loss models for fixed wireless access systems" Proceedings of the 61st IEEE Vehicular Technology Conference, Ipswich, UK, Volume 1, pp 73-77, 2005.

[94] Electronic Communication Committee (ECC) within the European Conference of Postal and Communications Administration (CEPT), "Derivation of a block edge mask (BEM) for terminal stations in the 2.6 GHz frequency band (2500-2690 MHz)", ECC report 131, Dublin, 2009.

[95] S. Ichitsubo, T. Furuno, T. Taga, and R. Kawasaki, "Multipath Propagation Model for Line-of-Sight Street Microcells in Urban Area" IEEE Transactions on Vehicular Technology, pp 422-427, 2000.

[96] D. Har, H. H. Xia, and H. L. Bertoni, "Path-Loss Prediction Model for Microcells" IEEE Transactions on Vehicular Technology, pp. 1453-1463, 1999.

[97] J. M. Keenan and A. J. Motley, "Radio Coverage in buildings", British Telecom Technology Journal, 8(1): 19-24, 1990.

[98] H. Hashemi, "The indoor radio propagation channel", Proceedings IEEE, 81(7): 943-968, July, 1993.

[99] S. Y. Seidel and T. S. Rappaport, "914 MHz path loss Prediction models for Indoor Wireless Communications in Multifloored Buildings", IEEE Transactions on Antennas and Propagation, 40(2): 207-217, 1992.

[100] K. W. Cheung, J. H. M. Sau and R. D. Murch, “A New Empirical Model for Indoor Propagation Prediction” IEEE Transactions on Vehicular Technology, 1997.

[101] Tapan K. Sarkar, Zhong Ji., Kyungjung Kim, Abdellatif Medour, and Magdalena Salazar-Palma “A Survey of Various Propagation Models for Mobile Communication” IEEE Antennas and Propagation Magazine ISSN 1045-9243, Vol. 45, Issue 3, pp. 51 – 82, 2003.

[102] R. Green, “Radio Link design for microcellular systems”, British Telecom Technology Journal, 8(1): 85-96, 1990.

[103] W. Honcharenko, H. L. Bertoni, J. L. Dailing, J, Qian and H. D. Yee, “Mechanisms goverining UHF propagation on single floors in modern office buildings”, IEEE Transactions on Vehicular Technologh, 41(4): 496-504, 1992.

[104] K. W. Cheung, J. H. M. Sau, and R. D. Murch, “A New empirical Model for Indoor Propagation Prediction,” IEEE Transactions on Vehicular Technology, VT-47, 3, pp. 996-1001, 1998.

[105] Erceg, V., Greenstein, L.J., Tjandra, S.Y. et al. “An empirically based path loss model for wireless channels in suburban environments” IEEE J. Select. Areas Communication, 17(7), pp 1205–1211, 1999.

[106] IEEE 802.16j-06/013r3, “Multi-Hop Relay System Evaluation Methodology (Channel Model and Performance Metric)” , 2007.

[107] IEEE 802.16.3c-01/29r4,“Channel Models for Fixed Wireless Apps”, 2001.

[108] IST (2004) 4-027756. WINNER II, D1.1.1 WINNER II Interim Channel Models

[109] H. L. Bertoni, “Radio Propagation for Modern Wireless Systems”, Upper Saddle River, NJ, Prentice Hall PTR, pp. 90-92, 2000.

[110] C. Tepedelenlioglu, A. Abdi, G. Giannakis, and M. Kaveh, “Estimation of Doppler spread and signal strength in mobile communications with applications to handoff and adaptive transmission” Wireless Communication Mobile Computer, volume 1, pp 221-242, 2001.

[111] M. Tayebi, M. Bouziani, “Performance analysis of OFDM systems in the presence of Doppler Effect” Journal of Electrical and Electronics Engineering (IOSR-JEEE) Vol. 4, pp 2278-1676, 2013.

[112] J. Won Lee, Hui-Ling Lou, d. Toumpakaris and J. Cioffi, “Effect of Carrier Frequency Offset on OFDM Systems for Multipath Fading Channels” Department of Electrical Engineering, Stanford University, IEEE 2004.

Appendix

List of publications

Journals:

[1] **Mohseni S.** and Matin M. A., "Study of the Sensitivity of the OFDM wireless systems to the Carrier Frequency OFFSET (CFO)", International Journal of Distributed and Parallel Systems (IJDPS) Vol. 4, No. 1, pp 73-80, 2013.

[2] **Mohseni S.** and Matin M. A., "Investigating the effect of the Carrier Frequency Offset (CFO) and Frequency synchronization on the performance of the OFDM Wireless systems", International Journal of Computer Science and Network Security, Vol. 12, No. 12, pp 85-92, 2012.

[3] **Mohseni S.** and Matin M. A., "Study of the estimation techniques for the Carrier Frequency Offset (CFO) in OFDM systems", International Journal of Computer Science and Network Security, Vol. 12 No. 6, pp 73-80, 2012.

[4] **Mohseni S.** and Matin M. A., "Investigating the Reducing Techniques for the Peak to Average Power Ratio (PAPR) in OFDM Systems", International Journal of Computer Science and Network Security, Vol. 12, No. 4, pp 1-8, 2012.

[5] **Mohseni S.** and Matin M. A., "Study of propagation path loss for OFDM mobile systems", International Journal of Computer Science and Network Security, Vol. 12, No. 9 pp 15-23, 2012.

[6] **Mohseni S.** and Matin M. A., "The Effects of Carrier frequency Offset in Wireless OFDM System", Journal of Optical Communication and Networking, 2013 (Submitted).

Proceedings:

[7] Bloul A., **Mohseni S**., Alhason B., Ayad M., Matin M. A.: "Simulation of OFDM technique for wireless communication systems", Proc. SPIE, Vol. 7797, 77971B, 2010.

[8] **Mohseni S**., Bader Alhasson, Matin M. A.**: "**Characterizations of Multi-segment DFB Laser"**,** Proc. SPIE, Vol. 7072, 70720C, 2008.